DET NORSKE
VERITAS

91-04793/

FRACTURE CONTROL FOR ARCTIC STRUCTURES: A MODEL FOR ANALYZING STRUCTURAL DETAILS

Final Report

by:
Det norske Veritas (Canada) Ltd.
#1110, 10201 Southport Road, S.W.
Calgary, Alberta
T2W 4X9

Work on the project was conducted under the auspices of the Canada Centre for Mineral and Energy Technology, Energy Mines and Resources Canada

6-9150
DSS File No. 03SQ.23440-~~6-9115~~
DSS Contract Serial No. 23440-6-9150/01-SQ
EMR Scientific Authority: Dr. W.R. Tyson

August 1988

171 pp

MICROMEDIA

DET NORSKE
VERITAS

CANADA

ADDRESS #1110, 10201 Southport Road S W
Calgary, Alberta T2W 4X9
Canada
TELEPHONE (403) 253-3422
TELEX 03-827808

Technical Report

Date	Department	Project No.
August 31, 1988	R & D	258

Approved by/sign

Touraj Nasseri, President

Client/Sponsor Clients ref
Canada Centre for Mineral & Energy Technology - Dr. W. R. Tyson

Summary

The study reported herein is the result of a research program, sponsored initially by The Canada Centre for Mineral and Energy Technology (CANMET), and Det norske Veritas (Canada) Ltd. During the course of the study, the Canadian Coast Guard Northern, also became a sponsor of the program.

Modern system reliability methods have been adapted and applied to analyse the uncertainties associated with the quantification of such steel characteristics that have critical effects on the performance of steel structures and vessels in the Arctic.

Limit-state functions delineating safe and failure spaces have been developed and used to compute the probabilities of critical modes of failures. The randomness of factors that have significant effect on steel performance, such as fracture toughness, strength and stress fields have been incorporated into the analysis by appropriate probability distributions for the factors. Furthermore, the sensitivity of failure probability to variation and uncertainties in key factors has been computed and comparative reliability analysis performed for different steels.

The study is a contribution towards a reliability-based integrated approach to the design and manufacturing of Arctic-specific steels. This is needed to deal with the uniquely demanding environment of the Arctic and the limited operational experience with Arctic vessels and structures. Recommendations on the further development and application of the methods presented in the study are also proposed for consideration in future programs.

VERITAS Report No.	Subject Group
88-CGY-003	Ship/Offshore

Title of Report

FRACTURE CONTROL FOR ARCTIC STRUCTURES:
A MODEL FOR ANALYZING STRUCTURAL DETAILS

4 Indexing terms
Arctic
Steel
Ship
Offshore

Date of last rev.	Rev. No.
February 1988	1

Distribution statement:

☒ No distribution without permission from the responsible department.

☐ Limited distribution within Det norske Veritas.

☐ Unrestricted.

Work carried out by/sign

M. Tomin	M. Nessim	A. Cormeau
M. T.	MN	AC

Number of pages
131

Det Norske Veritas has no liability for loss or damage caused by its officers, employees or other who act under assignment by the Foundation, whether or not such person has acted intentionally or negligently and whether or not the loss or damage has affected the owner of a ship, facility or system or a shipyard or other who have requested the Foundation's assistance, or any third party who without having any contractual relations with the Foundation has acted or made arrangements on reliance on decisions made or information given by or on behalf of the Foundation. Nor, in cases as mentioned in the preceding paragraph, can the individual or individuals who have personally caused the loss or damage be held liable.

TABLE OF CONTENTS

Page

1. INTRODUCTION 1
2. REVIEW OF PROBABILISTIC APPROACH TO SHIP STRUCTURAL DESIGN 3
3. STRUCTURAL RELIABILITY ANALYSIS 12
   - 3.1 Structural Reliability and Probability of Failure 12
   - 3.2 Levels of Reliability Methods 14
   - 3.3 First Order, Level 2 Reliability Method 16
   - 3.4 Computer Program PROBAN 21
   - 3.5 Targeted Probabilities of Structural Failure 24
4. MODES OF STRUCTURAL FAILURE & STRUCTURAL DETAILS 29
   - 4.1 Modes of Structural Failure 29
   - 4.2 Structural Details 30
5. DEVELOPMENT OF FAILURE MODELS 37
   - 5.1 Modelling Unstable Fracture 37
     - 5.1.1 The Stress Intensity Factor Approach 38
     - 5.1.2 Crack Tip Opening Displacement (CTOD) Approach 40
   - 5.2 Modelling Plastic Collapse 44
   - 5.3 Modelling Fatigue Crack Propagation 45
   - 5.4 Combined Probability of Failure (Serviceability) 49
   - 5.5 Modelling Crack Arrest 49
   - 5.6 Summary of Modelled Cases 50
6. PROBABILISTIC MODELLING OF INPUT RANDOM QUANTITIES 51
   - 6.1 Fracture Toughness 51
     - 6.1.1 Fracture Toughness Data 52
     - 6.1.2 Modelling Fracture Toughness vs Test Temperature 55
     - 6.1.3 Modelling Fracture Toughness vs Thickness 65
     - 6.1.4 Modelling Fracture Toughness vs Strain Rate 67
     - 6.1.5 Modelling Crack Arrest Toughness 73
   - 6.2 Modelling Yield Strength vs. Temperature 76

Page

6.3 Modelling Crack/Defect Size and Crack Shape 78
- 6.3.1 Modelling Initial Flaw Size 78
- 6.3.2 Surveyed Crack Size Distribution 80
- 6.3.3 Stress Intensity Factor (SIF) 81
- 6.3.4 Critical Crack Size Factor I_a 85

6.4 Modelling Stresses/Loads 88
- 6.4.1 Far-Away Stresses/Loads 88
- 6.4.2 Wave Induced Stresses/Loads 89

7. ANALYSIS AND DISCUSSION OF THE STUDY RESULTS 92

7.1 Probability of Fracture Based on Measured Crack Distribution 93
- 7.1.1 Probability of Unstable Fracture 93
- 7.1.2 Probability of Plastic Collapse 105
- 7.1.3 Probability of Failure Considering Unstable Fracture or Plastic Collapse 105

7.2 Probability of Failure Due to Fatigue Crack Propagation 106
- 7.2.1 Simple Plate 106
- 7.2.2 Welded T-Joint 109

7.3 Probability of Crack Arrest 115

8. CONCLUDING REMARKS AND RECOMMENDATIONS FOR FUTURE WORK 116

REFERENCES 119

APPENDICES

1. INTRODUCTION

The materials used for the construction of Arctic structures and vessels are exposed to low ambient temperatures, high local ice loads and intermediate to high strain rates. All these factors can significantly affect the risk of unstable fracture in these structures.

Current regulatory requirements for material selection are based on relatively high service temperatures. For example, the design temperature for worldwide shipping is considered 0°C which represents the 3-percentile of the temperature distribution for year-round worldwide shipping. IACS (1980) allows hull steel selection down to -50°C for primary and secondary categories and to -40°C for the so called "special" category. However, considerable penalties are imposed in terms of reduced thickness so that for example at -40°C, only E and EH steels are allowed in special category areas and even then they have a 10 mm maximum thickness.

The steel requirements for offshore structures in UK waters are based on a design temperature of -10°C, however the revised DOE guidelines (1986) allow steel selection in the range -20°C to +10°C while altering the Charpy V-Notch test temperature by 0.7°C for every 1°C that the design temperature differs from -10°C.

Boyd (1969), when reviewing the fracture failures of Liberty ships and T2 tankers, noted that, "There seems to be a strong element of chance in brittle fracture. In comparison with the enormous numbers of successful welded structures, the number of serious failures has been remarkably small. It is almost certain that many of the structures that have not failed contain features known to be conducive to brittle fracture and have sustained similar service conditions to those which have failed."

Indeed, unstable (brittle) fracture requires the joint occurrence of many unfavourable conditions. The most important seem to be the following: low temperature, high strain rate, high loads, high residual stresses, low fracture toughness (degraded fracture toughness at the crack tip), high constraint due to large thickness and a crack-like defect. The fatigue crack propagation itself is a random process.

It is therefore appropriate to model the fracture event probabilistically, capturing the random character of fatigue crack propagation and of various parameters affecting unstable fracture. Comparing probabilities of failure for service temperatures at which structures perform satisfactorily with those for low temperatures calculated from the developed models may help to substantiate steel selection requirements for low temperatures.

A probabilistic approach to the unstable fracture of tubular joints was developed in a preceding DnV study (Tomin and Lantos, 1986) and the results encouraged initiation of the current project financed jointly by CANMET, DnV and Canadian Coast Guard.

2. REVIEW OF PROBABILISTIC APPROACH TO SHIP STRUCTURAL DESIGN

The objective of this review is to identify the areas in ship structural reliability analysis where extensive work has been carried out and those where further work is required. The question of safety of ship structures is probably as old as ship building. The classical ship design approach relies on ensuring safety at sea by having a conservatively large margin between the maximum expected hull stress and the strength of the material. This approach has of course been successful for many years due to the fact that the demands on the ship structure were not as high as they are today. Using this classical method of ship reliability/safety with such high demands becomes less efficient than the more recently developed probabilistic methods. These new methods have been shown to yield considerably more economical ship structures (in some cases by more than 30 percent savings) and produces more clearly identified failure modes and associated failure probabilities.

This explains the recent interest (since the beginning of the 1970's) in probabilistic design methods as they apply to ship structures. Many publications have appeared which deal with this subject. The first serious application of reliability methods in ship design was proposed by Abrahmsen, et al (1970). This approach was subsequently adopted with some modification as the basis for the rules of the construction and classification of steel ships published by the ship classification society, Det norske Veritas (1975).

It should be emphasized that the review presented in this section is by no means exhaustive. Many references were identified, both through manual and computerized library search techniques, but were not fully reviewed due to resource and time constraints.

In the following literature review, attention is focused on providing the reader with the necessary background as to the state-of-the-art in this field in order to provide the basis which lead to the work presented in this investigation.

Previous work on ship structural safety and reliability may be divided into the following areas:

(a) Development of safety formats and models for analytically evaluating the safety/reliability of the structure.

(b) Application of developed probabilistic models to actual operations to identify the probabilities associated with various failure modes in order to determine the optimum operational profile.

(c) The economic aspects of the target safety and the practical implications of trade-offs between safety and cost.

The development of analytical formulations for safety and reliability of structure dates back to the time when statistical methods were developed in the twenties. The last three decades have, however witnessed a very rapid development in these theories and analytical models (see Section 3).

The application of probabilistic methods to the evaluation of the safety and reliability of a ship or a structure requires data on the following:

(i) The environment in which the operation takes place.

(ii) The loads exerted on the structure due to the environment.

(iii) The response of the structure under these loads. This response involves both the global and local stress states and stress concentration factors.

(iv) Identification of the failure modes of interest. These include yielding, plastic flow, buckling, fatigue and fracture.

Finally, the basis for the selection of the target safety levels was noted to be the subject of a few references which describe the trade-off between safety and the socioeconomic factors related to the structure under consideration. In these socioeconomic studies, the definition of the "adequate" safety targets requires the evaluation of such parameters as the annual life loss rate, the life of the structure, the economic cost of failure/unserviceability and the annual failure probability. The failure probability depends on the level of redundancy built or to be implemented, and the severity of the consequence of failure enters into the analysis through the definition of the economic costs of failure.

Individual failure modes are described in more detail in Section 4. In the following a brief description is given of the reviewed literature. This review is presented in chronological order dating back only to 1970.

As mentioned earlier in this section Abrahamsen et al (1970) proposed the use of probabilistic methods in ship structural design. The failure probability was calculated using the simple limit state function:

$$R - F \leq 0 \tag{2.1}$$

where R is the resistance and F is the load. The probability of failure is calculated using the two probability density functions (pdf's) of R and F. The paper gave several closed form solutions for the cases where these pdf's were represented by standard distributions such as the normal, the log normal, the exponential, and the Rayleigh distributions. Applications were presented for still water and wave bending moments for short term and long term failure probability estimation. Using the bending moment as the measure of hull stresses suggests that only the yield failure mode was considered.

Boe et al (1974) discussed the reliability design criteria as applied to the shipping industry and gave a formula for calculating the reliability for equipment and systems as function of time in the form

$$R(t) = \exp\left\{-\int_0^t H(x)\,dx\right\} \tag{2.2}$$

where the integral in the exponent is a hardware dependent hazard rate. For a constant hazard rate Eq. 2.2 reduces to the standard exponential distribution, otherwise the equation fits into a Weibull distribution which was considered by the authors to be an unnecessary complication. However, it might be reasonable to say here that such complication may not have been too much of a problem had the use of accurate computational methods and powerful computers been considered.

Mansour (1974) employed a level II mean value first order second moment reliability method (MVFOSM) where the limit state function was linearized using its Taylor series expansion. This method was proposed for application in calculating the ship longitudinal strength.

Hasofer and Lind (1974) defined an invariant reliability index. In this method, instead of using the mean point as the linearization point (Mansour, 1974), they used a point on the limit state surface which is closest to the origin. The shortest distance in the transformed variable space represents the safety index. This method proved to be effective when applied to the hull girder response of a vessel.

The Det norske Veritas Rules (1977) employed a level I safety format whereby a split load and resistance partial safety factors format was adopted. The proposed partial safety factors are based on reliability analysis using the level II method. This format is similar to that used by the Comite Euro-International du Beton (CEB, 1976, 1978) which has the general form

$$R_d \geq S_d \qquad (2.3)$$

or

$$\frac{1}{\gamma_m} R_K \geq S \{\sum \gamma_{fi} \; F_{ki}\} \qquad (2.4)$$

where R_d is the design resistance, S_d is the design load effect, R_K and F_K denote the characteristic design resistance and load, and γ_{fi} and F_i are the partial safety factor and the associated load, respectively. Two types of partial safety factors γ_m and γ_f are used related to the strength and the loads. An excellent review of the details of the code formats is given by Mansour (1984).

The Ship Structures Committee (SSC - 275, 1978) published a comprehensive report on the fracture toughness/behaviour of ship plate materials involving both experimental and analytical work. The loading rate influence was investigated using seven ship grade steels. The work concluded that the effect of strain rate on ship steels is very significant. In 1981 the SSC conducted a study (SSC - 301) on the probabilistic structural analysis of ship hull longitudinal strength. This committee has also been active in collecting data on ship extreme stresses (SSC - 304) and in studying the fatigue and fracture criteria for ship steels (SSC - 303, 305 and 307).

Flint (1979) discussed the treatment of safety for marine structures design codes. The paper discusses the socioeconomic aspects involved in evaluating target safety levels and introduces a social criterion factor in calculating the annual probability of failure. A lack of such work is apparent in the literature.

A comprehensive study of the reliability of ship steels under cold climate conditions was carried out by Fenco (1980) for the Transportation Development Centre. A method for calculating the probability of fracture was proposed. In this procedure the stress and the temperature ranges are discretized and a probability is associated with each range. The joint probabilities are then calculated considering the assumption of independence to be valid. For every temperature and stress combination where the calculated stress intensity factor is larger than the critical value (fracture toughness), fracture is assumed to occur. The probabilities of all stress-temperature ranges causing fracture are summed up to obtain the total fracture probability. This simplified procedure does not account for the fact that the flaw length, shape and boundary conditions are also probabilistic variables. In addition, the proposed method assumes a normal pdf and an exponential pdf to represent the stress and the temperature, respectively. The critical stress intensity factor was not considered as a probabilistic variable. These assumptions affect the accuracy of the results and thus considerably limit the applicability of the method.

Several good papers were published in 1981 in this area. Examples are Faulkner (1981), Soreide (1981) and Hutchinson (1981). Faulkner's paper gives an excellent review of the basis of the three levels of reliability analysis. In this paper examples are shown where the employment of reliability design methods lead to savings in steel for large ships of more than 30 percent due to the more realistic modelling of the limiting conditions and the more rational choice of load factors (consistent safety factors). Faulkner presented the results from 23 naval and merchant ships to support his claim. Soreide reviewed the basis of the level II method and employed the DnV code format in carrying out ultimate load analyses of marine structures. Hutchinson presented a comprehensive study where the reliability analysis was applied in the optimization of ship operation in marine environments. Factors such as climatology, seamanship, season, location and ship response were all considered. A Markov mapping process was proposed in order to more reliably forecast seastates incorporating the effect of seamanship. The author introduced a new parameter denoted the independence time defined as the time required in order for two subsequent observations to be independent or uncorrelated. Similarly, an independence distance was defined. These parameters were shown to improve the reliability of the method. The application presented dealt only with hull girder bending stresses due to seastates.

Olsen and Bratfos (1982) of DnV carried out a fracture mechanics analysis of an LPG storage vessel design using reliability methods. This represents one of a few references where reliability methods have been applied to determine the probability of catastrophic failure due to fracture. The method was employed to determine the critical crack size and the critical corrosion level for fracture to occur. The probability of failure during a specific time interval was estimated on a per defect basis and then integrated over the pdf of the number of defects. The method employed pdf's of the following variables: critical crack opening displacements (lognormal), flaw size (log-normal), material yield strength (normal), material crack propagation parameter (lognormal). The results from this analysis enabled the designer to achieve better understanding of the relative importance of the different parameters and to accordingly allocate his efforts.

Another interesting study which deals with brittle fracture of ship structures was carried out by the Technical Research Centre of Finland (VTT, 1983) for the Canadian Coast Guard. The probability of brittle fracture for the M.V. Arctic steel grades was evaluated using a level II reliability analysis. Probability density functions were evaluated for the following parameters: existing crack length, extreme stress, fracture toughness, and temperature. The analysis assumed intervals of time during each of which these distributions are considered constant. This time increment was taken as one month. The annual probability of failure was then calculated as:

$$P_f = \sum_{i=1}^{n} p_{fi} \, p_i \tag{2.5}$$

where p_{fi} is the failure probability in period i and p_i is the probability of operating in period i during a year. The target probability of brittle fracture was estimated to be in the range 10^{-3} to 10^{-4} per ship year based on ship casualty statistics. The probability density function of the existing crack lengths was combined using linear Elastic Fracture Mechanics (LEFM) with the pdf of the extreme stresses to produce the "demand" or stress intensity factor distribution. Similarly, the fracture toughness or "capability" of the material was calculated by combining the temperature pdf with the conditional pdf of the fracture toughness given a specific temperature. Both wave and ice induced stresses were accounted for in the analysis. The extreme stress was assumed to follow the Gumbel I distribution. A Monte-Carlo simulation technique with importance sampling was used to obtain the distribution of stress intensity factors K_I from the extreme stress and the crack length distributions. This procedure gave reasonable estimates of the probabilities of fracture and led to the upgrading of the vessel's steel in some of the critical areas. The procedure did not, however consider any other failure modes and did not include the effects of such parameters as the number of defects, fatigue cracking, and corrosion which could significantly influence the results.

Det norske Veritas (1983) carried out an investigation for the Canadian Coast Guard regarding the M.V. Arctic steel grades. In this investigation the computer program PROBAN was employed to calculate the probability of brittle fracture using a limit state condition of the form

$$\frac{K_{IC}}{F\sqrt{\pi a}} - \sigma < o \qquad (2.6)$$

where K_{IC} is the fracture toughness, a is the crack length, F is a geometry factor and σ is the applied stress. In addition, a crack growth criterion was employed in order to determine the fatigue risk. The results from this analysis have also led to the recommendation of upgrading some of the steels in this vessel which was adopted in the vessel's upgrading that took place in 1985.

Mansour et al (1984) published an excellent state-of-the-art review and a comprehensive study of the implementation of reliability methods to marine structures. The paper compared the formats of the existing design codes such as the American Petroleum Institute (API), the National Bureau of Standards (NBS), the Comite Euro-International du Beton (CEB), Det norske Veritas (DnV) and the American Bureau of Shipping (ABS). The various methods of reliability analysis were critically reviewed and compared. A methodology for calculating partial safety factors from level II reliability analysis was presented and applied. The results were compared with those of ABS.

Madsen, Krenk, and Lind (1986) published a monograph on the methods of structural safety. This excellent book gives the basics as well as the advanced methods developed to date in this field. The book entails several illustrations which demonstrate the applicability of the various methods. Madsen and Moghtaderi-Zadeh (1986) presented a paper on the application of reliability methods to calculate the nominal failure probabilities which are used to compare different elements or designs. The paper deals only with the fatigue ultimate limit state and uses the Miner damage index to compute the damage due to cyclic loading. The applications showed how, such an analysis, can lead to making optimum decisions regarding the increase of the fatigue life of an existing tubular joint in an offshore platform structure.

As recently as October 5 - 6, 1987, a symposium on marine structural reliability was held in Arlington. Several papers give further applications of the reliability design methods to offshore structures. None of the 18 published papers dealt with the material reliability except for one paper on fatigue design criteria. Also one paper discussed the question of selecting safety factors in design of marine structures. Further in-depth review to these proceedings is required.

Finally, several papers have been published recently on the subject of extremal analysis which constitutes an input to the reliability analysis process. Ochi (1981) gave an excellent review and applied extremal modelling techniques to ship structures. Maes and Jordaan (1986) proposed an extremal analysis procedure which uses short data extremal techniques for use in Arctic environmental design. Exchangeability techniques were shown to result in improved extremal values when the available data record is short.

This literature review demonstrates that very little work has been carried out in the area of material reliability for ship structures which accentuates the need for the present investigation.

3. STRUCTURAL RELIABILITY ANALYSIS

3.1 Structural Reliability and Probability of Failure

The structural reliability can be defined as a "measured chance" (probability) P_R, that a structure will withstand without failure, the loads to which it is subjected during some specified time (often the projected or design life). The failure probability, P_f, is then defined as a complement of the structural reliability, so that

$$P_f = 1 - P_R. \tag{3.1}$$

The quantities (variables) which affect the probability of failure form a vector of basic quantities $\underline{Z} = (Z_1, Z_2, ..., Z_n)$ where $\underline{Z}$ is a random vector in an n-dimensional vector space. It is common to use lower case letters ($\underline{z}$) to denote particular realisations (vectors) in the basic quantity space ($\underline{Z}$). Any limit (failure) state can be defined using a failure function $g(\underline{Z})$. Then the failure surface, corresponding to a given limit state, can be defined by $g(\underline{z}) = 0$, Figure 3.1. The failure surface then divides the space into a subspace of no failure states ($g > 0$) and its complement ($g < 0$) of failure states.

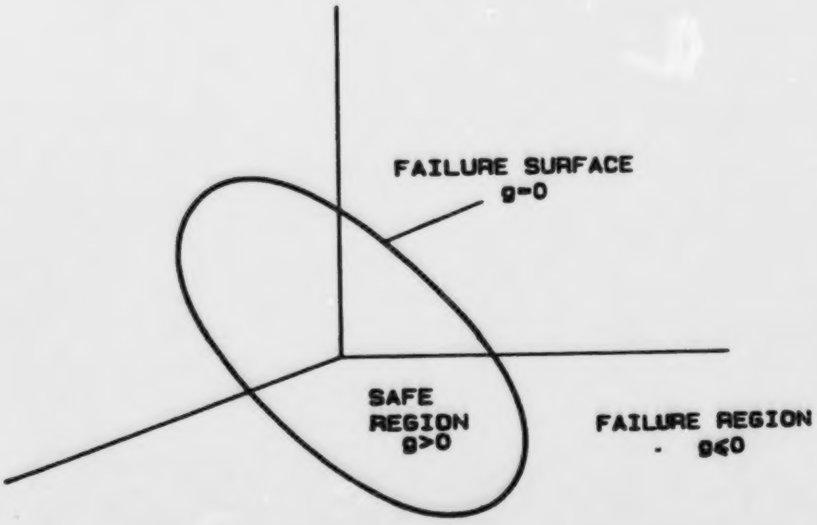

Fig. 3.1 Failure Surface

Then, the reliability P_R of a structure is the probability that the realization of $\underline{Z}$ falls in the safe region. Conversely, the probability of failure P_f is the probability that the realization of $\underline{Z}$ falls in the failure region.

The basic quantities can be divided in two groups, those affecting capacity (C), and those affecting demand (D) with corresponding resultant distributions, Figure 3.2. The probability of failure then corresponds to the overlapped region and can be expressed in terms of the probability density function of demand (f_D) and the cumulative distribution function of capacity (F_C) as:

$$P_f = \int_0^\infty F_C(x)\ f_D(x)dx \tag{3.2}$$

It is convenient to use the above approach and define a new random quantity, M = C - D, as the margin of safety. The probability of failure is then simply

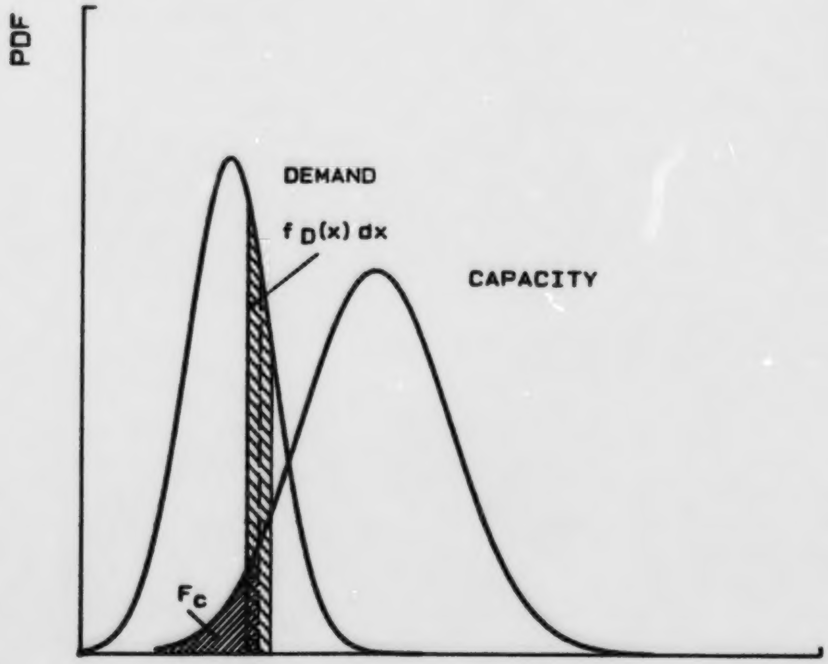

Fig. 3.2 Overlapped Region of Capacity and Demand

$$P_f = P\ (M < 0), \tag{3.3}$$

so that the margin of safety coincides with the previously introduced failure function, i.e.

$$M(\underline{Z}) = g(\underline{Z}).$$

The probability of failure is then given by the lower tail of the margin of safety cutoff at M = 0, Figure 3.3.

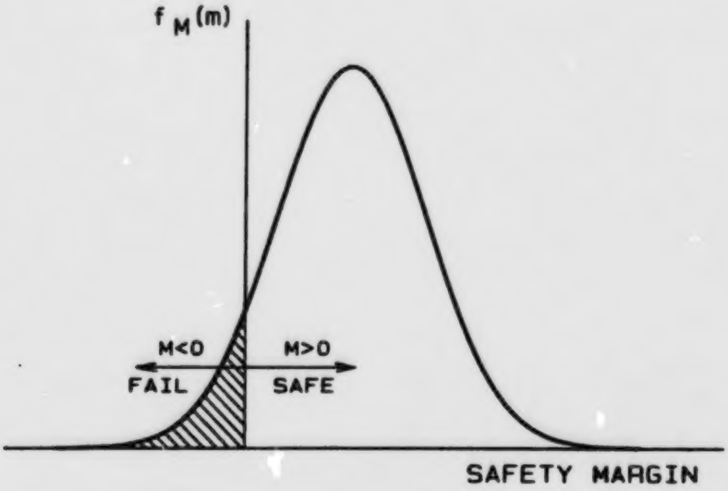

Fig. 3.3 Probability Density Function of the Safety Margin

3.2 Levels of Reliability Methods

In using the reliability-based methods, various degrees of simplification led to the definition of several levels of reliability analysis (CIRIA, 1977; Røren, Madsen and Lereim, 1986).

Level 1:

The reliability of structural elements is based on characteristic values (such as means and variances) of the basic quantities and expressed in terms of partial safety factors. In general, the design value, Z_i^* of the quantity Z_i is given by:

$$Z_i^* = m_i - \alpha_i \beta \sigma_i = m_i(1 - \alpha_i \beta V_i)$$

$$= \left(\frac{1 - \alpha_i \beta V_i}{1 + k_i V_i}\right) Z_{ki} = \gamma_i Z_{ki}, \tag{3.4}$$

where m_i is the mean value of Z_i;
V_i is the coefficient of variation of Z_i;
σ_i is the standard deviation of Z_i;
Z_{ki} is the characteristic value of Z_i;
k_i is a coefficient depending on the probability level p associated with the characteristic value of Z_i, and the nature of the probability distribution of Z_i;
α_i is a coefficient depending on the form of the failure boundary;
γ_i is the desired partial safety factor; and
β is the reliability index (see Section 3.3).

For example, ISO 2394 (1973) quotes seven partial factors to be applied to the loads or to the structural strength. The safety format of the DnV rules (1977) simplified this approach introducing two partial safety factors, one for loads, γ_f and one for material, γ_m. Then, the typical inequality regarding safety by applying the partial safety factor format is:

$$C(R_c/\gamma_m) > D\,(Lc\,\gamma_f)$$

where R_c is the characteristic resistance;
L_c is the characteristic load; and
C and D denote capacity and demand respectively

Level 2:

These methods use computational algorithms idealizing the failure surface at a selected point (design point) when calculating the failure probability of a structure. Often, these methods are based on Hasofer-Lind reliability index (Hasofer, Lind, 1974). This method was used in this project and will be discussed in more detail in the following section.

Level 3:

These reliability methods employ full joint probability distribution functions of basic quantities, making the analysis computationally much more demanding. Level 3 methods evaluate the probability content of the entire failure region. The reliability levels are commonly based on agreed failure probabilities, interpreted in the sense of relative frequencies. The Level 3 methods are currently being applied in the new generation of reliability software.

Level 4:

These methods make the reliability analysis a part of an overall engineering economic model under uncertainty, considering the cost benefits of construction, maintenance and repair, consequences of failure, etc. These methods are being developed at present.

3.3 First-Order, Level 2 Reliability Method

Rackwitz (1976) grouped the Level 2 reliability methods into three classes:

1. Mean value first-order second-moment methods;
2. Advanced first-order second-moment methods; and
3. Approximate full distribution methods.

These three distinct classes are discussed in detail in CIRIA (1977). The Level 2 reliability analysis, implemented in PROBAN (PROBability ANanalysis computer program; Tvedt, 1983) belongs to the third class of Rackwitz, which is a generalized class 2 for nonnormal distributions of basic quantities. Only the basics of the algorithm implemented in PROBAN used for this project will be described.

Cornell (1969) introduced the reliability index (safety index), β as:

$$\beta = \frac{\mu_M}{\sigma_M},$$

where μ_M is the mean and σ_M is the standard deviation of the safety margin, Figure 3.4. Thus, the number of standard deviations, by which the mean of the safety margin exceeds zero, became a convenient measure of reliability.

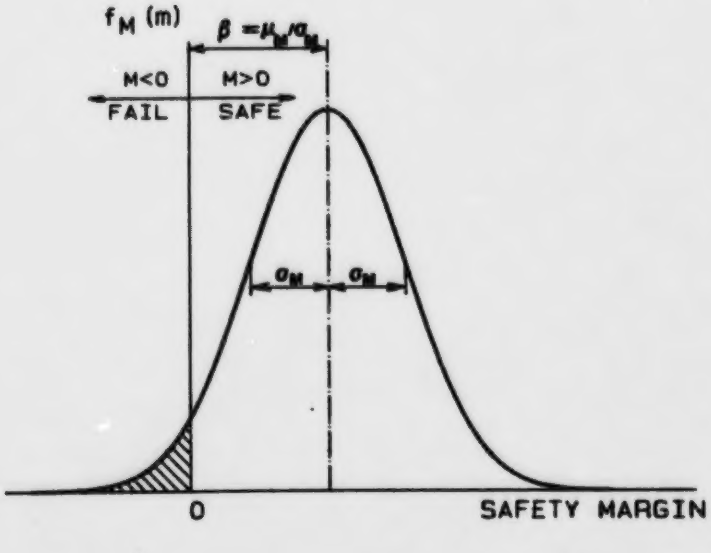

Fig. 3.4 Illustration of the Reliability Index β

The concept of the reliability index can be generalised and $\beta(\underline{z})$ can be interpreted as a measure of the distance from the origin to the failure surface in the n-dimensional space of the vector $\underline{Z}$. This is illustrated in Figure 3.5. As can be seen from this figure, the reliability index proposed by Hasofer and Lind (1974) β_{HL} corresponds to the minimum distance from the origin to the failure surface. The point on the failure surface defining this minimum distance is named the design point. When the margin of safety, M, is normally distributed (C and D are normally distributed and uncorrelated), then the probability of failure is simply:

$$P_f = P(M < 0) = \Phi\left(\frac{0 - \mu_M}{\sigma_M}\right) = \Phi(-\beta),$$

where Φ is the standard normal distribution function.

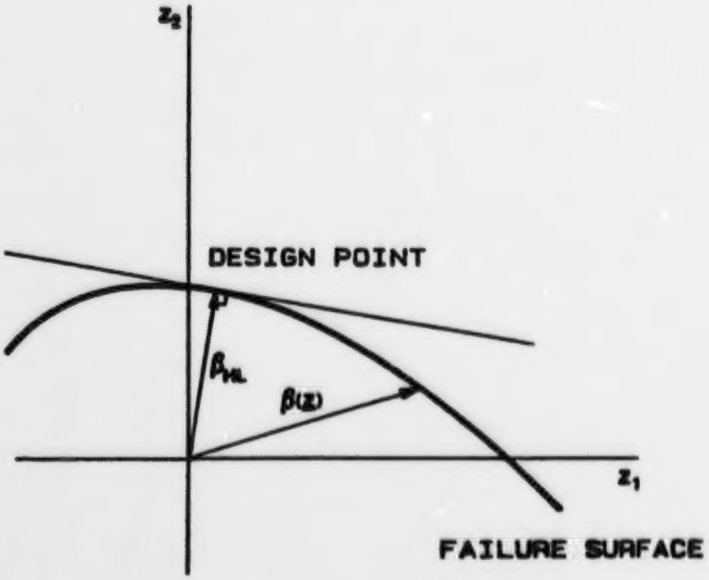

Fig. 3.5 Geometrical Interpretation of the Reliability Index

When the basic quantities are not normally distributed and possibly correlated, the first step in the reliability analysis is the one-to-one transformation of basic quantities $\underline{Z}$ into a set of independent and standardized, normally distributed variables $\underline{U}$, Figure 3.6. It is convenient to define a sensitivity, α_i, of the reliability index at the design point ($\underline{u}^*$) with respect to the basic quantity (u_i) as:

$$\alpha_i = \frac{u_i^*}{\left(\sum_{j=1}^{n} u_j^{*2}\right)^{1/2}} = \frac{u_i^*}{\beta_{HL}} \tag{3.7}$$

where β_{HL} is the Hasofer-Lind reliability index.

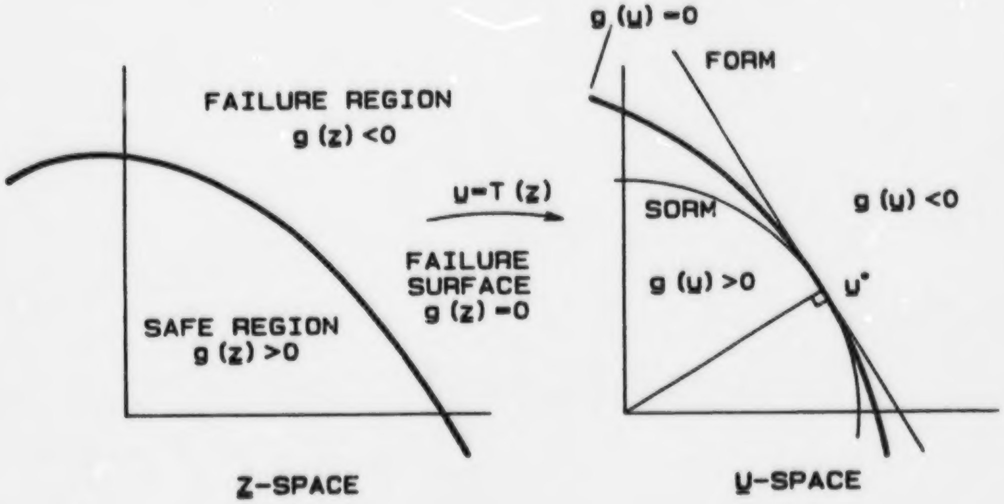

FAILURE REGION
g (z) <0
SAFE REGION
g (z) >0
u=T (z)
FAILURE SURFACE
g (z) =0
g (u) =0
FORM
SORM
g (u) <0
g (u) >0
u*
Z-SPACE
U-SPACE

Fig. 3.6 Transformation from $\underline{Z}$-Space to $\underline{U}$-Space

The sensitivity factors α_i are the directional cosines of the normal to the failure surface at the design point, Figure 3.7, so that:

$$\sum_{i=1}^{n} \alpha_i^2 = 1.$$

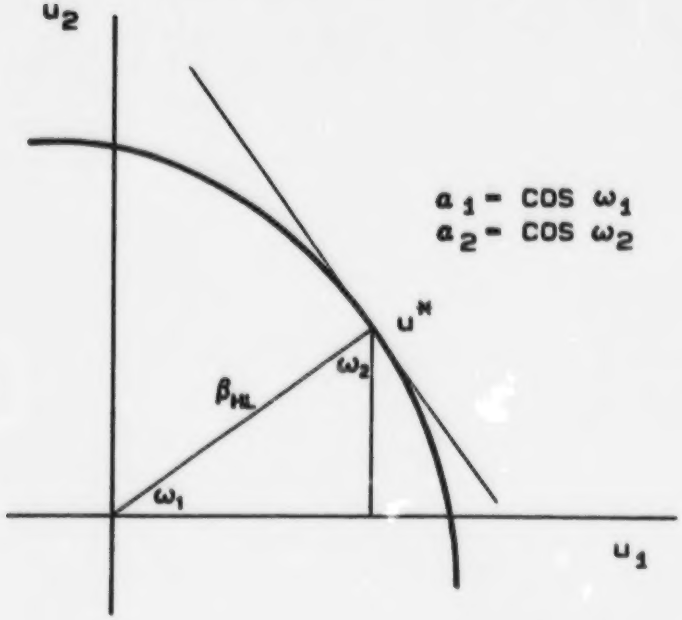

Fig. 3.7 Illustration of Sensitivity Factors

The First-Order Reliability Method (FORM) uses a hyperplane approximation of the failure surface at the design point, Figure 3.6. Correspondingly, the Second-Order Reliability Method (SORM) uses a quadratic approximation of the failure surface. It can be shown that FORM provides a good approximation for most engineering problems, since the major contribution to the failure probability stems from the shaded area in Figure 3.8. This is attributed to the fact that the probability density function of the basic quantities decreases as exp $(-r^2/2)$ with the distance r from the origin (Madsen, Krenk, Lind, 1986). The use of FORM reduces considerably the amount of computational work.

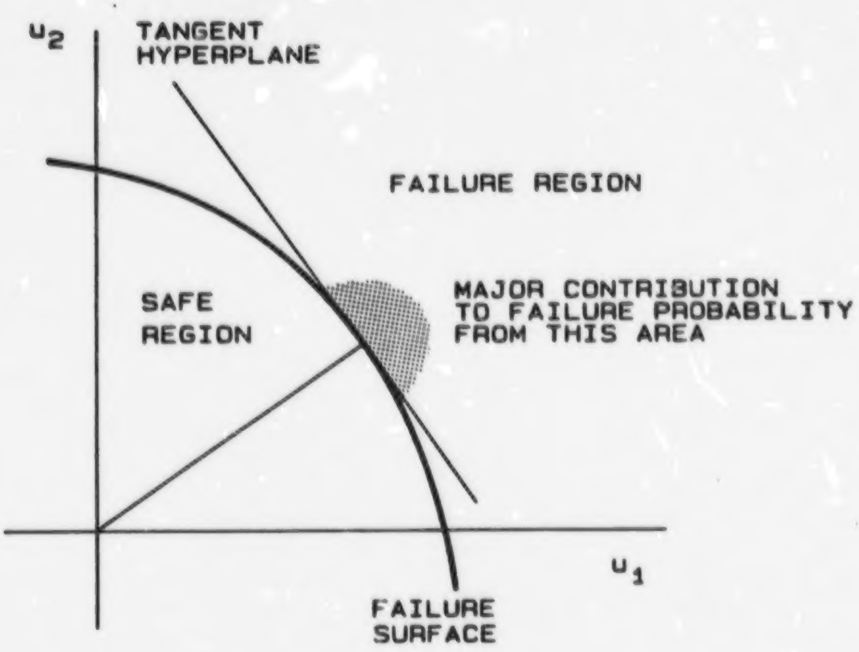
u2
TANGENT HYPERPLANE
FAILURE REGION
SAFE REGION
MAJOR CONTRIBUTION TO FAILURE PROBABILITY FROM THIS AREA
u1
FAILURE SURFACE

Fig. 3.8 FORM Hyperplane Approximation

3.4 Computer Program PROBAN

The computer program PROBAN was developed by DnV with sponsorship by CONOCO and U.S. Coast Guard (Tvedt, 1983a, 1983b). In PROBAN, the following algorithm was implemented (Rackwitz and Fiessler, 1978):

Step 1: Compute the mean and standard deviation of the equivalent normal distributions at the mean $\underline{z}_o$ of the basic distributions. This defines a linear transformation into the iteration space $\underline{u}_o$ that is fixed until the next transformation.

Step 2: Compute the u-space gradient to the limit state (failure) function at the mean of the $\underline{z}$-space distributions. Iterate until an intersection $\underline{u}_o(\underline{z}_1)$ with the surface is found. Set $i = 1$.

Step 3: Compute the mean and standard deviation of the equivalent normal distributions at $\underline{z}_i$. This defines the transformation into the $\underline{u}_i$ space for the next iteration. Compute $\beta_i = \text{sign}(g(\underline{z}_o))\,|\underline{u}_i(\underline{z}_i)|$ in this space.

Step 4: Compute the gradient $\nabla g(\underline{u}_i(\underline{z}_i))$. Define the plane given by $\underline{u}_i(\underline{z}_i)$ and the gradient. Iterate in this plane along the circle with center at the origin and radius $|\beta_i|$ until a second intersection α_s with the surface is found, i.e. solve

$$\underline{u}_i(\alpha) = \underline{u}_i(\underline{z}_i)\cos(\alpha) + \underline{v}_i\sin(\alpha),$$

where $\underline{v}_i$ is the orthogonal projection of $\nabla g(\underline{u}_i(\underline{z}_i))$ onto $\underline{u}_i(\underline{z}_i)$ scaled to the length $|\underline{v}_i| = |\underline{u}_i(\underline{z}_i)|$.

Step 5: Bisect the intersection angle α_s and iterate along the direction $\underline{u}_i(\alpha_s/2)$ until a new intersection with the surface is found. This defines the next iterate i+1.

Step 6: Stop-criteria:

1:

$$|\beta_{i+1} - \beta_i| \le 0.001$$

$$\text{Arccos}\left(\frac{\underline{u}_i \cdot \underline{u}_{i+1}}{|\underline{u}_i|\;|\underline{u}_{i+1}|}\right) \le 0.01$$

2:

$$2\beta_i(1 - \cos_\alpha)\;| \le 0.001$$

$$2\;|\;\alpha\;| \le 0.01$$

where

$$\alpha = \text{Arccos}\left(\frac{\underline{u}_i \cdot \nabla g(\underline{u}_i)}{|\underline{u}_i|\;|\nabla g(\underline{u}_i)|}\,\text{sign}(g(\underline{z}_o))\right).$$

The first criterion must be fulfilled two times in succession, or the second criterion must be fulfilled once. If one of the stop criteria are fulfilled, jump to 7 else jump to 3.

Step 7: Output results:

The iteration procedure applied in the program is a method of steepest descent on the failure boundary, Figure 3.9.

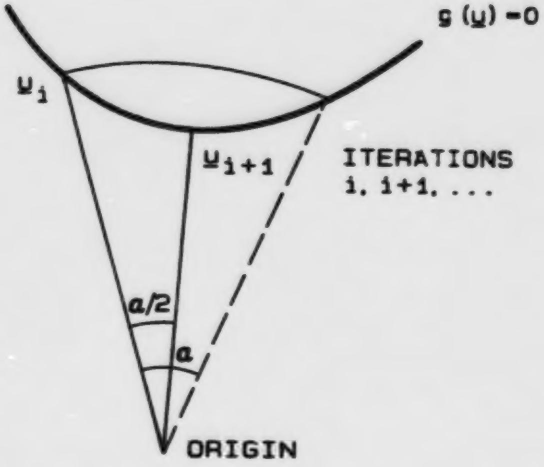

Fig. 3.9 Iteration Along the Failure Surface in the Standardized Normal Space

Presently, the following distributions of basic quantities are implemented in PROBAN:

- normal
- lognormal
- Weibull
- Gumbel
- Longuet-Higgins
- Nolte
- Generalized Gamma

The basic quantities can be independent or correlated. The number of random quantities is limited to 50 which surpasses the needs of most engineering problems. The user defines the failure surface (limit state) function $g(\underline{Z})$ in the user subroutine LIMST which is then compiled and linked to PROBAN, Figure 3.10.

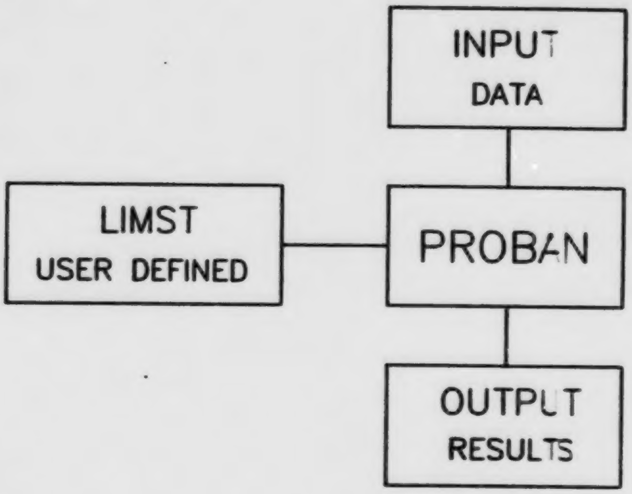

Fig. 3.10 Schematics of Running PROBAN

Appendix 1 lists continuous distributions in the form used for input to PROBAN.

3.5 Targeted Probabilities of Structural Failure

Even though the probabilities of failure obtained from the reliability analysis cannot in general be interpreted in terms of failure frequencies (time independent), it is still of interest to discuss the targeted (acceptable) occurrence of structural failures. Such targets of the probability of failure are implemented implicitly or explicitly in some structural codes (see Introduction), and are based on natural disasters, risks involved in various human activities, and the foreseeable consequences of structural failures. The consequence (a loss) can be divided into four categories: economic loss, damage to theenvironment, injury or death. The risk of death for in Table 3.1 (Madsen, Krenk and Lind, 1986).

Table 3.1

Risk of Death (Source, CIRIA, 1977)

Exposure	Risk of Death per Hour per 10^8 Persons Exposed	Hours of Exposure per Persons Exposed per Year	Risk of Death per 10^4 Exposed Persons per Year	Ratio of Wounded to Number of Deaths
Mountain climbing (international)	2700	100	27	
Trawl fishing (deep sea, 1958-1972)	59	2900	17	
Flying (crew)	120	1000	12	<<1
Coal mining	21	1600	3.3	
Automobile travel	56	400	2.2	20
Construction	7.7	2200	1.7	450
Flying (passengers)	120	100	1.2	<<1
Home accidents	2.1	5500	1.1	
Factory work	2	2000	0.4	
Building fires	0.15	5500	0.08	5
Structural failure	**0.002**	**5500**	**0.001**	**6**

For example, there are no internationally accepted target values for probability of failure in shipping, even though 10^{-4} is often regarded as acceptable (Lindeman, Odland and Strengehagen, 1977). Various authors have proposed formulae for the target values, e.g. Flint and Baker (1977) suggest:

$$P_f = 10^{-4} \frac{K_s}{N_r} N_d, \tag{3.9}$$

where N_d = design life in years;
N_r = number of people at risk; and
K_s = social criterion factor, varying from 5 (hazardous activities) to 0.5 (structures where sanctuary is provided).

If we assign, for example, $K_s = 3$ for Arctic shipping, $N_d = 20$ years and $N_r = 20$ people, the target value for failure probability from Eq. (3.9) is $P_f = 3 \times 10^{-4}$. In Figure 3.11, the risk of various events in terms of fatalities is shown (Boe, Joergensen, Mathiesen, and Røren, 1974).

Offshore steel structures, designed to meet recognized codes, generally have a theoretical probability of failure in the order of 10^{-4} to 10^{-6}. Concrete structures usually fall in the lower part of that range. DnV Rules (1977) for steel members and for the plasticity based analysis (partial material factor of 1.3) target on a probability of failure of about 10^{-6} (Fjeld, 1976). It is argued that targeted risk levels for offshore structures should not be much higher than those accepted for onshore industry.

The failure probabilities (per fatalities per year) can be classified in the following four categories (Fjeld, Andersen and Myklatun, 1978):

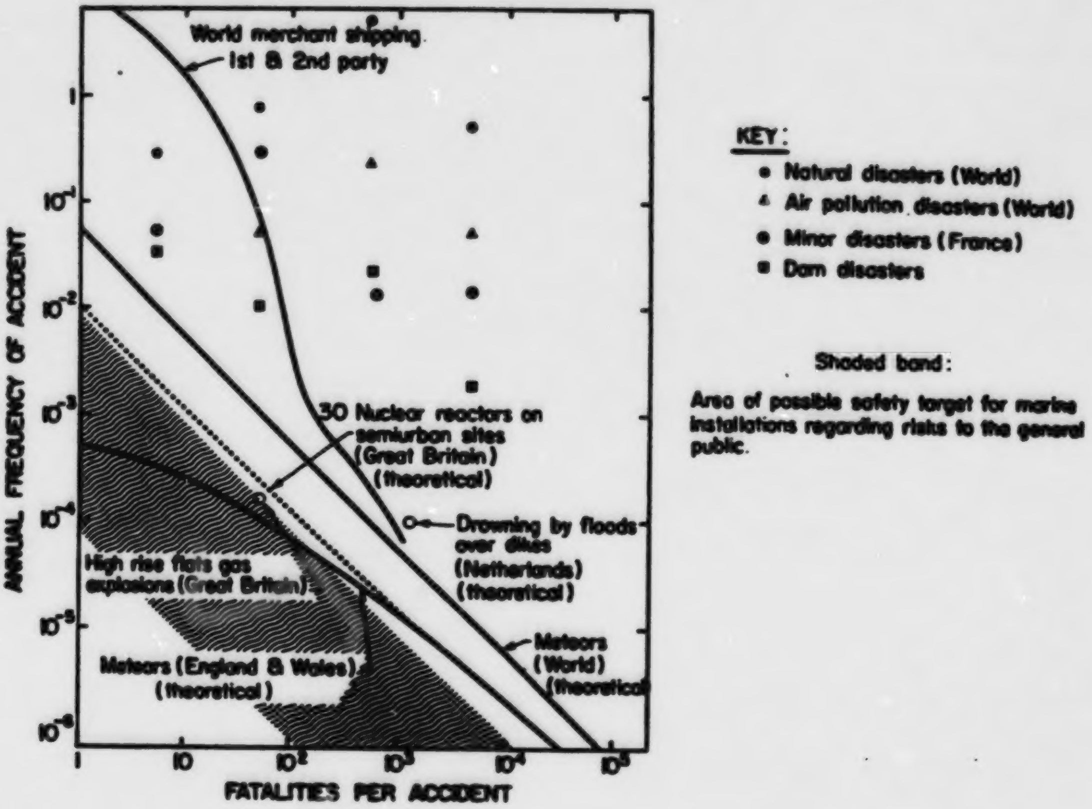

Fig. 3.11 Compiled Data on Accident Frequency and Related Consequences (Fatalities)

$P_f < 10^{-6}$ negligible

$10^{-6} < P_f < 10^{-4}$ low

$10^{-4} < P_f < 10^{-2}$ medium

$P_f > 10^{-2}$ high

The probabilities of failure targets, as implemented in various structural codes, are shown in Table 3.2 (Fjeld, 1976):

Table 3.2

Probability of Failure Targets in Some Codes

Code	Prob. of failure during life	Annual prob. of failure
IMPLICIT PROBABILITIES		
AISC 1969	$3 \cdot 10^{-3}$	10^{-4}
ACI 318 · 71	$9 \cdot 10^{-5}$	$3 \cdot 10^{-6}$
Canadian structural codes	10^{-3}	$3 \cdot 10^{-5}$
EXPLICIT PROBABILITIES		
ECCS general		10^{-5}
dangerous consequences		10^{-6}
CIRIA report 63 Onshore industry		10^{-6} - 10^{-7}
Offshore industry		10^{-4} - 10^{-6}

4. MODES OF STRUCTURAL FAILURE AND STRUCTURAL DETAILS

4.1 Modes of Structural Failure

Modes of failure discussed in this report are related to the damage or collapse of structural components caused by structural demand (defined by loads and geometry considerations) exceeding the load carrying capability/capacity (defined by material properties, geometry and boundary conditions) of a given component.

A component is considered damaged either when its original form has changed (e.g. from local yielding, buckling or appearance of fatigue cracks or short arrested cracks caused by local brittleness) or when material properties have changed adversely during the service of the structure (e.g. strain hardening as a result of permanent local deformations or a local decrease of toughness due to aging or improper repair procedure).

A damaged component may still be capable of sustaining service loads, however, with reduced margins of safety to various failure modes or their combinations and a repair aims at restoring margins of safety to the original design values.

A collapse is induced by severe damage when the margin of safety to any particular failure mode is reduced to zero. For example, this might happen when a fatigue crack reaches a critical size, causing thus unstable fracture of a component or causing buckling instability or plastic collapse due to reduced cross-section of the component.

A large part of all damages in structures having high load-path redundancy such as ships are initiated in brackets, lugs, openings, poor quality welds and other types of local irregularities. The failure modes involved are usually caused by fatigue cracks. Although such failures may have economical consequences, the "fail-safe" concept applies to most of these structures. This means that a certain amount of cracking is accepted. Only for some critical details a "safe-life" approach is justified (prevention of crack initiation).

Figure 4.1 (Odland, 1975) shows modes of failure divided into two categories:

a) those not involving fracture; and
b) those involving fracture.

When there is no experience as to what are the dominant failure modes of a component, all possible modes should be initially considered. This requires a systematic analysis and classification of structural elements according to their geometry and function in the integrated structure as well as to the consequences of their failure.

Both the demand and capability in structural failure calculations depend on random quantities making the margin of safety a random quantity and justifying a probabilistic approach to these calculations. This type of calculation combines structural design with material design into an integrated approach which can be used to design safer and more cost effective structures. Figure 4.2 shows random quantities to be considered in unstable fracture calculations.

4.2 Structural Details

Excellent surveys of ship structural details and their classification were performed by Jordan and Cochran (1978) and Jordan and Knight (1979). More than half a million details were observed, their damage assessed, and placed into twelve detail families, Table 4.1. The total number of configurations was 634. The average failure rate among all the details surveyed was 1.13%.

To model fracture for any structural details, the stress concentration factor along the assumed path of the crack must be known if a stress analysis is to be avoided for each crack configuration. Namely, the stress concentration cause propagation of the initial flaws.

Panel stiffeners (detail Family no. 12) placed third with respect to the failure rate behind beam brackets (Family No. 1) and tripping bracket (Family no. 2) in the second survey (Jordan and Knight, 1979). The structural details used in this project included a simple finite plate, a plate with stiffeners and a T-joint, Figure 4.5.

TABLE 4.1

Distribution of Detail Configurations

Detail Family Number	Detail Family	Number of Groups	Number of Configurations
1	Beam Brackets	14	145
2	Tripping Brackets	3	82
3	Non-tight Collars	3	49
4	Tight Collars	4	33
5	Gunwale Connections	2	21
6	Knife Edges	0	0
7	Miscellaneous Cutouts	8	72
8	Clearance Cutouts	5	39
9	Deck Cutouts	3	23
10	Stanchion Ends	3	94
11	Stiffener Ends	5	35
12	Panel Stiffeners	6	41
12	TOTAL	56	634

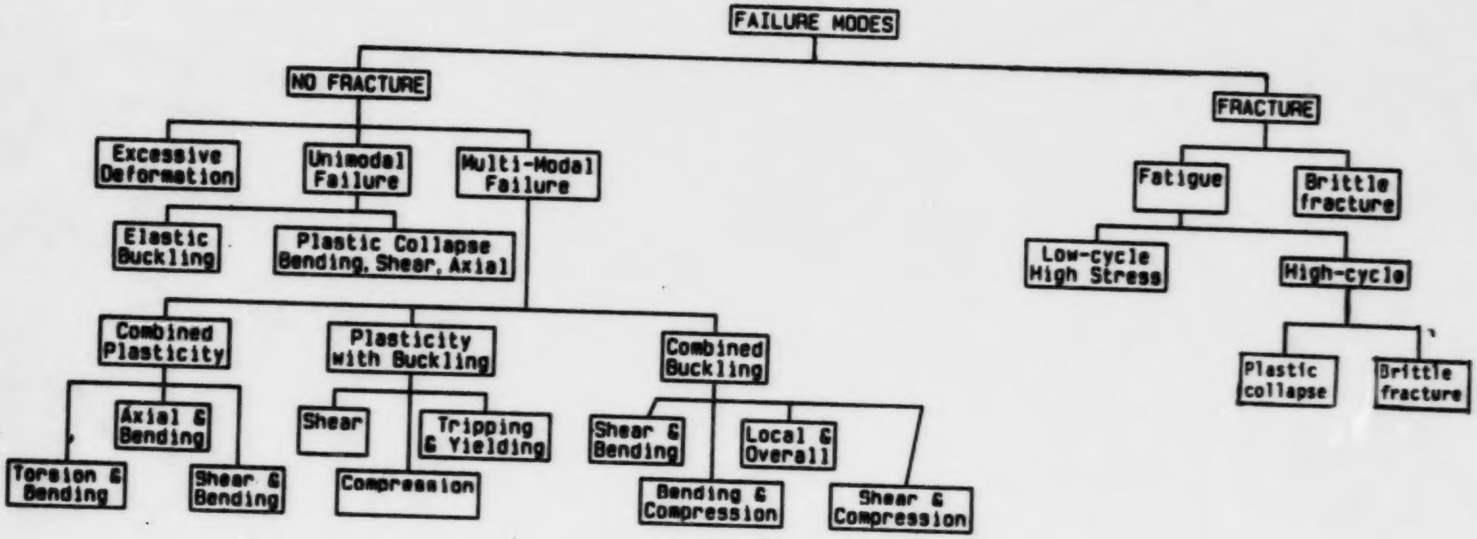
FAILURE MODES
NO FRACTURE
FRACTURE
Excessive Deformation
Unimodal Failure
Multi-Modal Failure
Elastic Buckling
Plastic Collapse Bending, Shear, Axial
Combined Plasticity
Plasticity with Buckling
Combined Buckling
Torsion & Bending
Axial & Bending
Shear & Bending
Shear
Compression
Tripping & Yielding
Shear & Bending
Bending & Compression
Local & Overall
Shear & Compression
Fatigue
Brittle fracture
Low-cycle High Stress
High-cycle
Plastic collapse
Brittle fracture

Figure 4.1: Failure Modes

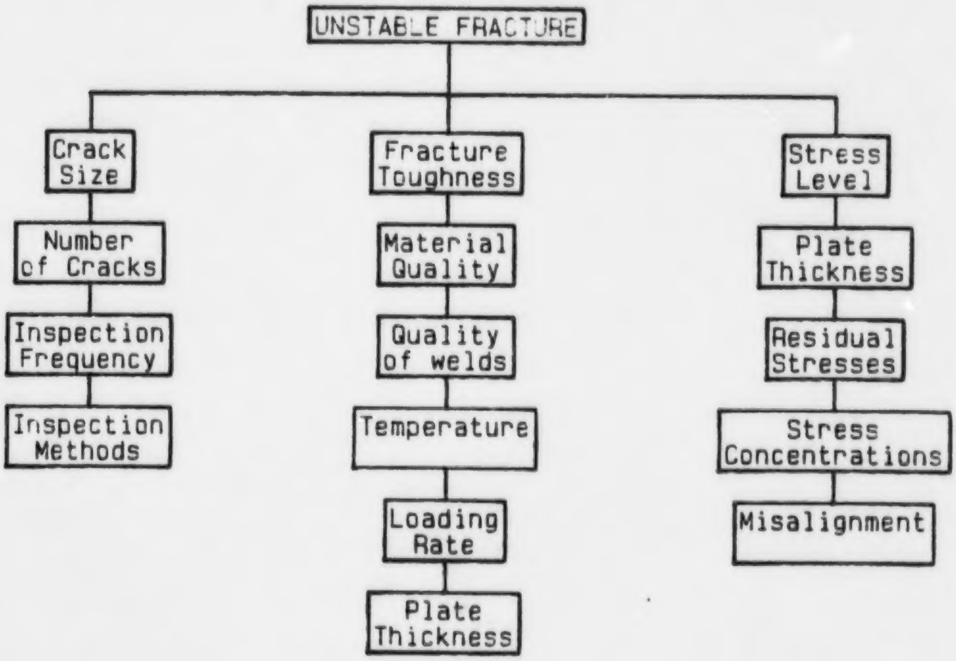
UNSTABLE FRACTURE
Crack Size
Number of Cracks
Inspection Frequency
Inspection Methods
Fracture Toughness
Material Quality
Quality of welds
Temperature
Loading Rate
Plate Thickness
Stress Level
Plate Thickness
Residual Stresses
Stress Concentrations
Misalignment

Figure 4.2: Random Quantities Considered for Unstable Fracture

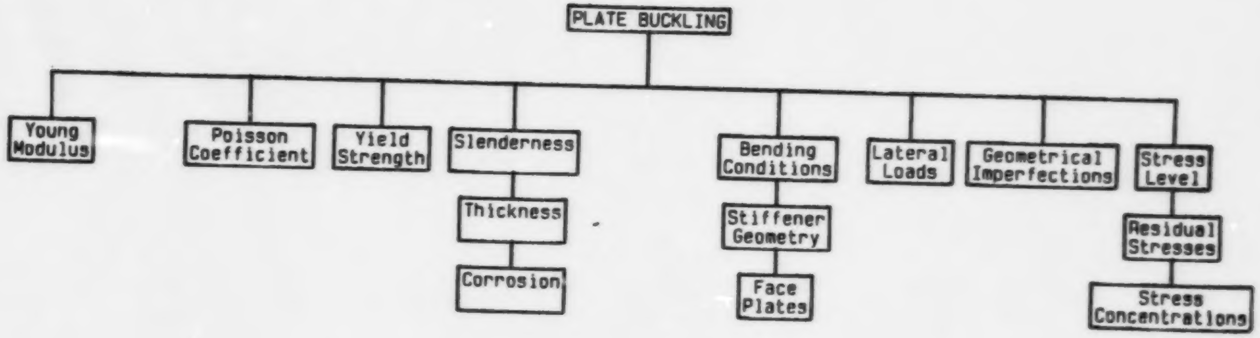
PLATE BUCKLING
Young Modulus
Poisson Coefficient
Yield Strength
Slenderness
Thickness
Corrosion
Bending Conditions
Stiffener Geometry
Face Plates
Lateral Loads
Geometrical Imperfections
Stress Level
Residual Stresses
Stress Concentrations

Figure 4.3: Random Quantities Considered for Plate Buckling

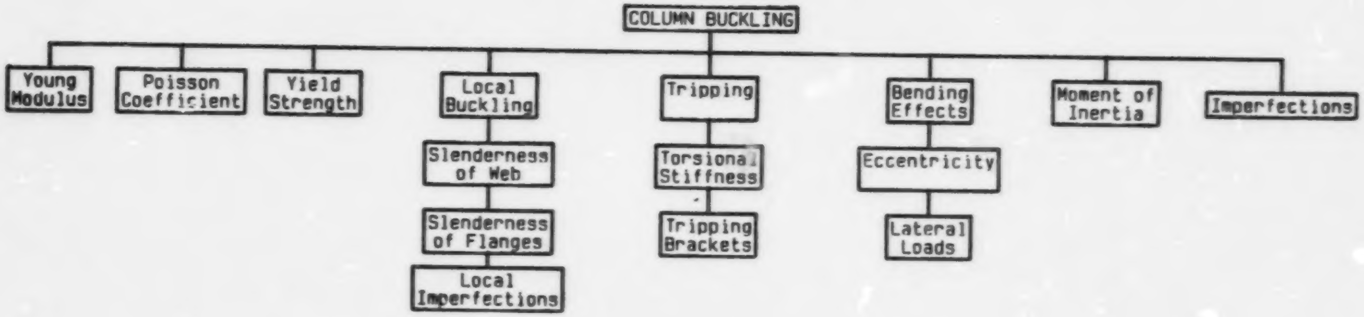
COLUMN BUCKLING
Young Modulus
Poisson Coefficient
Yield Strength
Local Buckling
Slenderness of Web
Slenderness of Flanges
Local Imperfections
Tripping
Torsional Stiffness
Tripping Brackets
Bending Effects
Eccentricity
Lateral Loads
Moment of Inertia
Imperfections

Figure 4.4: Random Quantities Considered for Column Buckling

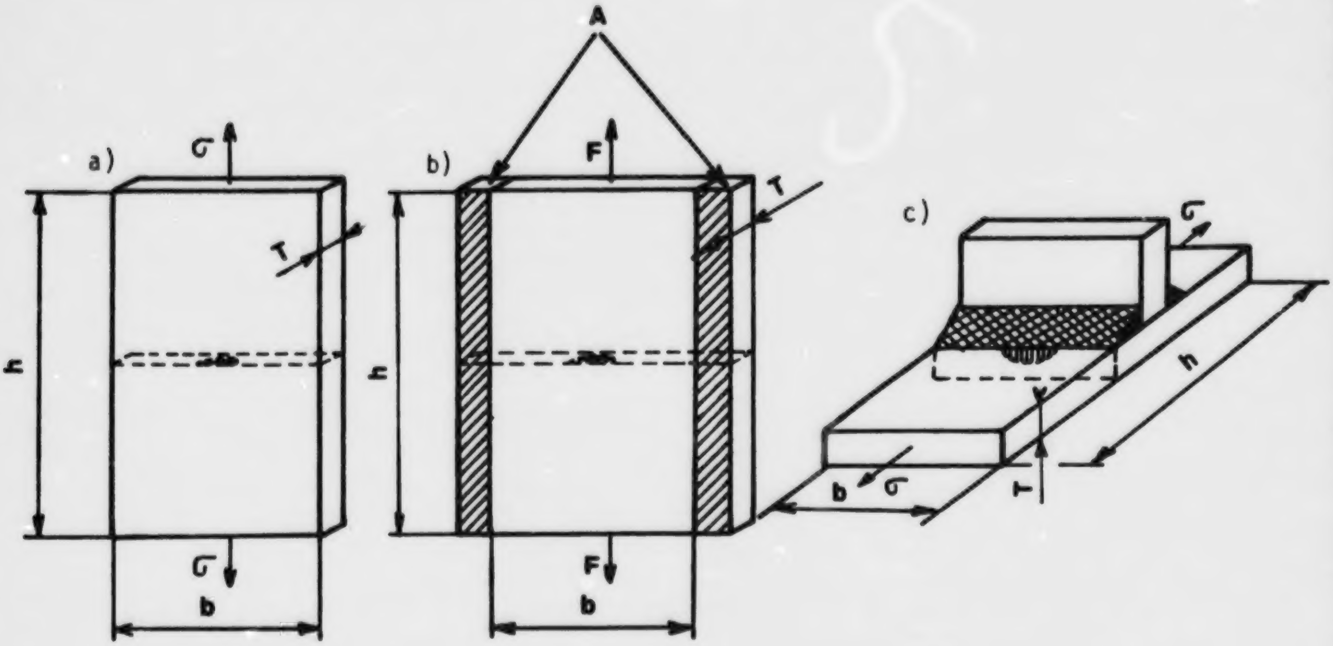

Figure 4.5: Structural Details Used in the Analysis a) simple plate; b) plate with stiffeners; and c) T-joint

b: width of the plate
h: height of the plate
T: thickness of the plate
A: section area of the stiffener
σ: far-away stress
F: force equivalent to σ

5. DEVELOPMENT OF FAILURE MODELS

This study is concerned with an assessment of failure modes of structural components affected by fatigue crack growth, see Figure 4.1. The following modes are considered in detail:

a) Brittle/unstable fracture
This type of failure occurs when the combination of crack size (initial or propagated crack), applied stresses and other factors will produce a fracture demand which is greater than fracture capacity of the component.

b) Plastic collapse
Due to the initial defect and fatigue crack growth, the effective cross section area of a structural component reduces which may cause global yielding of the component.

The overall performance of a component may be defined as a combination of the above two failure modes as follows:

- Collapse - this is defined as a failure of a component either in failure mode (a) or (c), i.e. unstable fracture and plastic collapse respectively. Thus the collapse failure criterion is a union of the first and second type of failure events.

- Serviceability - this is defined as the failure of a component to provide a minimum requirement, i.e. failure of the component in failure mode (a).

5.1 Modelling Unstable Fracture

The unstable fracture criterion can be formulated differently, depending on how the resistance to fracture (fracture toughness) is measured. Fracture toughness may be given in terms of a critical stress intensity factor, in terms of a critical CTOD or a critical J-integral. The CEGB or CERL fracture assessment diagram (also called R6 failure assessment diagram) can be used for an assessment of combined unstable fracture and plastic collapse failures (Ingham and Harrison, 1981). In this study, the CDOD criterion was considered.

5.1.1 The Stress Intensity Factor Approach

This approach is used when the component is likely to fail in a brittle manner (the local plastic zone at the crack tip must be small relative to the crack size and other governing dimensions such as thickness). The handbook of stress intensity factors (Rooke and Cartwright, 1976) gives the ratios K/Ko where Ko is the normalizing stress intensity factor for the basic configuration and for which loading on boundaries are far away from the crack $K_o = \sigma \sqrt{\pi}\, a$. The ratio of K/Ko thus reflects the effect of the closeness of geometrical boundaries on the stress state at the crack tip and is often called the geometry function F, see Section 6.3.3. When the resultant function F is not readily available, different influences affecting K might be separated and the resultant stress intensity factor composed from these individual factors. Thus, K might be conveniently expressed as (e.g. Almar-Naess, 1985).

$$K = FK_o = F_E \cdot F_S \cdot F_T \cdot F_W \cdot F_G \cdot K_o \tag{5.1}$$

where:

F_E = basic crack shape factor
F_S = front face factor
F_T = back face or finite thickness factor
F_W = finite width factor
F_G = stress gradient factor

The stresses to which the crack is exposed must include the effect of stress concentrations, the residual stress and any dynamic stresses acting on the structural component. The resultant stress can be written as

$$\sigma = SCF(\sigma_o + S/2) + \sigma_{res} \qquad (5.2)$$

where:

SCF is the stress concentration factor
σ_{res} is the residual stress
S is the stress range (peak to trough).
σ_o normial stress (for field)

The residual stress component $_{res}$ can be expressed as a fraction of the yield strength σ_y

$$\sigma_{res} = C_r \sigma_y \qquad (5.3)$$

where the factor C_r is in the range $<0,1>$ depending on whether these stresses were eliminated during the post-weld heat treatment (PWHT). In the former case, it is common to assume $C_r = 1$ and in the stress relieved case $C_r = 0$. These are, however very idealized assumptions. In reality the value of C_r depends on the thickness and plate dimensions as well as the quality of the heat treatment. This will be discussed in more detail in Chapter 6.

The margin of safety for unstable crack propagation in the stress intensity factor formulations can be written as

$$M_{1k} = K_{Ic} - K \qquad (5.4)$$

where K_{Ic} is the critical stress intensity factor (fracture toughness) which is a material property and depends, among other factors, on thickness, temperature and rate of loading (strain rate).

Expressing the critical flaw size a_c as a function of K_{Ic}, and F, the safety margin can be rewritten in terms of crack demand and crack capacity as

$$M_{1a} = a_{1c} - a \tag{5.5}$$

where a is the initial or propagated crack size which will be obtained from the crack growth model (Section 5.3) or in a special case, a can be a crack size discovered during an inspection. The latter case is interesting, because having the crack size information (crack size distribution) and knowing that the structure did not collapse by unstable fracture, it is possible to assess the structural redundancy of the structure. This will be the case of large tankers (Antoniou, 1977) which will be considered later in this report.

For the rectangular plate with crack, Eq. (5.5) can be written as

$$M_{1a} = \frac{1}{\pi} \left(\frac{K_{Ic}}{F\sigma}\right) - a \tag{5.5a}$$

and for the plate with stiffened edges and centrally located crack (see Section 6.3.3)

$$M_{1a} = \frac{1}{\pi} \left(\frac{K_{Ic}}{F \frac{P}{2bt}}\right)^2 - a \tag{5.5b}$$

where t is the thickness of the plate and 2b is the plate width.

5.1.2 Crack Tip Opening Displacement (CTOD) Approach

The crack tip opening displacement approach was developed (Burdekin and Dawes, 1971) to account for a significant amount of plasticity associated with unstable crack propagation in materials demonstrating high levels of fracture toughness. The CTOD design curve, Figure 5.1, relates the strains surrounding the crack tip to the dimensionless CTOD defined by

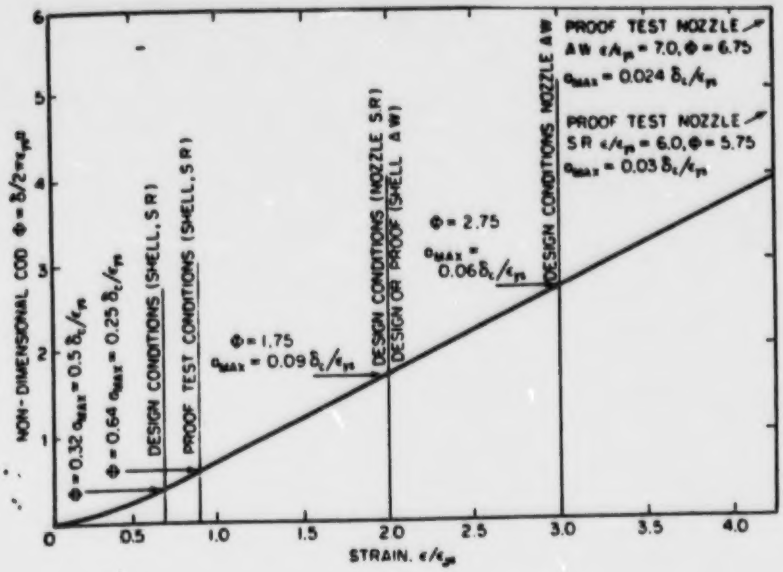

Fig. 5.1 CTOD Design Curve

$$\Phi = \sigma/\sigma_y - 0.25 \text{ for } \sigma/\sigma_y > 0.5 \tag{5.8a}$$

When the actual configuration differs significantly from that of the infinite plate with a through-thickness crack, an equivalent crack size of equal severity must be found and used for the CTOD design. This is conveniently done by assuming that the equivalent through-thickness crack in an infinite plate would produce the same stress intensity at its crack tip as the one considered.

Equating the stress intensity factor $K = F\,\sigma\sqrt{\pi a_f}$ for the rectangular plate of finite dimensions with a crack of dimension a_f to the stress intensity factor of the infinite plate with a crack for which $K_o = \sigma\sqrt{\pi a_\infty}$, the equivalent crack size is given by

$$a_\infty = F^2 a_f \tag{5.9}$$

$$\phi = \frac{\delta_c}{2\pi\varepsilon_y a_\infty} \tag{5.6}$$

where:

δ_c is the critical CTOD obtained from the CTOD tests (BS 5762, 1979)

ε_y is the yield strain and

a_∞ is the allowable size (half length) of the through thickness crack in a wide (infinite) plate loaded in tension.

Based on the original experimental data obtained from wide plate tests, the design curve is defined by

$$\phi = (\varepsilon/\varepsilon_y)^2 \text{ for } \varepsilon/\varepsilon_y \leq 0.5 \tag{5.7}$$

and

$$\phi = \varepsilon/\varepsilon_y - 0.25 \text{ for } \varepsilon/\varepsilon_y > 0.5 \tag{5.8}$$

The PD 6493 (1980) recommends the use of the CTOD approach for stresses (including residual component) not exceeding $3\sigma_y$. For higher stresses, a full elastic-plastic analysis should be carried out. It is assumed that the Hooke's law can be used to express stresses in term of strains in Eqs. 5.6, 5.7 and 5.8, obtaining thus

$$\phi = \frac{\delta_c E}{2\pi\sigma_y a_\infty} \tag{5.6a}$$

and

$$\phi = (\sigma/\sigma_y) \text{ for } \sigma/\sigma_y \leq 0.5 \tag{5.7a}$$

Similarly, for the sheet with stiffened edges containing a crack, the equivalent crack size is given by

$$a_\infty = F^2 (1 + s)^2 a \tag{5.10}$$

where $s = E_2 A/(E_1 bt)$ is the relative stiffness (A is cross-sectional area of one stiffener, E_1 and E_2 are Young's modulae of the plate and stiffener respectively, t is thickness of the plate and $2b$ is the width, see Figure 6.28).

The appropriate equivalent allowable crack size a_∞ is then to be substituted in the expression for the dimensionless CTOD, Eq. 5.6a to arrive at the allowable crack sizes for the above two cases as follows:

Rectangular sheet

$$\begin{aligned} a_f &= \frac{\delta_c E \sigma_y}{2\pi F^2 \sigma^2} \qquad \text{for} \qquad \sigma/\sigma_y \leq 0.5 \\ a_f &= \frac{\delta_c E}{2\pi \sigma_y F^2 (\sigma/\sigma_y - 0.25)} \qquad \text{for} \qquad \sigma/\sigma_y > 0.5 \end{aligned} \tag{5.11}$$

Stiffened plate

$$\begin{aligned} a_f &= \frac{\delta_c E \,\sigma_y}{2\pi F^2 (1 + s)^2 \sigma_s^2} \qquad \text{for} \qquad \sigma_s/\sigma_y \leq 0.5 \\ a_f &= \frac{\delta_c E}{2\pi \sigma_y F^2 \,(1 + s)^2 (\sigma_s/\sigma_y - 0.25)} \qquad \text{for} \qquad \sigma_s/\sigma_y > 0.5 \end{aligned} \tag{5.12}$$

where σ for plain rectangular sheet is given by Eq. 5.2 and σ_s for the stiffened plate is given by

$$\sigma_s = \frac{SCF}{2bt(1 + s)} (P + \Delta P/2) + \sigma_{res} \qquad (5.13)$$

where P is the static force (see Figures 5.2 and 5.3), ΔP is the dynamic range of the force, b is the width of the sheet and t is the thickness.

The CTOD design curve was chosen so as to provide safety against unstable crack propagation so the crack size in Eq. 5.6a is an allowable crack size rather than the critical crack size. To use the CTOD design approach for evaluation of the probability of unstable crack propagation, the margin of safety must be expressed in terms of the critical crack size a_c

$$a_{1c} = I_a \, a_{a\ell} \qquad (5.14)$$

where:

$a_{a\ell}$ is the allowable crack size obtained from the CTOD design curve (Eqs. 5.11 and 5.12).

I_a is the safety factor built into the CTOD design curve.

5.2 Modelling Plastic Collapse

The third failure mode considered is plastic collapse. The critical crack size in this case is obtained from the general yielding of the structural component. Due to the initial defect or due to propagated crack, the effective cross section reduces which may lead to plastic yielding of the material. Thus the safety margin against plastic collapse may be written as

$$M_2 = \sigma_y - \sigma_{eff} \qquad (5.15)$$

where σ_y is the yield strength of the material and σ_{eff} is the effective stress at the cross section containing the crack. Assuming a uniform plastification of the remaining cross section area (2b - 2a) under a far field stress σ_o, the effective stress is given by

$$\sigma_{eff} = \sigma_o \left(\frac{b}{b - a}\right) \tag{5.16}$$

Substituting now $\sigma_{eff} = \sigma_y$ into Eq. 5.16, the critical crack size which would cause plastic collapse is given by

$$a_{2c} = b(1 - \sigma/\sigma_y) \tag{5.17}$$

and the safety margin can be rewritten as

$$M_{2a} = a_{2c} - a \tag{5.18}$$

where a is again the initial or propagated crack size or a crack size discovered during an inspection.

5.3 Modelling Fatigue Crack Propagation

The two failure criteria above can be expressed in terms of the corresponding margins of safety (Eqs. 5.5 and 5.18) in the following generalized form

$$M_{ia} = a_{ic} - a \qquad i = 1, 2 \tag{5.19}$$

where failure in the i-th failure mode occurs when $M_i < = 0$. Thus the size of a crack plays an important role in both failure modes.

In various components of structures exposed to dynamic loading (such as ships), fatigue cracks may develop and propagate during the life of the structure.

In the linear fracture mechanics approach, based on Paris and Erdogan (1963) relation, the crack growth rate is governed by the stress intensity factor range as follows:

$$da/dN = C(\Delta K)^m \tag{5.20}$$

where a is the crack size, N is the number of stress (load) cycles and C and m are the crack growth parameters which depend on material and on the environment.

The stress intensity factor range can be expressed as

$$\Delta K = FS\sqrt{\pi a} \tag{5.21}$$

where S is the stress range given by the dynamic far field stress component $\Delta\sigma$ or by the load fluctuations ΔP in which case $S = \Delta P/2bt$.

The crack propagation equation can be then expressed as

$$da/dN = CF^m S^m (\sqrt{\pi a})^m \tag{5.22}$$

The time (number of cycles) to failure (i.e. fatigue life) N_f may be divided into a crack initiation period N_o and a crack growth period N_p so that

$$N_f = N_o + N_p \tag{5.23}$$

The crack growth period, N_p, can then be calculated as

$$N_p = N_f - N_o = \int_{N_o}^{N_f} dN = \int_{a_o}^{a_f} \frac{da}{da/dN} \tag{5.24}$$

where a_o is the initial and a_f is the final crack size respectively. Substituting from Eq. 5.22 into Eq. 5.23 results in

$$N_p = \int_{a_o}^{a_f} \frac{da}{CF^mS^m \ (\sqrt{\pi a})^m} \tag{5.25}$$

For a constant amplitude loading (S = const) and for constant crack growth parameters C and m, the previous equation can be rewritten as

$$N_p = \frac{1}{CS^m} \quad \int_{a_o}^{a_f} \frac{da}{(F \ \sqrt{\pi a})^m} \tag{5.26}$$

It is convenient to introduce a new function (Madsen et al, 1986)

$$\psi(a_f) = \int_{a_o}^{a_f} \frac{da}{(F\sqrt{\pi a})^m} \tag{5.27}$$

where a is the integration variable. It is appropriate to call this function damage capacity. a_f is the critical crack size (crack capacity). The damage function monotonically increases with a_f. Thus the greater the critical crack size, the higher the damage capacity.

Substituting Eq. 5.27 into Eq. 5.26, the fatigue crack growth period for a crack of size a_o to reach size a_f is then

$$N_p = \frac{\psi(a_f)}{CS^m} \tag{5.28}$$

It is convenient to formulate various probability statements in terms of cycles to failure, N_f. The probability of failure after N-th cycle is obtained as

$$P_f = P\,(N_f \ <= N\ ) \tag{5.29}$$

Substituting for N_f from Eq. 5.23 and for N_p from Eq. 5.28, the failure probability can be expressed as

$$P_f = P(N_o + N_p < = N) = P(\{\Psi(a_f) - (N-N_o)CS^m\} < = 0) \tag{5.30}$$

Thus, using the general definition for the two margins of safety (Eq. 5.19), it is

$$M_i = \Psi(a_{if}) - CS^m (N - N_o) \qquad i = 1,2 \tag{5.31}$$

In the presence of welds when initial flaws are present, the initiation period is neglected and it is assumed that $N_o = 0$.

The failure crack size (crack capacity), a_{if}, is given for the two failure modes as follows:

1. Unstable fracture:

$a_{1f} = a_{1c}$ given by Eq. 5.14 for CTOD

2. Plastic collapse:

$a_{2f} = a_{2c}$ given by Eq. 5.18

It should be noted that safety margins given by Eq. 5.31 in terms of the damage capacity function, which in turn is a function of critical crack size for each failure mode, are extensions of safety margins given by Eq. 5.20. The formulation given by Eq. 5.31 is preferable, since in this formulation the fatigue crack growth is taken into account directly, whereas the safety margins given by Eq. 5.21 are for a given crack size which is to be obtained from fatigue crack growth calculations.

5.4 Combined Probability of Failure (Serviceability)

The probability of a combined failure is a probability that either unstable fracture or plastic collapse occur. The probability of failure (serviceability criterion) is then given by the combined probability of the two events, i.e.

$$P_f = P\,(M_1 \leq 0 \cup M_2 \leq 0) \tag{5.32}$$

where M_1 and M_2 represent the margin of safety against unstable fracture and plastic collapse respectively.

5.5 Modelling Crack Arrest

Assume a given crack distribution in a plate with crack arresters (stiffeners). The probability that the structural element will fail is given by

$$P_f = P_{fp} \cdot P_{fs|fp} \tag{5.33}$$

where P_{fp} is the probability that the assumed crack size causes an unstable crack propagation in the plate; and

$P_{fs|fp}$ is the probability that a crack will propagate through the crack arrestors given it propagated already through the plate.

The conditional probability $P_{fs|fp}$ can be obtained by using a deterministic crack size of the size 2b (see Figure 6.28) in the margin of safety against unstable crack propagation.

The probability that a crack which propagated through the plate will get arrested by the crack arrestors, P_a, is then given by

$$P_a = 1 - P_{fs|fp} \tag{5.34}$$

5.6 Summary of Modelled Cases

Table 5.1 lists routine names for all the models developed. The cases are divided into two major groups - (1) simple plate; and (2) stiffened plate. Each group is divided into three subgroups - (a) through-thickness crack propagation; (b) crack size given (no crack propagation); and (c) surface crack propagation. Within each subgroup, three limit state functions are defined: (i) CTOD; (ii) critical crack size and (iii) plastic collapse.

Table 5.1

Names of Limit State Function Routines

Simple Plate	Stiffened Plate	
CTOD	SCTOD	Through-Thickness Crack Propagation
CRTCK	SCRCK	
COLPS	SCLPS	
CTODI	STOI	Crack Size Given
CRTCI	SCRCI	
COLPI	SCLPI	
CTODS	SCTSI	Surface Crack Propagation
CRTCS	SCRSI	
COLSS	SCLSI	

6. PROBABILISTIC MODELLING OF INPUT RANDOM QUANTITIES

The use of the probabilistic approach to the limit state analysis requires a representative statistical data base for each random quantity which affects the limit state function (margin of safety). The statistical data for the input quantities (basic variables) is commonly approximated by one of the existing distributions which is then used as an input to PROBAN (see Section 3).

In this Section, the data, to be used in this study for individual input quantitites introduced in the models developed in Section 5, is presented and approximated through appropriate continuous probability distributions.

6.1 Fracture Toughness

As was already concluded in the previous probabilistic study (Tomin and Lantos, 1986), the probability of fracture at low temperatures becomes most sensitive to fracture toughness due to its transition character. This fact became apparent in early fifties and led to intensive studying of this material property for structural materials when fracture mechanics was developed as a tool for designing against fracture.

The resistance of structural materials to fracture (fracture toughness) can be measured in many different ways, such as K_{Ic} (critical stress intenstiy factor in the crack-opening mode in plane-strain state), J_{Ic} (critical value of the J-integral in the crack-opening mode in plane-strain state), δ_c (critical value of the crack-tip-opening-displacement) or CVN (Charpy V-Notch toughness). Even though CVN cannot be readily quantified for use in fracture models, it has a widespread application as a quality control tool for selection of materials for low temperatures.

Fracture toughness, besides being strongly dependent on the test temperature, is also a function of thickness and strain rate and these effects will be also a subject of this study. The dependence of fracture toughness on thickness is usually studied in the range between plane stress and plane strain states, Figure 6.1.

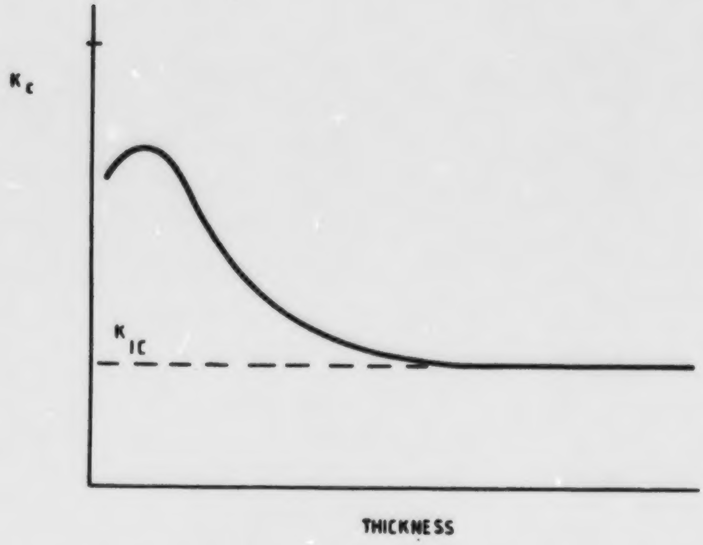

Fig. 6.1 Variation of Fracture Toughness with Thickness

Also, fracture toughness shows high anisotropy and its value can vary considerably depending on the orientation of the specimen with respect to the direction of rolling. Here, two orientations are investigated: T-L (low toughness) and L-T (high toughness), Figure 6.2.

For crack arrest models, the quantity K_{ca} (resistance of material to fast running crack) will be used.

6.1.1 Fracture Toughness Data

The effort in this study is aimed at studying application of ship hull steel Grades A, D and E36, (which are medium to high strength, carbon-manganese steels) to low temperatures.

This class of steels is broadly used in the shipping and offshore industry and the fabrication practices are well established. Unified requirements for these steels were

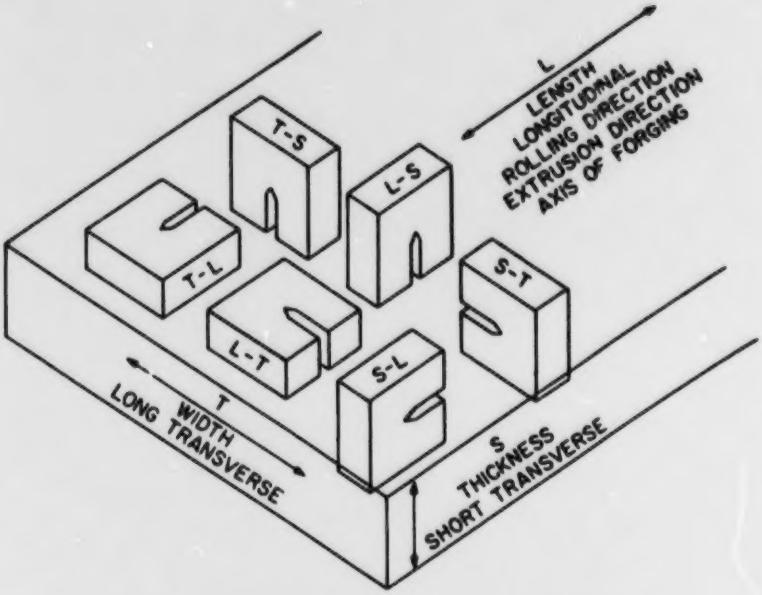
T-S
L-S
T-L
L-T
S-L
S-T
L
LENGTH
LONGITUDINAL
ROLLING DIRECTION
EXTRUSION DIRECTION
AXIS OF FORGING
T
WIDTH
LONG TRANSVERSE
S
THICKNESS
SHORT TRANSVERSE

Fig. 6.2 Notation for Specimen Orientation

adopted by Classification Societies (IACS, 1979) minimizing the differences between the steels approved by individual Classification Societies and produced by different steel manufacturers.

It is important to study limitations of the use of these steels with respect to their application for structures intended for service in the Canadian Arctic.

For this study, a data base generated for ship steels certified to DnV requirements, i.e. NVA, NVD and NVE 36 was used. This experimental data base was developed at DnV through a joint DnV/NTNF program (Saether, 1980; Larsson et al, 1983a and Melve et al, 1983). The chemical composition of these steels is given in Table 6.1.

The data is presented in Appendix 2. Tables A2.1 to A2.3 list the static CTOD values for Grades A (NVA), D (NVD) and E 36 (NVE 36) in T-L and L-T specimen orientations respectively. The dynamic CTOD data is given in Table A2.4 (Grade A), Table A2.5 (Grade D) and Table A2.6 (Grade E 36).

Table 6.1
Chemical Composition and Characterisation of the Examined Steel Plates

Quality	C%	Si%	Mn%	P%	S%	Ni%	Cr%	Al%	N%
NVA	0.12	0.16	0.48	0.017	0.021	$<$ 0.02	$<$ 0.02	$<$ 0.005	0.007
NVD	0.16	0.28	0.89	0.022	0.027	$<$ 0.02	$<$ 0.02	0.009	0.008
NVE 36	0.14	0.20	1.46	0.010	0.014	0.02	$<$ 0.02	0.044	0.007

NVA:	Hot rolled, ferritic-pearlitic structure, grain size ASTM 5-6.
NVD:	Normalized, ferritic-pearlitic structure, grain size ASTM 7-8.
NVE 36:	Normalized, ferritic-pearlitic structure, grain size ASTM 9.

The fracture toughness values (K_{Ic}) for Grades A, D and E 36 are given in Tables A2.7 to A2.9. The crack arrest stress intensity factor, K_{Ia}, for Grade E 36 in the temperature range - 30° to - 40°C is given in Table A2.10.

The Charpy V-Notch energy is tabulated in Tables A2.11 (Grade A), A2.12 (Grade D) and A2.13 (Grade E 36).

The critical CTOD as a function of the strain rate is tabulated in Table A2.14 (Grade A, orientation T-L), Table A2.15 (Grade A, orientation L-T), Table A2.16 (Grade D, orientation T-L), Table A2.17 (Grade D, orientation L-T), Table A2.18 (Grade E 36, orientation T-L) and Table A2.19 (Grade E 36, orientation L-T). The strain rate range covered is approximately from 10^{-4} sec^{-7} (static CTOD) to 10^{1} sec^{-1} (dynamic CTOD).

6.1.2 Modelling Fracture Toughness vs Test Temperature

There were several attempts to model the transitional behaviour of fracture toughness as a function of test temperature.

Oldfield (1975) used a hyperbolic tangent function for the nonlinear regression which modelled constant value lower and upper toughness shelves.

The variability of fracture toughness measured in experiments for different temperatures and thicknesses have been rigourously analysed by Tyson and Marandet (1988) and by Faucher and Tyson (1988).

For this project, the algorithm developed at Battelle by Bishop et al (1983), was used. Bishop assumed that the randomness in fracture toughness can be modelled at any temperature using Weibull's two-parametric distribution. Details of the algorithm are described in the unpublished report by Bishop et al (1985).

Critical CTOD

Figures 6.3, 6.4 and 6.5 show 5-, 50- and 95-pct curves for the static critical CTOD and for A (T-L, L-T), D(T-L, L-T) and E 36 (T-L, L-T) Grades respectively.

Tables 6.2, 6.3 and 6.4 list the Weibull parameters for static CTOD for Grades A, D and E 36 respectively.

Table 6.2

Weibull Parameters for Static CTOD Grade A

Temp.	Orientation	T-L	Orientation	L-T
°C	ALPHA	BETA	ALPHA	BETA
0	2.001	4.216	0.00956	8.027
- 10	2.664	4.227	0.158	6.791
- 30	13.172	4.250	14.524	4.860
- 50	545.89	4.273	189.71	3.4779

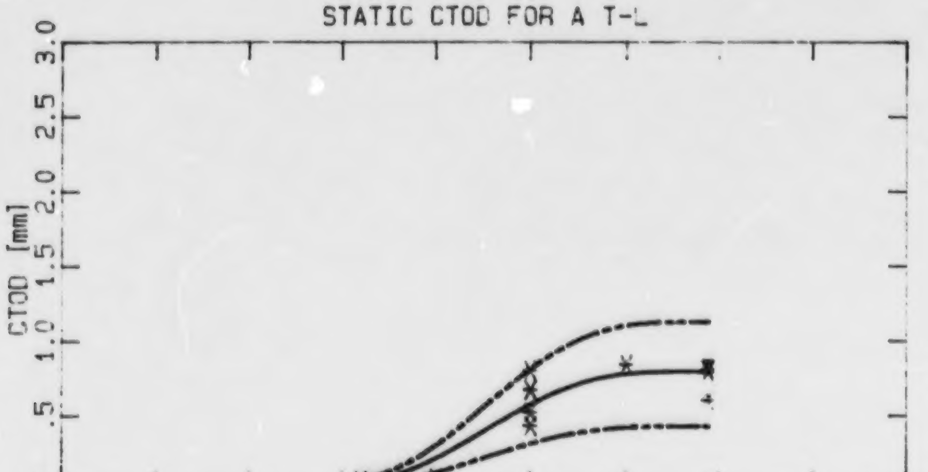

Figure 6.3 Static CTOD for Grade A

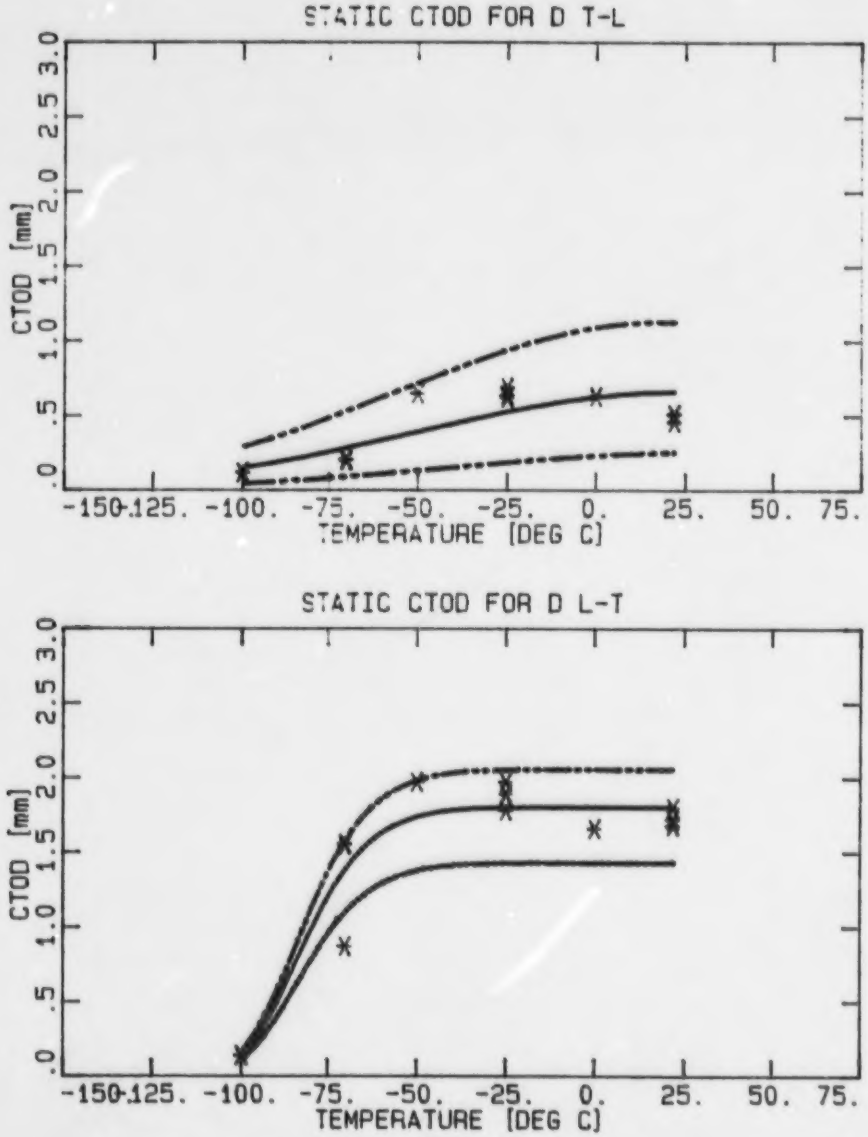

Figure 6.4 Static CTOD for Grade D

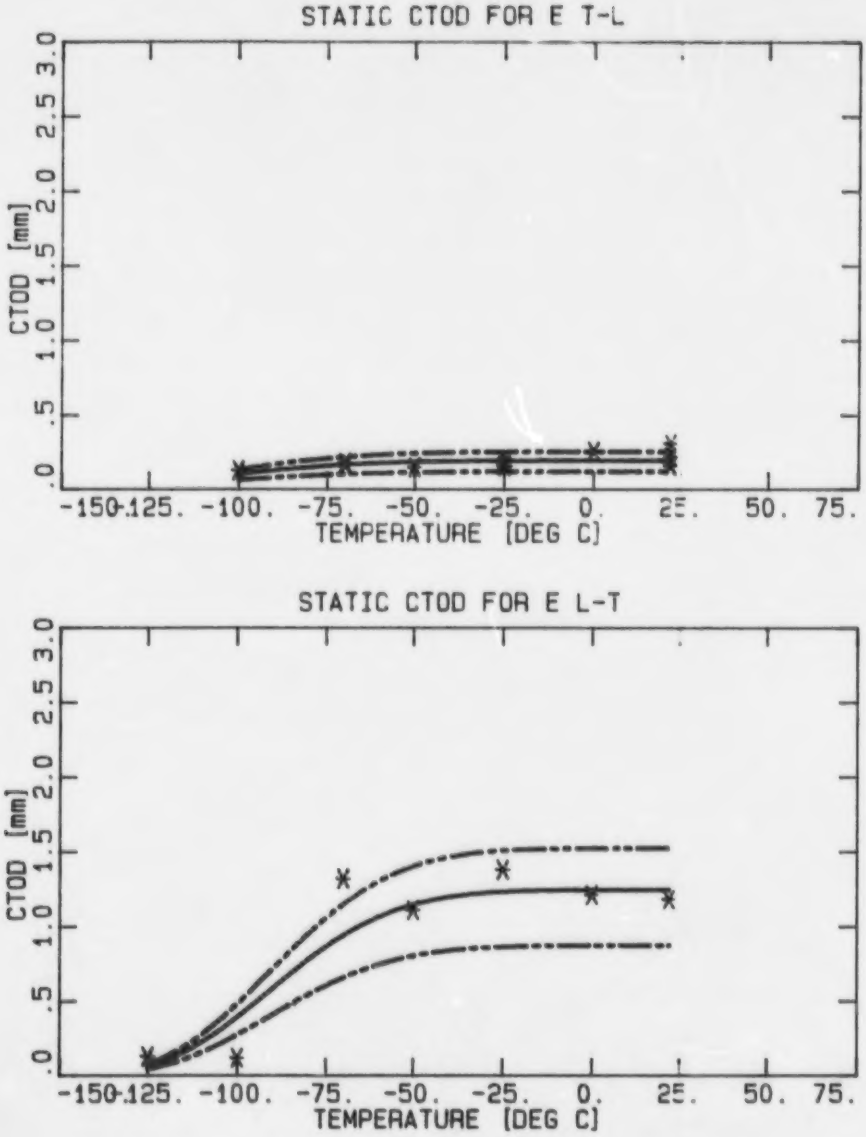

Figure 6.5 Static CTOD for Grade E 36

Table 6.3
Weibull Parameters for Static CTOD Grade D

Temp. °C	Orientation ALPHA	T-L BETA	Orientation ALPHA	L-T BETA
0	2.365	2.648	0.000906	11.2
- 10	2.669	2.604	0.000907	11.2
- 30	3.884	2.519	0.000935	11.2
- 50	6.646	2.436	0.00138	11.2

Table 6.4
Weibull Parameters for Static CTOD Grade E 36

Temp. °C	Orientation ALPHA	T-L BETA	Orientation ALPHA	L-T BETA
0	5252.5	5.546	0.137	7.31
- 10	5271.4	5.546	0.138	7.31
- 30	5508.4	5.546	0.154	7.31
- 50	6709.5	5.546	0.250	7.31

The dynamic CTOD data is shown in Figures 6.6, 6.7 and 6.8 for Grades A, D and E 36 respectively. The Weibull parameters for dynamic CTOD data are given in Tables 6.5 and 6.6. It should be noted that lack of data did not allow computation of Weibull parameters in some cases.

Table 6.5

Weibull Parameters for Dynamic CTOD Grade A

Temp. °C	Orientation ALPHA	T-L BETA	Orientation ALPHA	L-T BETA	Note	
0	*	*	62.06	2.597	* Fixed	0.11
- 10	*	*	70.96	2.515	* Fixed	0.093
- 30	*	*	89.43	2.359	* Fixed	0.066
- 50	*	*	107.76	2.214	* Fixed	0.047

Table 6.6

Weibull Parameters for Dynamic CTOD Grade E 36

Temp. °C	Orientation ALPHA	T-L BETA	Orientation ALPHA	L-T BETA	Note
0	72.6	4.21	*	*	* Not sufficient
- 10	74.2	4.21	*	*	data
- 30	96.1	4.21	*	*	
- 50	306.9	4.21	*	*	

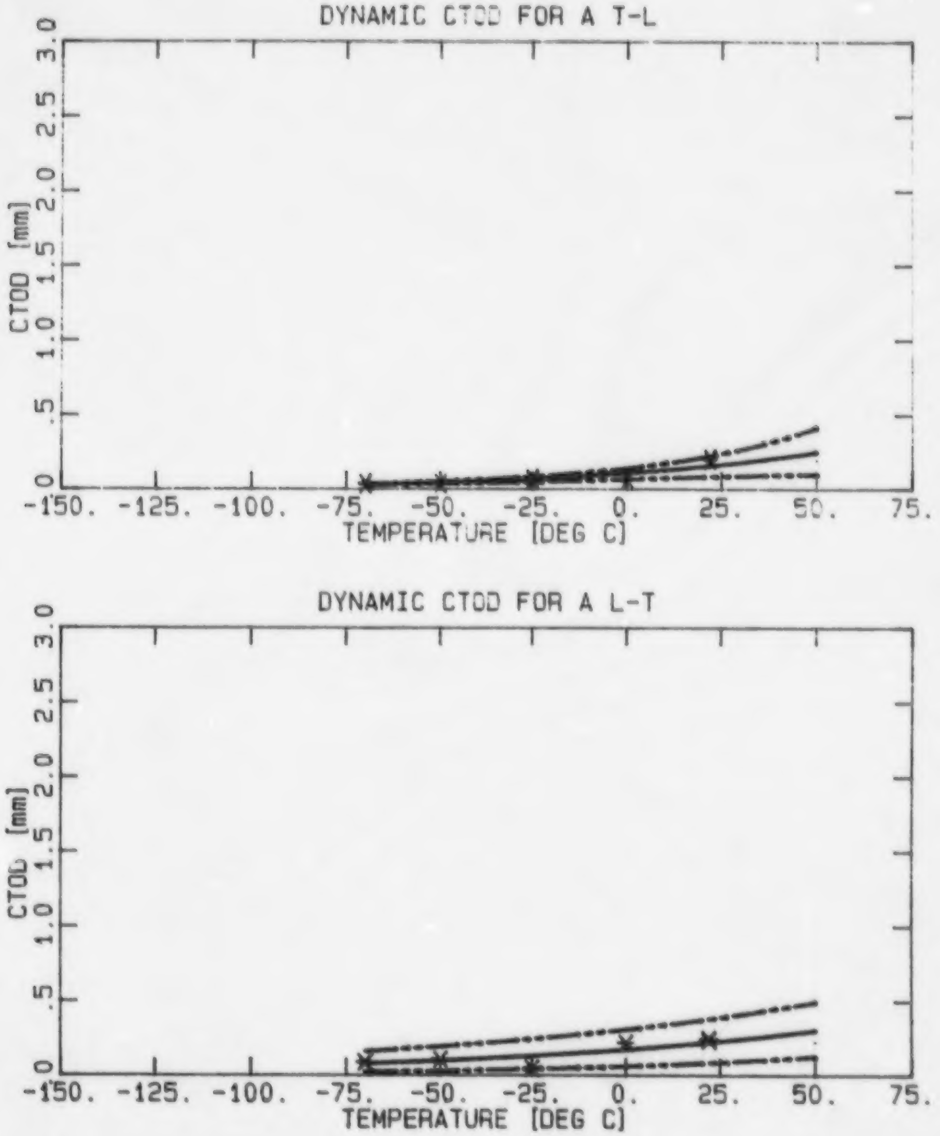

Figure 6.6 Dynamic CTOD for Grade A

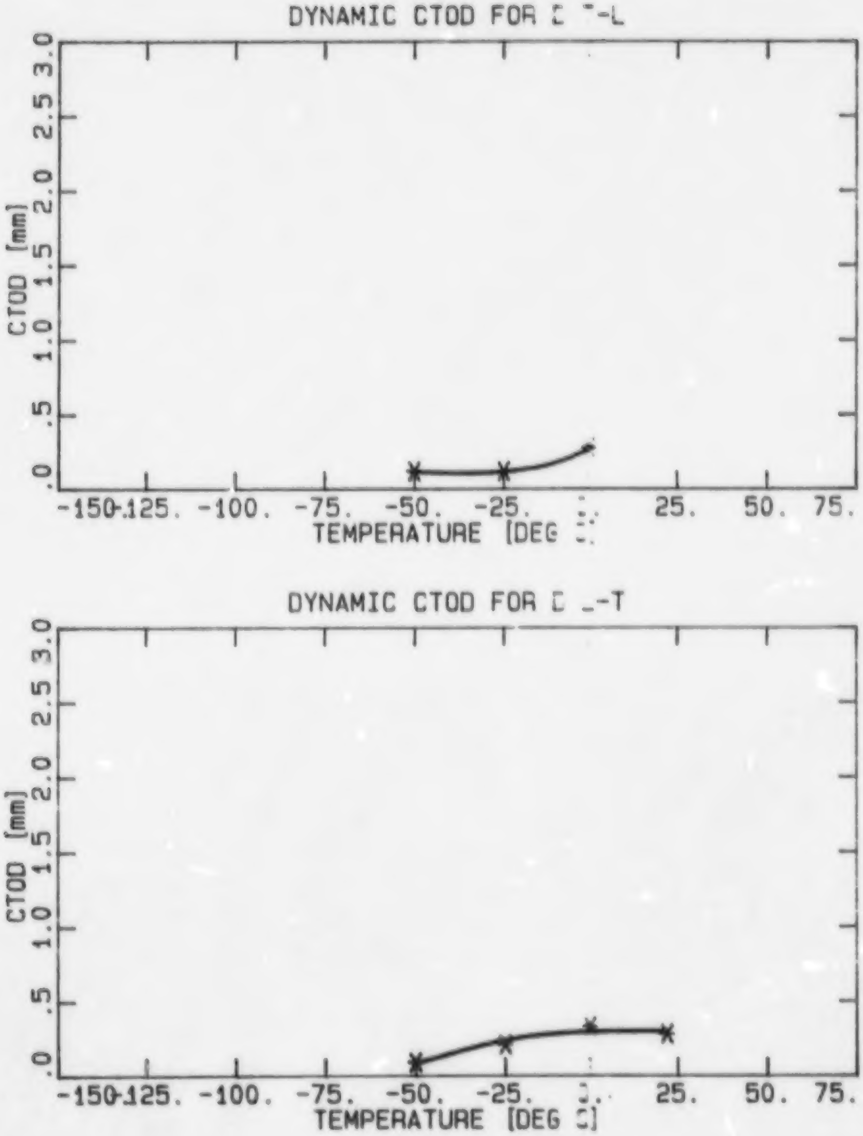

Figure 6.7 Dynamic CTOD for Grade D

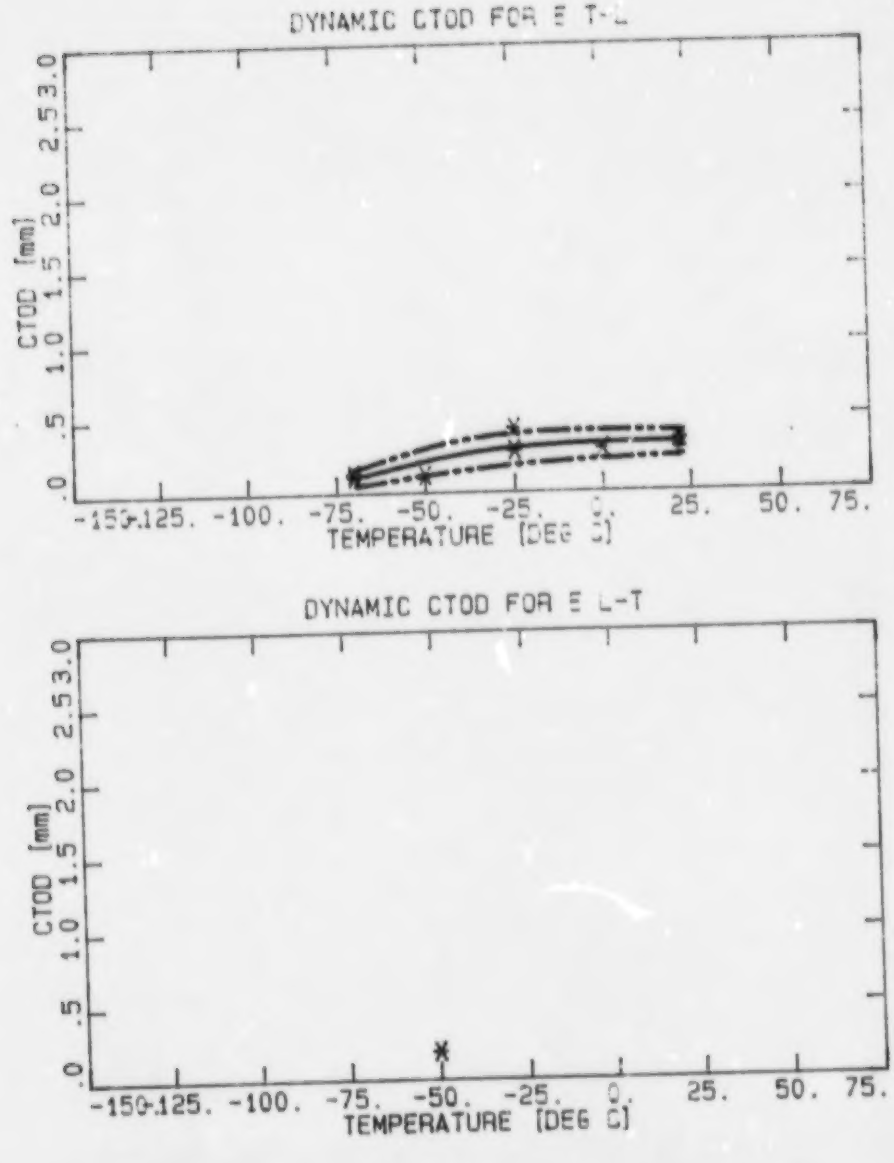

Figure 6.8 Dynamic CTOD for Grade E 36

Critical Stress Intensity Factor K_{IC}, K_C

In the case fracture toughness is given in terms of the critical stress intensity factor (SIF), the following relationships are assumed to be valid (e.g. Rolfe and Barsom, 1977).

$$\delta = \frac{K_{IC}^2 \, (1-\nu^2)}{2E\sigma_y} \quad \text{planestrain} \tag{6.1a}$$

and

$$\delta = \frac{K_C^2}{2E\sigma_y} \quad \text{planestress} \tag{6.1b}$$

where δ is CTOD;

ν is Poisson's ratio;

E is Young's modulus;

σ_y is yield strength; and

K_{IC}, K_C are plane-strain and plane-stress fracture toughness respectively.

6.1.3 Modelling Fracture Toughness vs. Thickness

As shown in Figure 6.1, resistance to fracture is governed by the stress state around the crack which depends on thickness. The fracture toughness-thickness relationship for Grade A steel at three temperatures (-10, -25 and -40°C) is shown in Figure 6.9 (Karlsen, 1979). The curves for -10 and -25°C are sufficiently close to justify a joint sample space for this data. It can be observed that the lower shelf of fracture toughness is reached at 25 mm thickness at -40°C, while it is reached at 100 mm thickness at both -10 and -25 degrees C.

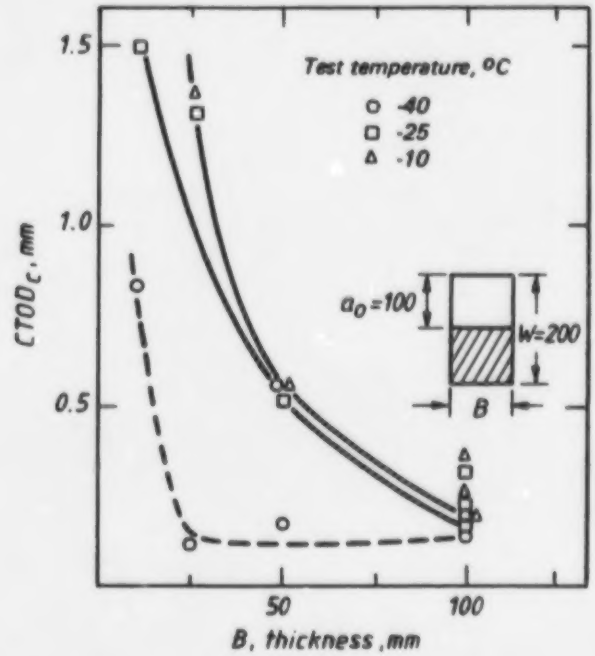

Figure 6.9 Effect of Plate Thickness on CTOD$_c$ for Through-Thickness SENB Specimens

The data was processed using Bishop's technique (Bishop et al, 1983 and 1985) and Figures 6.10 and 6.11 show the 5-, 50- and 95-pct exceedance curves for -10, -25°C, and -40°C respectively. Table 6.7 shows the corresponding Weibull parameters. The effect of thickness on fracture toughness has been studied, using a statistical model, by Faucher and Tyson (1988).

Table 6.7

Weibull Parameters for CTOD as a Function of Thickness

Grade A

Thickness mm	Temp. -10 & -25°C		Temp. -40°C	
	ALPHA	BETA	ALPHA	BETA
10	0.04416	4.492	6.173	4.599
30	0.60336	4.292	952.205	4.599
50	4.668	4.101	1968.613	4.599
70	21.732	3.918	2073.481	4.599
100	88.596	3.676	2075.277	4.599

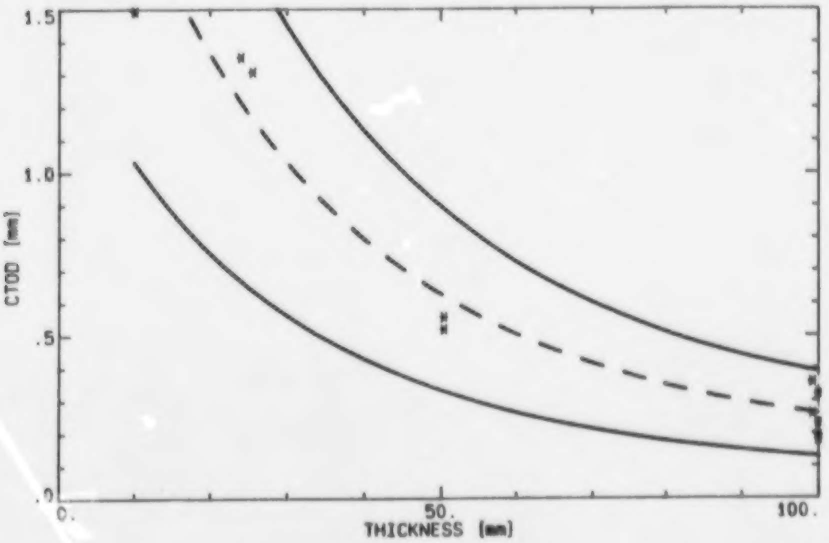

Figure 6.10 CTOD as a Function of Thickness for Grade A Steel at -10 and -25° C

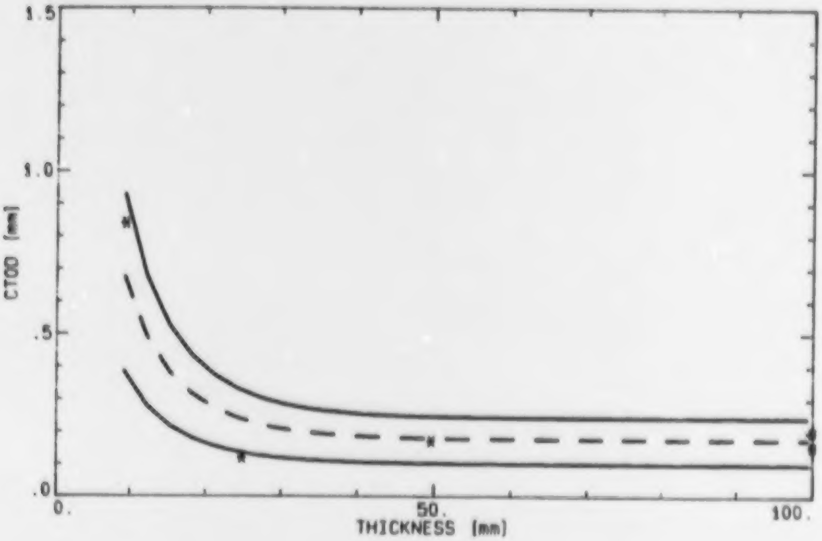

Figure 6.11 CTOD as a Function of Thickness for Grade A Steel at -40° C

6.1.4 Modelling Fracture Toughness vs. Strain Rate

Fracture toughness as a function of strain rate was plotted in Figures 6.12 to 14 (Grade A T-L), Figures 6.15 to 17 (Grade A L-T) and Figures 6.18 to 20 (Grade E36 T-L). These figures show again 5-, 50- and 95-pct exceedance curves of the Weibull distribution. The Weibull parameters used in the analysis are tabulated in Tables 6.8 and 6.9.

Table 6.8

Weibull Parameters for CTOD as a Function of Strain Rate

Grade A

	Orientation T-L		Orientation L-T		Note
Log $\dot{\varepsilon}$	ALPHA	BETA	ALPHA	BETA	
	Temperature 22°C				
-4.0	1.538	2.530	3.904E-7	25.722	
-2.0	20.169	2.530	6.644E 7	25.722	
0.0	73.030	2.530	8.668E14	25.722	
	Temperature -25°C				
-4.0	4.054	1.901	4.557	2.897	
-2.0	66.572	1.901	675.050	2.897	
0.0	269.778	1.901	8215.852	2.897	
	Temperature -70°C				
-4.0	*	*	8.785E 6	6.525	* Fixed
-2.0	*	*	8.785E 6	6.525	0.04 mm
0.0	*	*	8.785E 6	6.525	

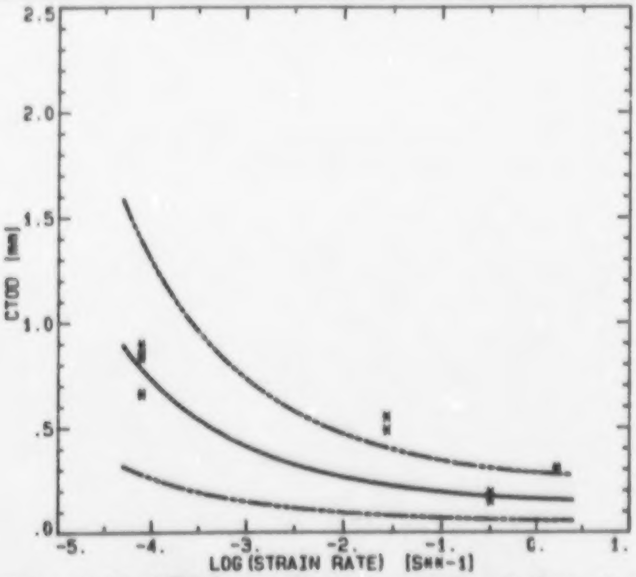

Figure 6.12 CTOD as a Function of Strain Rate for A Grade T-L Steel at 22°C

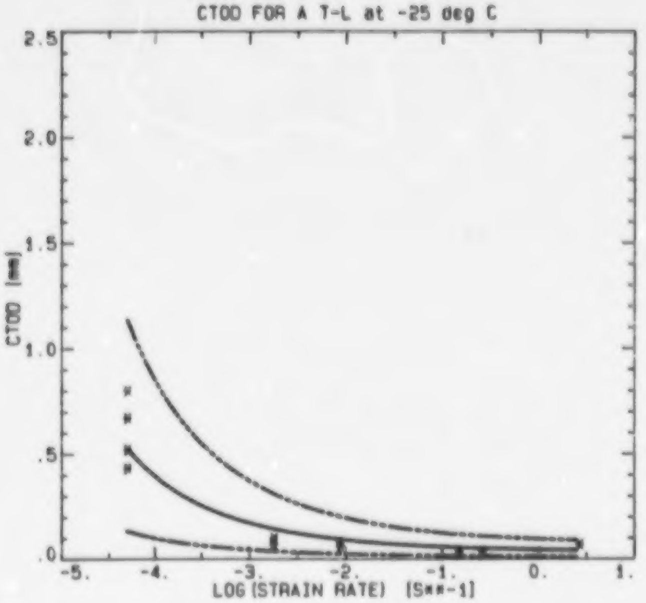

Figure 6.13 CTOD as a Function of Strain Rate for A Grade T-L Steel at -25°C

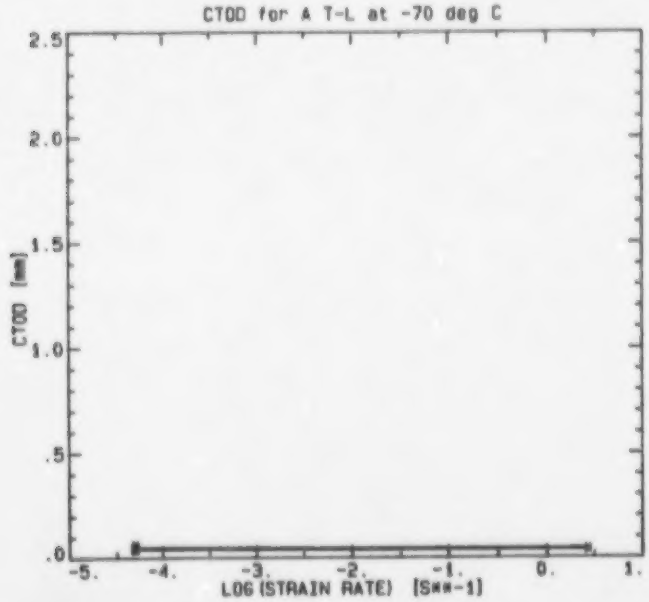

Figure 6.14 CTOD as a Function of Strain Rate for A Grade T-L Steel at -70°C

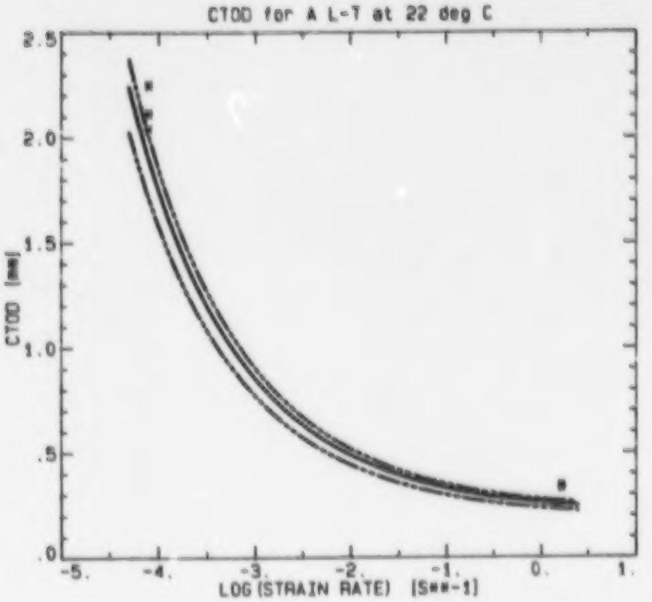

Figure 6.15 CTOD as a Function of Strain Rate for A Grade L-T Steel at 22°C

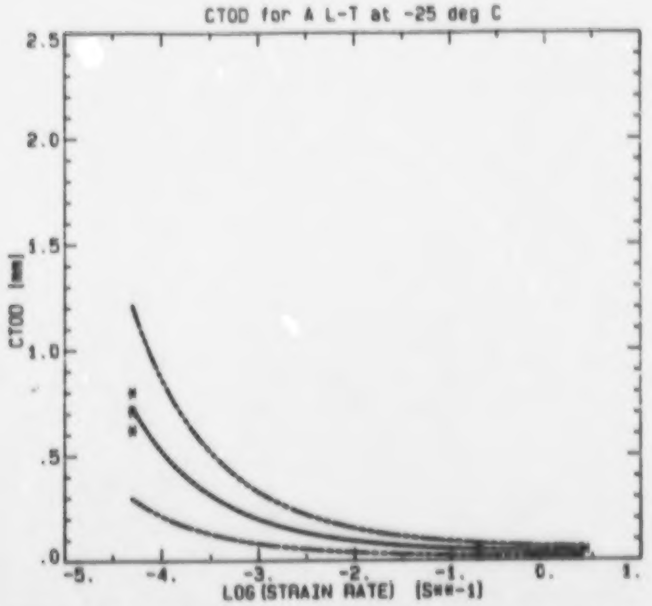

Figure 6.16 CTOD as a Function of Strain Rate for A Grade L-T Steel at -25°C

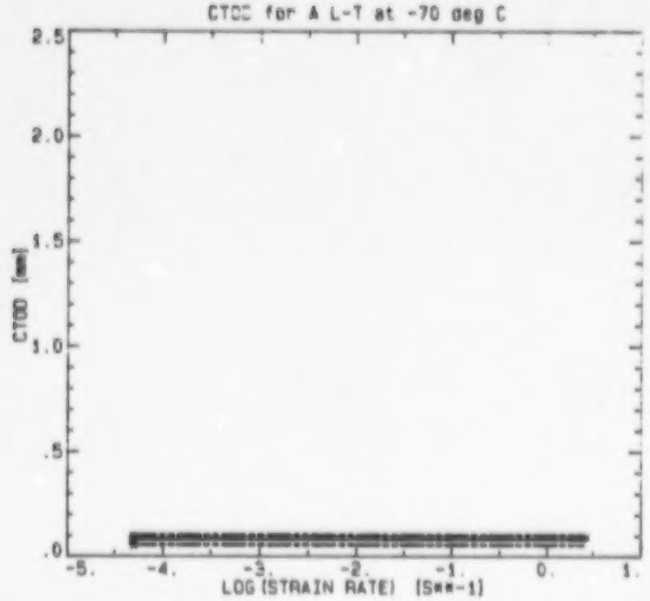

Figure 6.17 CTOD as a Function of Strain Rate for A Grade L-T Steel at -70°C

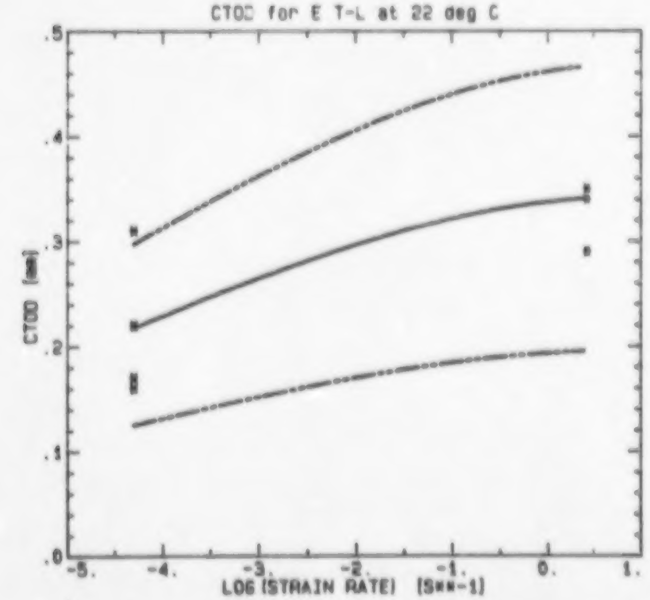

Figure 6.18 CTOD as a Function of Strain Rate for E36 Grade T-L Steel at 22°C

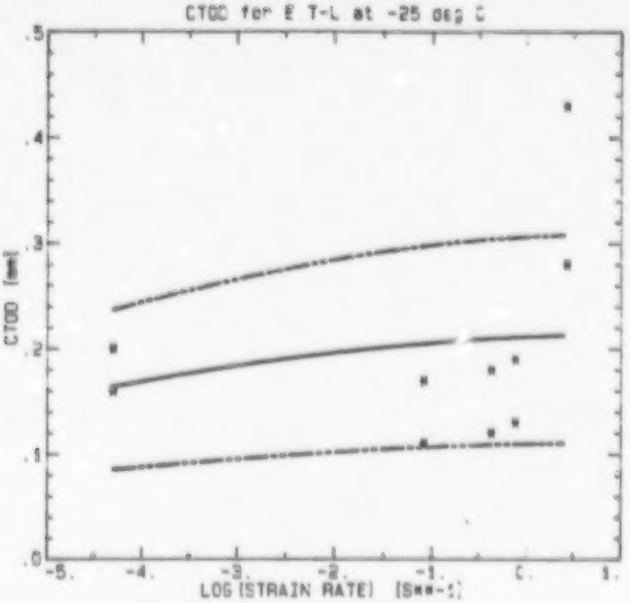

Figure 6.19 CTOD as a Function of Strain Rate for E36 Grade T-L Steel at -25°C

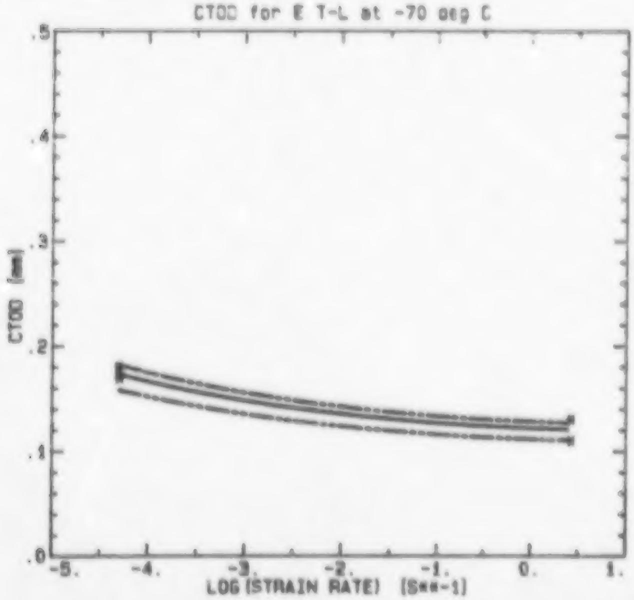

Figure 6.20 CTOD as a Function of Strain Rate for E36 Grade T-L Steel at -70°C

Table 6.9
Weibull Parameters for CTOD as a Function of Strain Rate
Grade E36 Orientation T-L

Log $\dot{\varepsilon}$	ALPHA	BETA
	Temperature 22°C	
-4.0	68.609	4.670
-2.0	204.347	4.670
0.0	111.522	4.670
	Temperature -25°C	
-4.0	819.144	3.970
-2.0	447.047	3.970
0.0	330.255	3.970
	Temperature -70°C	
-4.0	1.966E22	28.795
-2.0	7.875E24	28.795
0.0	1.576E26	28.795

As can be seen from the above tables and figures, there is not sufficient data at -70°C, however, it seems that the lower shelf of fracture toughness was reached and that fracture toughness at this lower shelf does not depend on strain rate.

6.1.5 Modelling Crack Arrest Toughness

There are two approaches to crack arrest: (1) static and (2) dynamic. Both methods assume that there is a material property K_m which is the lowest value of the stress intensity factor which will support a continued propagation of a running crack (e.g. Crossley and Ripling, 1980). The static approach approximates K_m by measuring the static value of the critical stress intensity factor, K_{ca}, following the arrest. The dynamic approach maintains that the dynamic effects accompanying a running crack are not negligible. The dynamic (running crack) toughness, K_d, is measured as a function of velocity and its minimum value, K_{dm}, is used as an approximation of K_m.

The static concept of crack arrest is generally accepted for relatively short cracks in the range of 200 to 300 mm (Yoshiki et al, 1968). This approach is widely used by the Japanese steel makers for the characterization of the crack arresting properties of their newly developed steels using special Thermo-Mechanical Control Processes (TMCP) (Nakano et al, 1987 and Watanabe et al, 1986). The use of K_{ca} fracture toughness as a crack arresting property was discussed in Nagamoto et al (1982) and the value of K_{ca} = 190 MPa$\sqrt{}$ m was found to be the minimum requirement for an effective crack arrestor in structural configurations encountered in bulk carriers Nakano et al (1987) suggest the value 180 MPa$\sqrt{}$ m for crack arrestors in ice-breaking vessels.

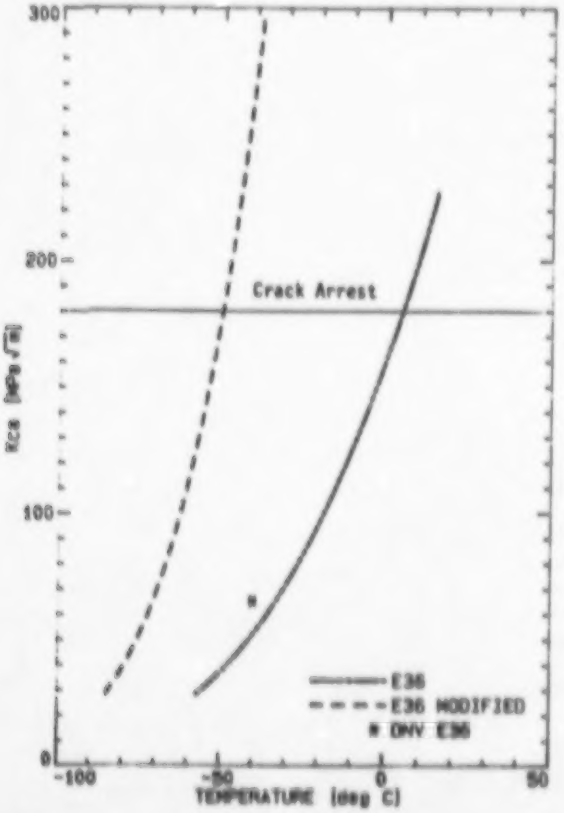

Figure 6.21 Crack Arrest Toughness K_{ca} for E36 and E36 Modified Steels

Figure 6.21 shows K_{ca} for Grade E36 (Watanabe et al, 1986) and E36 Mod (Nakano et al, 1987). Also, a single point in the figure denotes a series of tests performed at DnV (Melve et al, 1983) on E36 steel.

The results (K_{ca}) obtained by DnV are summarized in Table A2.18 (Appendix 2) and are plotted in Figure 6.22 as a function of crack propagation velocity. As can be seen, the static crack resistance does not significantly depend on the crack propagation velocity or temperature in the temperature range investigated (-29 to -40°C). This fact led to pooling all the results into one point (65 MPa$\sqrt{}$ m) in Figure 6.21. Figure 6.23 shows K_d as a function of crack propagation velocity and when compared with Figure 6.22, it is obvious that the K_{ca} lies below the minimum K_d value. However, the valid (elastic) region for propagated crack length was a < 92 mm.

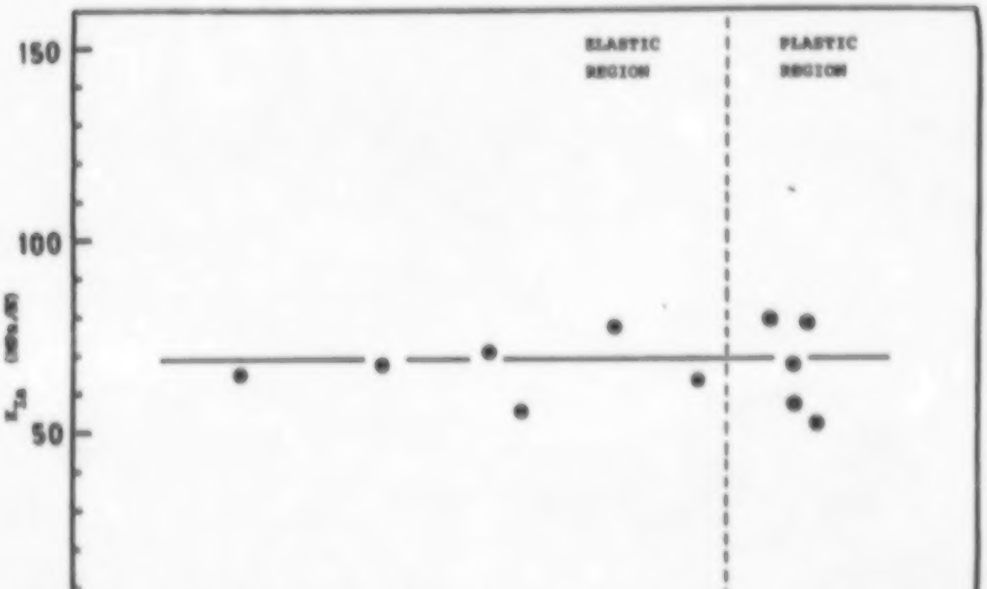

Figure 6.22 Crack Arrest Toughness Versus Calculated Crack Propagation Velocity for Grade E 36 in T-L Orientation. Plastic Region Means that the Testpieces are Plastically Deformed During Loading

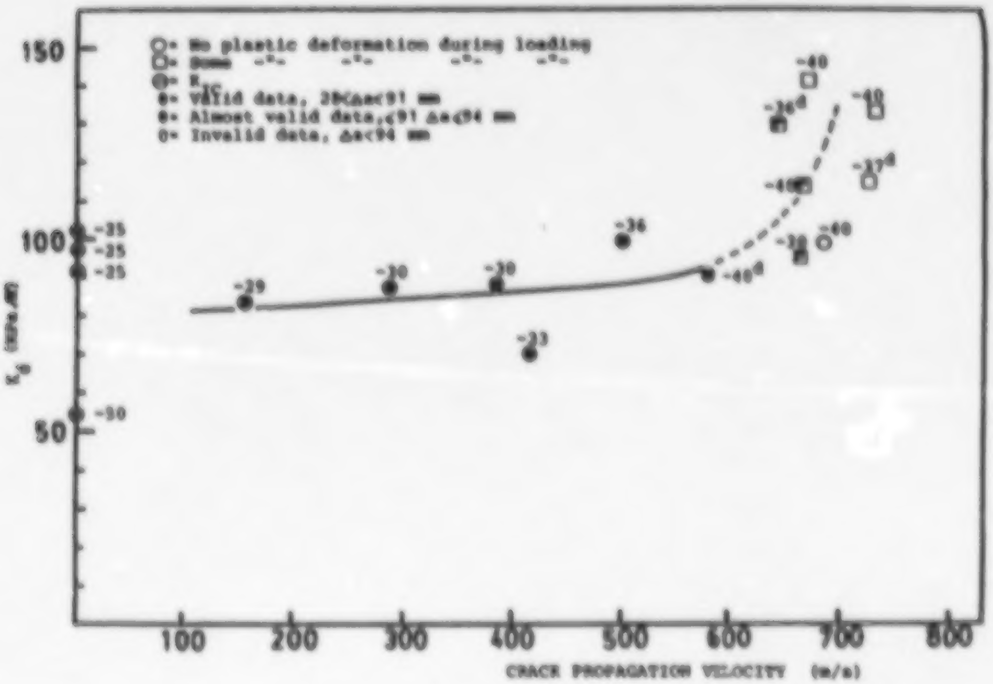

Figure 6.23 Dynamic Toughness, K_d, Versus Calculated Crack Propagation Velocity for Grade E36 in T-L Orientation. d Designates Side Groove Angle of 140° in the Testpiece

The values K_{ca}, shown in Figure 6.21 were used for comparison of crack arresting properties of E36 and E36 Mod steels using the probabilistic model.

6.2 Modelling Yield Strength vs Temperature

The yield strength data for Grades A, D and E 36 is given in Tables A2.20 and A2.21 and A2.22 in Appendix 2. It can be seen that yield strength does not significantly depend on the orientation of the specimen. Therefore the data for both L-T and T-L orientations was pooled together and a 3rd degree polynomial regression used to approximate the yield strength vs temperature dependency, Figure 6.24.

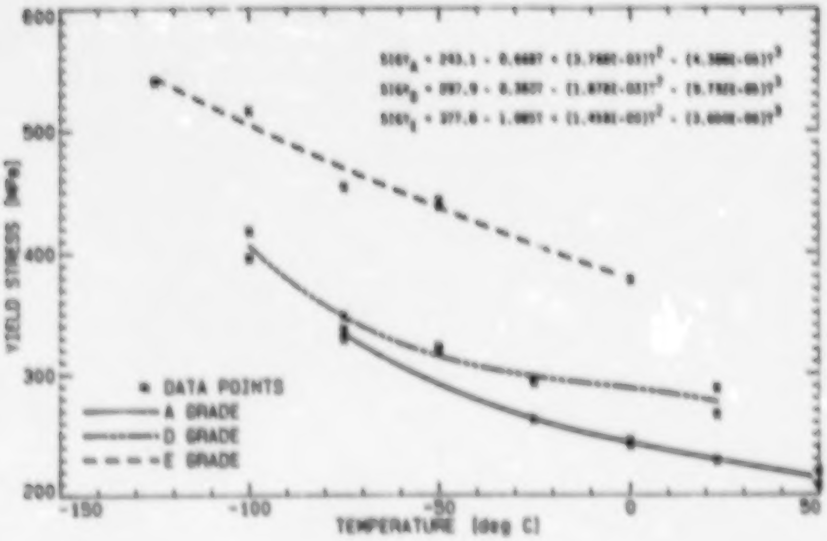

Figure 6.24 Yield Strength of Grades A, D and E36 Steels as a Function of Temperature

The variability of the yield strength at a given temperature was assumed to be 4%, Table 6.10.

Table 6.10
Yield Strength as a Function of Temperature

	Grade A		Grade D		Grade E 36	
Temp °C	Mean MPa	Std Dev	Mean MPa	Std Dev	Mean MPa	Std Dev
0	243	9.7	279	11.2	378	15.1
- 10	250	10.0	283	11.3	389	15.6
- 30	268	10.7	296	11.8	411	16.4
- 50	291	11.6	316	12.6	436	17.4

6.3 Modelling Crack/Defect Size and Crack Shape

There are two types of cracks/defects considered in this study:

1) Distribution of initial defects (flaws) which are introduced in a component during the fabrication process (usually welding);

2) Distribution of cracks discovered during regular (two year) survey of tankers.

The first type of data is used as an input to the fatigue crack propagation model and the second type of data is used to investigate the probability of failure of a given component based on one existing crack distribution. The latter allows us to draw conclusions with respect to the role of structural redundancy, knowing that the cracks discovered did not cause catastrophic failure of the ships investigated.

6.3.1 Modelling Initial Flaw Size

For any investigation of fatigue crack propagation, the knowledge of the initial flaw (crack) size is of paramount importance. The probability of finding a flaw of a given size (introduced in the structure during fabrication) is related directly to the detection probability for the non-destructive evaluation (NDE) method applied (Bokalrud and Karlsen, 1982). It has been shown (Wong and Rogerson, 1983) that Weibull probability distribution can be used to describe the weld defect size, Figure 6.21. This distribution gives conservative values for large defect sizes which are most important for the determination of the probability of failure. The Weibull probability distribution, with parameters $\alpha = 0.91$ $\beta = 0.8$ and $\gamma = 0.1$ mm, was used in the analysis (see Appendix 1 for the meaning of the parameters).

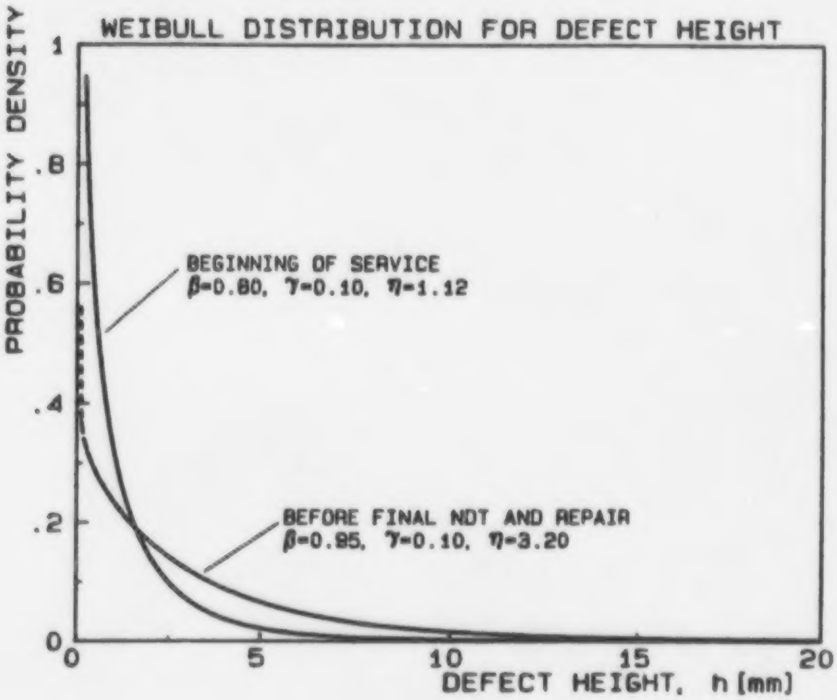

Figure 6.25 Weibull Distribution of the Initial Defect Size

6.3.2 Surveyed Crack Size Distribution

Antoniou (1977) published data on cracks reported over eight years of repairs done on 233 tankers ranging from 30,000 to 100,000 dwt. In total, 25,652 cracks were found and reported. Antoniou found that the marginal distribution of crack size (irrespective of the age of ships) is lognormal, Figure 6.26, with the following parameters $\epsilon = 0.5494$, $\xi = 5.4359$ and $\gamma = 40.5$ mm (see Appendix 1 for the meaning of the parameters).

Antoniou also found from ships returning from repairs to the shipyard on a regular basis, that the average crack growth rate was approximately 250 to 300 mm/year.

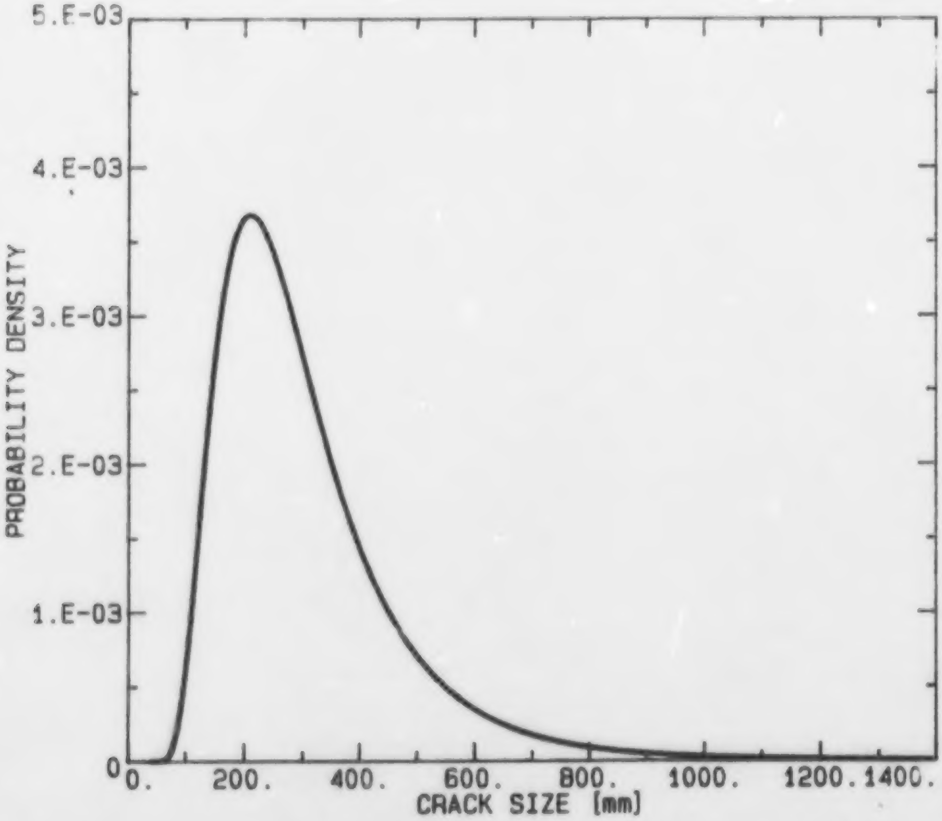

Figure 6.26 Probability Density Function for Crack Size in Tankers

6.3.3 Stress Intensity Factor (SIF)

a) Plate with a Through-Thickness Crack

The basic stress-intensity factor $K_o = \sigma \surd \pi a$, for an infinite centrally cracked plate, is adjusted for the proximity of the boundaries using the geometry factor $F = K/K_o$, Figure 6.27 (Rooke and Cartwright, 1976).

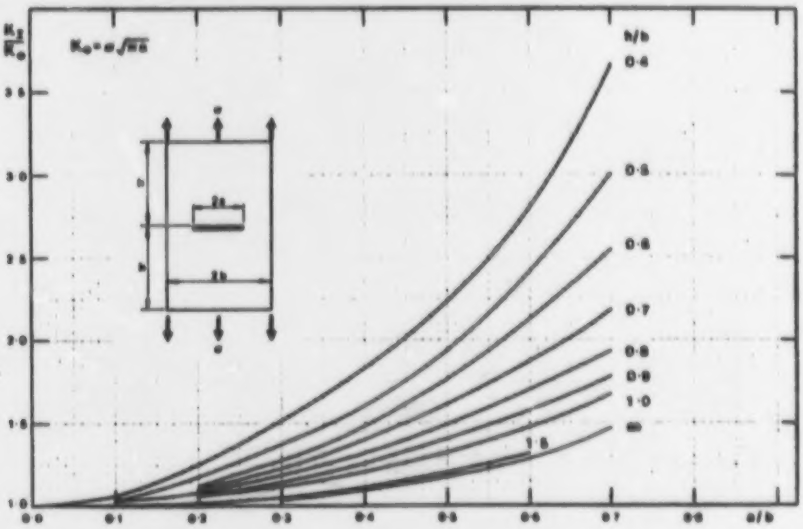

Figure 6.27. K/K_o for Centrally Cracked Plate (from Rooke and Cartwright, 1976)

b) Stiffened Plate with a Through-Thickness Crack

The stress-intensity factor is expressed in terms of the load P and the relative stiffness, defined as

$$s = AE_2/(btE_1) \tag{6.2}$$

where A is the cross-sectional area of one stiffener;

E_1 and E_2 are Young's moduli of the plate and the stiffener respectively; and
t is thickness of the plate.

Dimension b is shown in Figure 6.28.

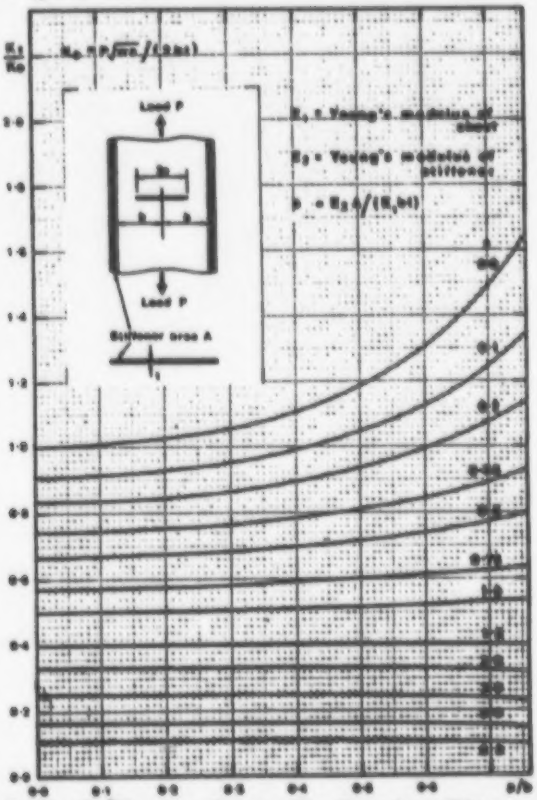

Figure 6.28. K/K_o for Centrally Cracked Plate with Stiffeners (from Rooke and Cartwright, 1976)

In both cases a) and b) the curves were digitized and approximated by polynominal functions which were then used in the algorithm for fatigue crack propagation to adjust for the change in the crack-plate configuration as the crack size increases.

c) Plate with Surface Crack

The stress intensity factor for a part-through "thumbnail" crack in a plate subjected to uniform tensile stress, Figure 6.29, is given by

$$K = 1.12 \sqrt{\pi a/Q} \qquad (6.3)$$

where the shape factor Q is plotted in Figure 6.30 as a function the crack aspect ratio a/2c.

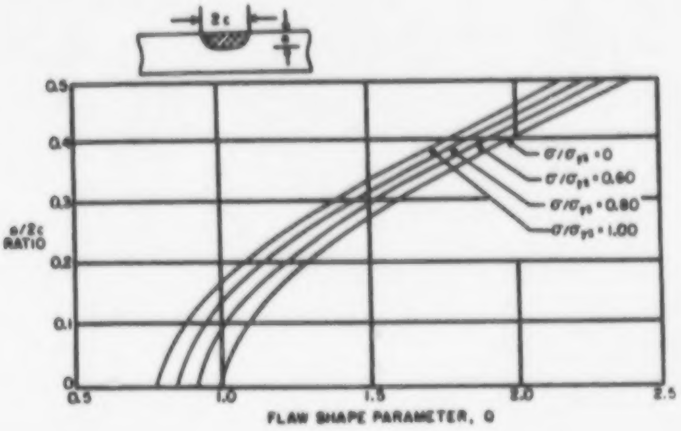

Figure 6.30 Crack Shape Factor as a Function of Aspect Ratio

d) Welded T-Joint

A welded T-joint in tension was selected to represent a large family of structural details, Figure 4.5c. This element is characterized by a complex state of stress at the crack tip dominated by stress concentration near the weld toe.

The basic crack shape factor F_E (see Eq. 5.1) is given by (Almar-Naess, 1985)

$$F_E = \{ 1 + 4.5945(a/2c)^{1.65} \}^{-0.5} \tag{6.4}$$

Assuming a/2c = 0.4, $F_E = 0.71$.

The crack front face factor F_S for 45° weld profile is given by

$$F_S = 1 - 0.16(a/2c) = 0.94 \tag{6.5}$$

The finite thickness factor F_T is shown as a function of the ratio a/2c in Figure 6.31.

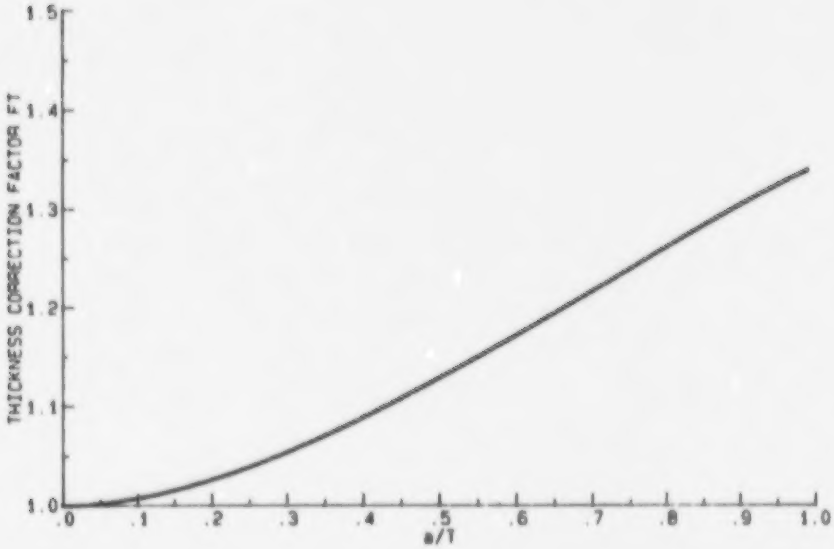

Figure 6.31 Thickness Correction Factor as a Function of a/2c

This function can be approximated through a polynomial

$$F_T = 1 + 0.01652\,(a/T) + 0.633(a/T)^2 - 0.306(a/T)^3 \qquad (6.6)$$

where T is the thickness of the plate.

The finite width correction factor F_W for the crack propagation through the thickness is assumed to be 1.

The stress gradient factor depends on the stress concentration factor SCF, the stress decay coefficient d and stress decay exponent q as follows

$$F_G = SCF/\ (1 + d^{-1}(a/T)^q\ ) \tag{6.7}$$

For a T-joint d = 0.3602, q = 0.2487 and SCF = 1.621log(l/T) + 3.964 (Almar-Naess, 1985), where l = 20 mm is the leg of the weld and T = 35 mm is the thickness of the plate. For this configuration, SCF = 3.57 at the weld toe.

The resultant stress gradient factor is then

$$F_G = 3.57/\ (1 + 2.78(a/T)^{0.25}\ )$$

The resultant correction factor is a function of a/T and is obtained by multiplying all the above factors (see Eq. 5.1).

$$F = 0.67F_T(a/T)F_G(a/T) \tag{6.8}$$

This factor was used in the fatigue crack propagation algorithm implemented in PROBAN.

The aspect ratio was assumed to be a/2c = 0.4 for both the simple plate as well as for the T-joint with surface crack. The cross-sectional area of the stiffeners used in the calculations was A = 8000 mm^2. The ratio of the height/width of the simple plate and the T-joint was > 1.5 so that the bottom curve in Figure 6.27 was used.

6.3.4 Critical Crack Size Factor I_a

As already discussed in section 5, a CTOD design curve is based on the allowable crack size. To use this curve for establishing the margin of safety against unstable crack initiation, a crack safety factor (CTOD model factor) was introduced in Eq. 5.14.

Figure 6.32 shows a comparison between the critical crack size obtained from wide plate tests (Kamath, 1981 and Pisarski, 1983) with the corresponding allowable crack size obtained from the CTOD design curve. As can be seen from this figure, there is only 3.3% probability that the allowable crack size exceeds the critical crack size. Alternatively, there is approximately a 50% probability that the allowable crack size exceeds 33% of the critical crack size, i.e. the safety factor is approximately equal to 3. Madsen et al (1985) used lognormal distribution to fit the above data for wide plate tests to obtain

$$F_{I_a}(X) = \Phi\left(\frac{\ell nx - 1.099}{0.535}\right) \tag{6.2}$$

Madsen et al (1985) also found that for a large diameter pipe (OD = 1 m) the safety factor I_a = 11.7. For small crack sizes which were important for the analysis, no significant correlation was observed between I_a and the critical crack size and that the lognormal distribution for I_a fitted the data well.

Depending on the structural detail, the parent and weld materials, the safety factor I_a can be as low as 2 (PD 6493, 1980) or as high as 20 (Almar-Naess, 1985).

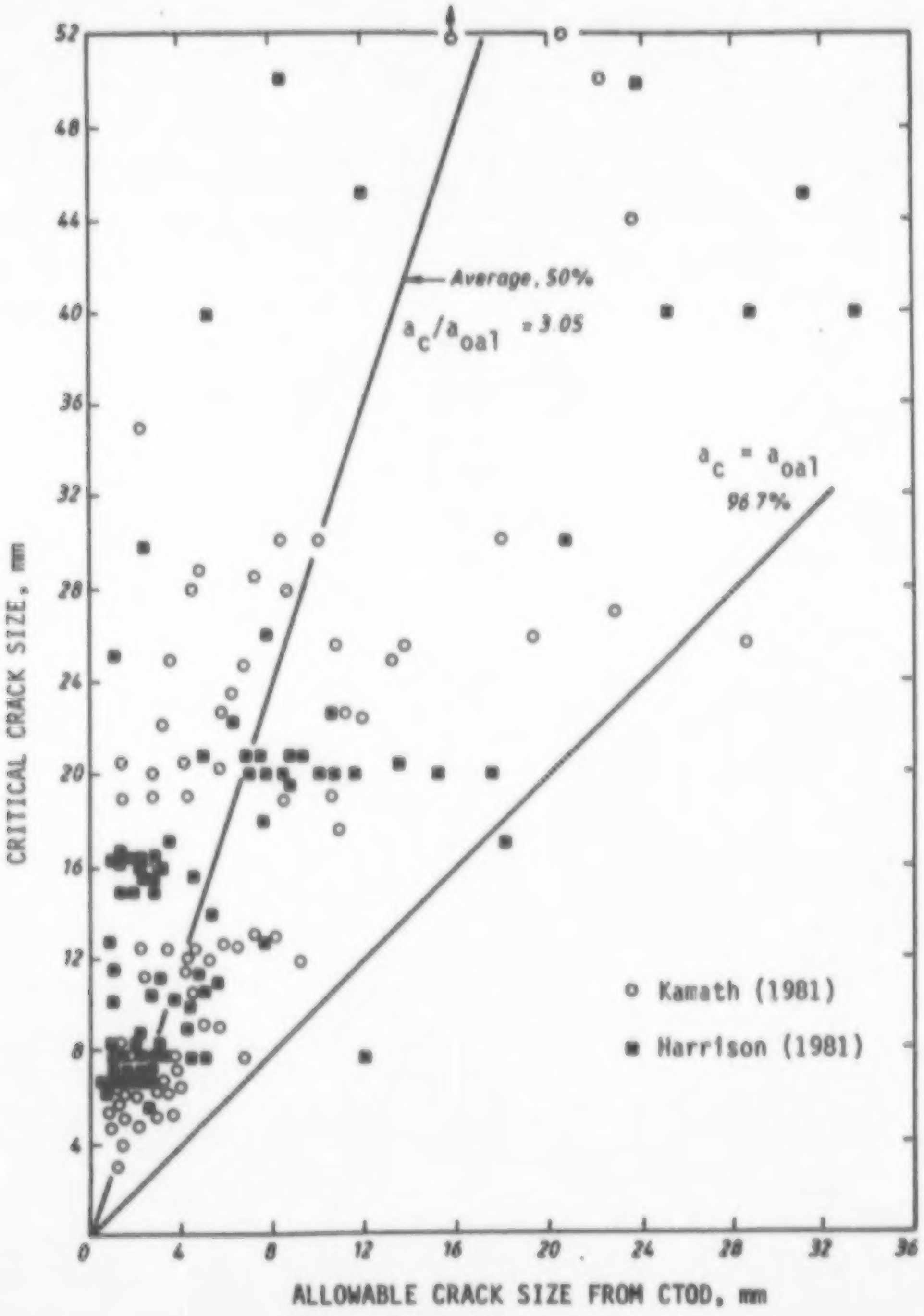

Figure 6.32 Comparison of Allowable (CTOD) Crack Size and Critical Crack Size for Wide Plates

6.4 Modelling Stresses/Loads

There are two stresses (loads) to be modelled: a) far-away stress (load); and b) cycling stress (load).

6.4.1 Far-Away Stresses/Loads

The allowable stresses for hull structures depend on the strength group of the steel considered, location in the hull, length of the ship and the stress state. For example, DnV Rules (1984) define the requirement for the allowable bending stress for longitudinally stiffened strength deck plating as

$$\sigma_{al} = 120f_1$$

where f_1 = 1.00 for NS structural steel
f_1 = 1.08 for NV-27 steel
f_1 = 1.28 for NV-32 steel
f_1 = 1.39 for NV-36 steel
f_1 = 1.43 for NV-40 steel

The thickness of plating is selected based on the lateral pressure.

However, the stresses measured in ship hulls are usually lower. For example, the T2 tanker Schenectady which broke in two in 1943 was exposed, at the time of failure, to only about 68 MPa in tension (Boyd, 1969). Based on actual measurements, Rolfe and Barsom (1977) estimate that 97 MPa is a reasonable maximum nominal stress level in ship hulls.

The stresses in the deck from the still water bending moments calculated for M.V. Arctic were 60 MPa under ballast condition (Sukselainen and Kujala, 1983).

In the current study it was assumed that the nominal far-away stress will be treated deterministically and the analysis will be performed for 60, 80 and 100 MPa. In the case of the stiffened plate, an equivalent load $P = \sigma$ bt was used in the analysis.

6.4.2 Wave Induced Stresses/Loads

The sea wave loading is a highly stochastic process. Various theories were developed to model seastates. For example, for the North Sea, two spectra have been defined (e.g. see Almar-Naess, 1985): a) Pierson-Moskowitz spectrum which is applicable to a fully developed sea; and b) JONSWAP spectrum for the extreme wave conditions (limited by the size of the generation area).

The long-term wave induced stress histories match well the two-parametric Weibull distribution (Munse et al, 1983). Figure 6-33 shows a histogram of peak-to-trough stresses with a corresponding Weibull distribution measured in the SL-7 Research Program (Fain and Booth, 1979). Each stress range in the scratch gauge data represent the maximum peak stress to the minimum trough stress which occurred during a four-hour sampling period and corresponds to one occurrence in the histogram. It is assumed that the average wave period is 7.5 seconds. The number of cycles experienced by the ship in one occurrence is thus 1920.

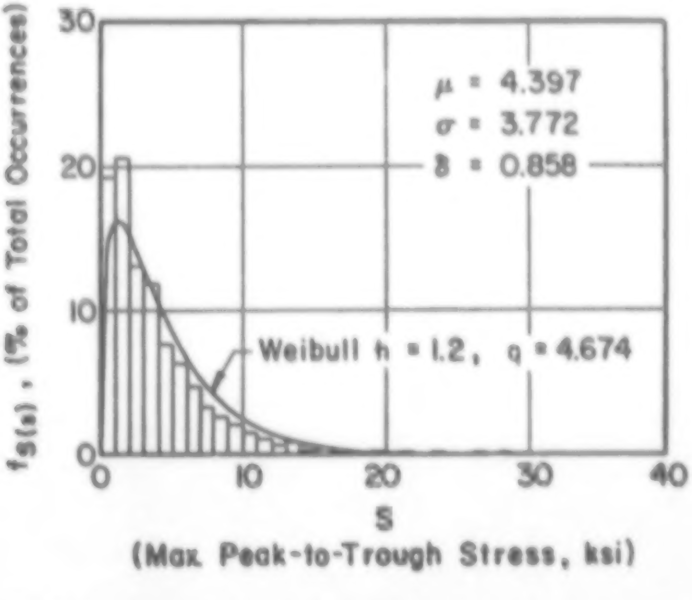

Figure 6.33: Scratch Gauge Stress Data with Corresponding Weibull Distribution

For the fatigue crack propagation using Paris-Erdogan law (Eq. 5.20), it is advantageous to calculate an equivalent stress range (e.g. Almar-Naess, 1985). The algorithm is based on equal damage ratio in the case of the real and the equivalent spectra calculated on the basis of the Miner-Palmgren damage cumulation law. Assuming that the long-term distribution of stress ranges is represented by a two-parametric Weibull distribution:

$$Q(\Delta\sigma) = \exp\left(-\left(\frac{\Delta\sigma}{q}\right)^{h}\right) \tag{6.9}$$

where Q is the probability that the stress range will be exceeded
$\Delta\sigma$ is the stress range
h, q are Weibull parameters

The Weibull parameter q is related to the stress range with the return period equal to the ship lifetime (20 years) as follows:

$$q = \frac{\Delta\sigma_o}{(\ln N_o)^{1/h}} \tag{6.10}$$

where N_o is the total number of cycles during the ship lifetime
and $\Delta\sigma_o$ is the stress range exceeded once during N_o cycles.

The equivalent stress range $\Delta\sigma_{ev}$ can be expressed as:

$$\Delta\sigma_{ev} = q\left(\Gamma(m/h+1)\right)^{1/m} \tag{6.11}$$

where Γ is the gamma function and m is the crack propagation parameter in the Paris-Erdogan propagation law.

The equivalent stresses together with the maximum stress exceeded once in $N_o = 10^8$ cycles are listed in Table 6.11 for a number of ships (Munse et al, 1984).

Table 6.11
Equivalent Stresses for Various Ship Loading Histories

	h	Δσo (MPa)	Δσev (MPa)	Note
Dry Cargo				
Wolverine State	1.2	114	17.1	
California State	1.0	124	12.3	
Mormascan	1.3	84	12.3	North Atlantic voyages
Mormascan	1.0	69	6.8	South American voyages
Large Tankers				
Idemitsu Maru	1.0	85	8.4	
R.G. Follis	0.8	207	14.8	
Esso Malaysia	0.8	150	10.7	
Universe Ireland	0.7	129	6.7	
Bulk Carrier				
Fotini L.	0.9	204	16.8	
SL-7 Containerships				
	1.2	235	31.3	Eight ships surveyed

7. ANALYSIS AND DISCUSSION OF THE STUDY RESULTS

In this chapter results obtained by applying the probabilistic model of material failure modes to three types of steel will be presented and discussed.

Three types of ship steel have been considered: Grade A, D, and EH36. Probability of failures for typical structural elements have been estimated on the basis of measured distribution of cracks as well as on the basis of assumed initial flaw sizes.

Types of Steel

To interpret the results, one has to discuss first the fracture properties of the three steels used as a basis for the calculations and comparisons.

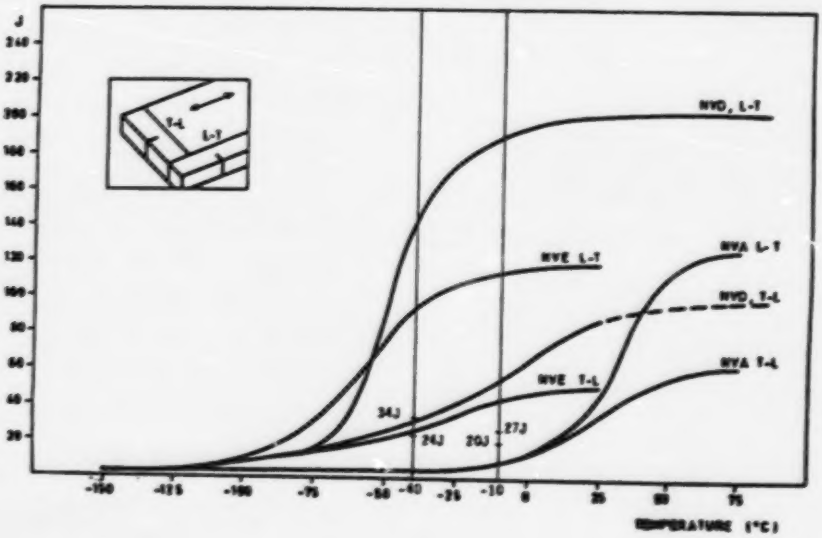

Figure 7.1. Charpy V-Notch Transition Curves for Grades A, D and E36 Steels

Figure 7.1 shows Charpy V-Notch transition curves for steels Grade A, D and E36 in both orientations T-L and L-T. It can be seen that both steel Grade D and E36 exceed the minimum quality CVN requirements (20 J for D T-L, 27 J for D L-T at -10°C and 24 J for E36 T-L, 34 J for E36 L-T at -40°C). There are no toughness requirements for Grade A steel.

However, Grade E36 T-L satisfies the requirement only marginally. Grade D is superior to Grade E36 in both T-L and L-T directions.

Sulphide inclusions together with the texture of the plates due to rolling caused a very pronounced difference between the T-L and L-T fracture toughness results. For example a tensile test for E36 steel in the through thickness direction (S-direction, Figure 6.2) resulted in UTS = 545 MPa as compared to 1333 MPa in the T-direction (Saether, 1980).

For interpreting results of the probabilistic analysis, it is important to keep in mind the critical CTOD transition curves in Figures 6.3 to 6.5. Only Grade A shows a distinct transition in the CTOD values in the temperature range 0 to -50°C investigated in the study.

7.1 Probability of Fracture Based on Measured Crack Distribution

The measured crack size distribution used in the model was described in Section 6.3.2. It was assumed that cracks propagated away from welds and stress concentrators. Two modes of failure were considered: a) unstable fracture; b) plastic collapse.

7.1.1 Probability of Unstable Fracture

Effect of Temperatures and Stiffness

Figure 7.2 and 7.3 show probabilities of failure for two nominal stresses 60 MPa and 100 MPa in a static loading regime. In each figure, the cases for simple plate and

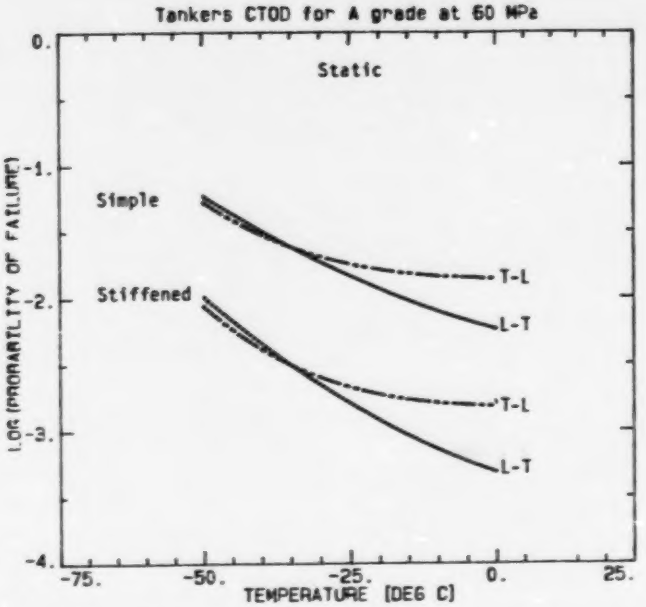

Figure 7.2: Probability of Unstable Fracture as a Function of Temperature for 60 MPa Nominal Stress and Static Loading

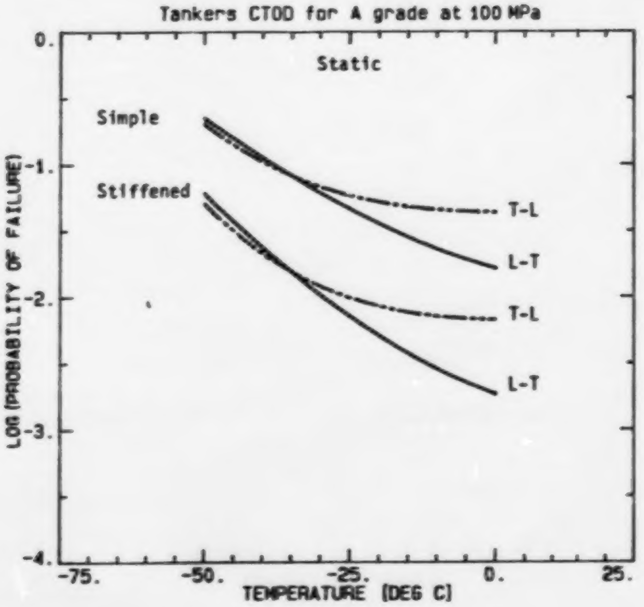

Figure 7.3: Probability of Unstable Fracture as a Function of Temperature for 100 MPa Nominal Stress and Static Loading

stiffened plate are compared for both T-L and L-T specimen orientations. The temperature dependency of the probabilities of failure is caused by fracture toughness and yield strength both of which depend on temperature (Figures 6.3 to 6.11). The effect of fracture toughness is more pronounced due to its transitional behaviour than that of the yield strength.

The closeness of the T-L and L-T curves at low temperatures (below -35°C) suggests that fracture toughness for the tested Grade A steel reaches identical values close to the lower shelf for both T-L and L-T orientations. The probabilities of unstable fracture are about one order of magnitude lower for the stiffened plate than for the simple plate at 0°C. The difference decreases with decreasing temperatures. The shape of respective curves for 60 MPa and 100 MPa is identical, however the curves shift towards high probabilities of failure with increasing nominal stress. The probability of failure at 100 MPa for stiffened plate is approximately same as that at 60 MPa for simple plate (-50°C).

Even though the effect of strain rate on the probability of fracture is discussed later in this section in more detail, the static and dynamic cases are compared below (correspond to the static and dynamic CTOD, see Section 6.1.2).

Figures 7.4 to 7.6 show probability of failure curves for steels Grade A, D and E36 respectively for the case of simple plate. In each figure, the static and dynamic loading cases are compared. For Grade A steel, the strain rate effect is more pronounced than the effect of specimen orientation, Figure 7.4. Figure 7.5 shows an anomalous behaviour. The probability of fracture actually slightly decreases with decreasing temperature for static loading and L-T orientation. This is caused by the fact that the upper shelf for the tested Grade D steel extends down to -50°C (Figure 6.4) and the increase of the yield strength with decreasing temperature (Figure 6.10) causes the slight drop of the probability of failure. The curves for dynamic loading are based on scarce fracture toughness data, see Figure 6.7, and the crossing of the curves at approximately -45°C is not regarded as a significant phenomenon.

Figure 7.6 does not show the curve for dynamic loading in L-T orientation due to lack of fracture toughness data, see Figure 6.8. In the static case, the probability of

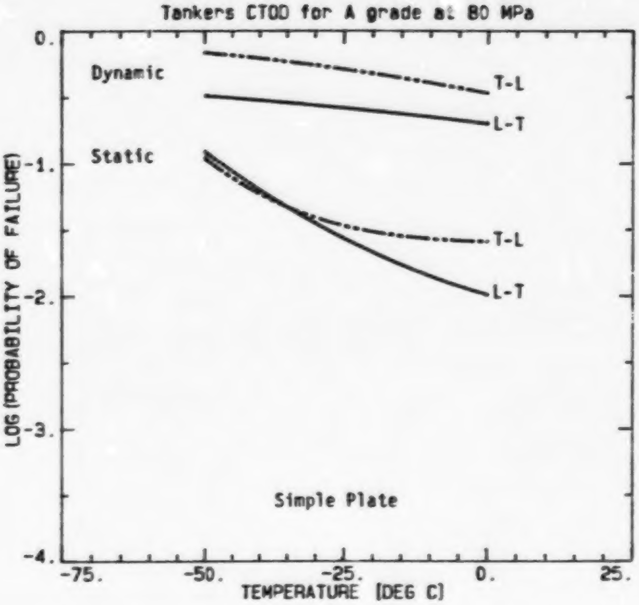

Figure 7.4: Probability of Unstable Fracture as a Function of Temperature for Simple Plate, Steel Grade A

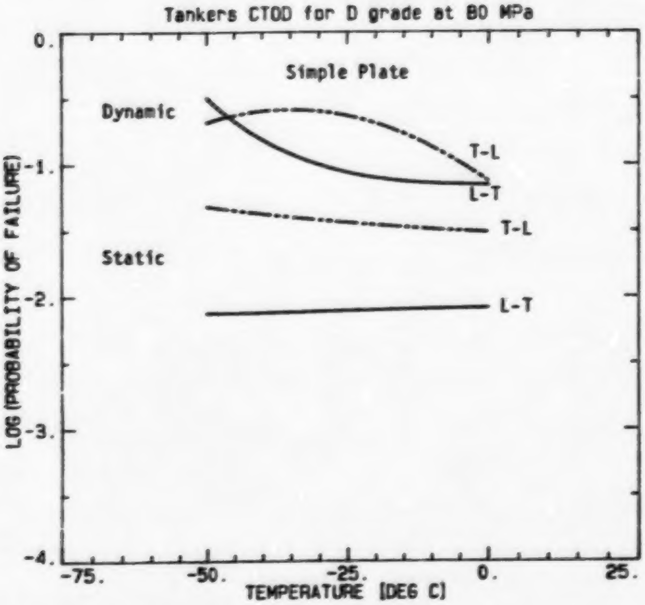

Figure 7.5: Probability of Unstable Fracture as a Function of Temperature for Simple Plate, Steel Grade D

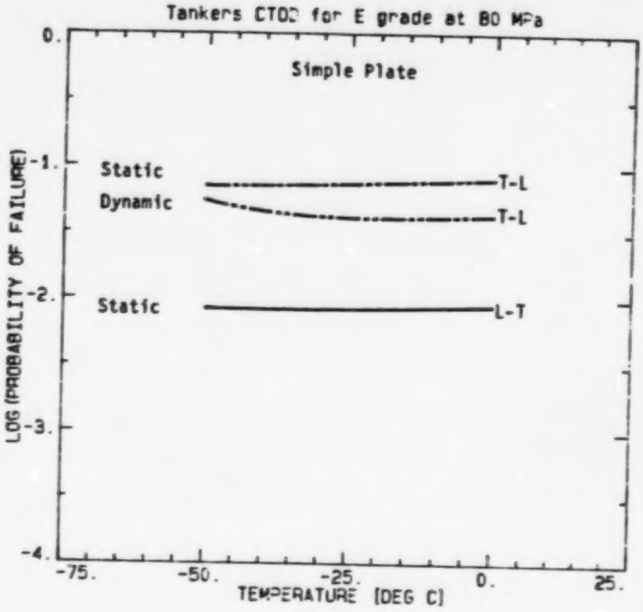

Figure 7.6: Probability of Unstable Fracture as a Function of Temperature for Simple Plate, Grade E36

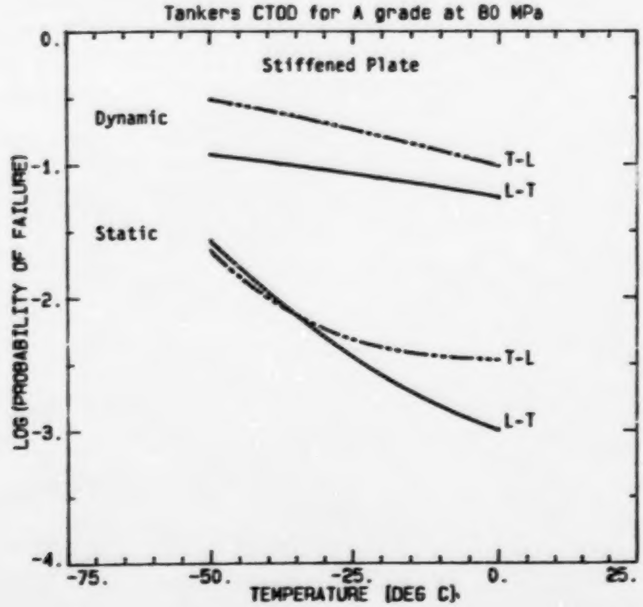

Figure 7.7: Probability of Unstable Fracture as a Function of Temperature for Stiffened Plate, Grade A

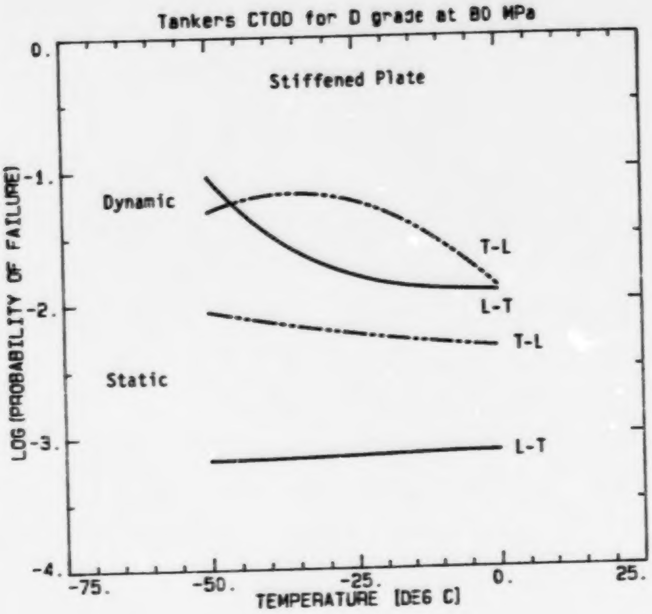

Figure 7.8: Probability of Unstable Fracture as a Function of Temperature for Stiffened Plate, Grade D

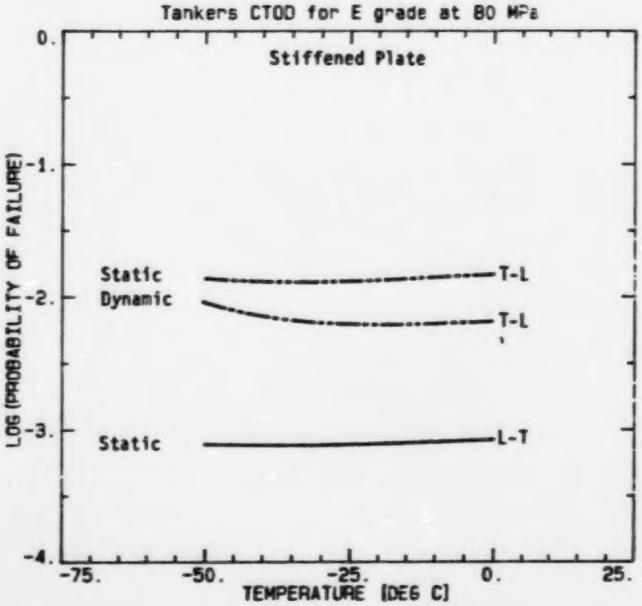

Figure 7.9: Probability of Unstable Fracture as a Function of Temperature for Stiffened Plate, Grade E36

failure for the T-L orientation is about one order of magnitude lower than that for the L-T orientation and both curves maintain approximately constant probability of failure throughout the temperature range 0° to -50°C.

Figures 7.7 to 7.9 show the results for a stiffened plate geometry, Grade A steel and 80 MPa nominal stress. The probability of unstable fracture is favourably affected and is 5 to 10 times lower than the respective value in the case of simple plate. The curves have the same shape as in the case of simple plate and are shifted to lower probabilities.

Effect of Strain Rate

The data presented in Section 6.1.4 allowed to investigate the effect of strain rate on the probability of failure in the range between 10^{-4} to $1\ s^{-1}$.

Figures 7.10 and 7.11 show the probability of unstable fracture as a function of strain rate in the log-log scale for simple and stiffened plates respectively for steel Grade A. The far field stress on the plate was 80 MPa. It should be observed that for both simple plate and stiffened plate, even though the probability of fracture differs by less than one order of magnitude between T-L and L-T orientations at $10^{-4}\ s^{-1}$, this difference disappears completely for -25°C or remains fairly constant for both -70°C and $+22^{\circ}$C. For low temperature (-70°C) there is no effect of strain rate on the probability of fracture since there is no change of fracture toughness with strain rate (see Section 6.1.4). It seems that the insensitivity of the probability of fracture to strain rate at low temperature is due to the fact that fracture toughness reached its minimum value (lower shelf). Also, it should be observed that the effect of stiffening in reducing the probability of fracture is about ten times higher than the effect of change in orientation of the specimens at low strain rates. At high strain rates, the effect of stiffening gets less pronounced.

Figure 7.12 shows sensitivity factors for individual quantities as functions of strain rate for A grade steel T-L orientation at -25°C. At low strain rates, the probability of unstable fracture is sensitive to CTOD, CTOD factor (see Ia p.45), crack

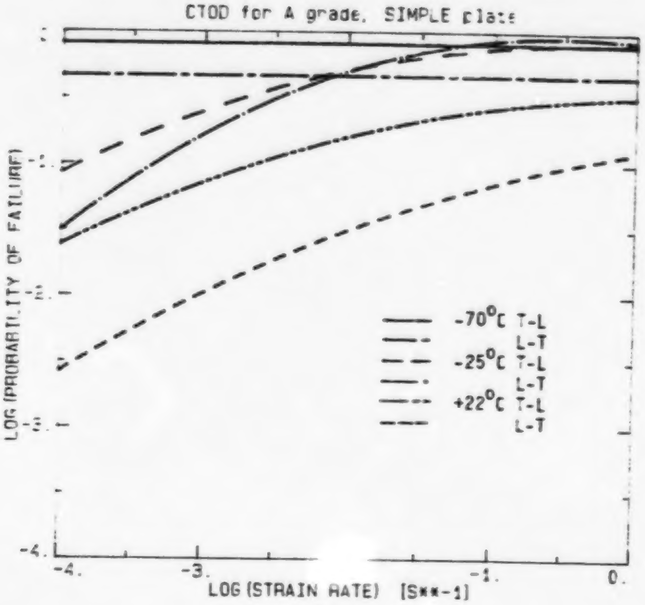

Figure 7.10: Probability of Fracture as a Function of Strain Rate for Simple Plate, Grade A Steel

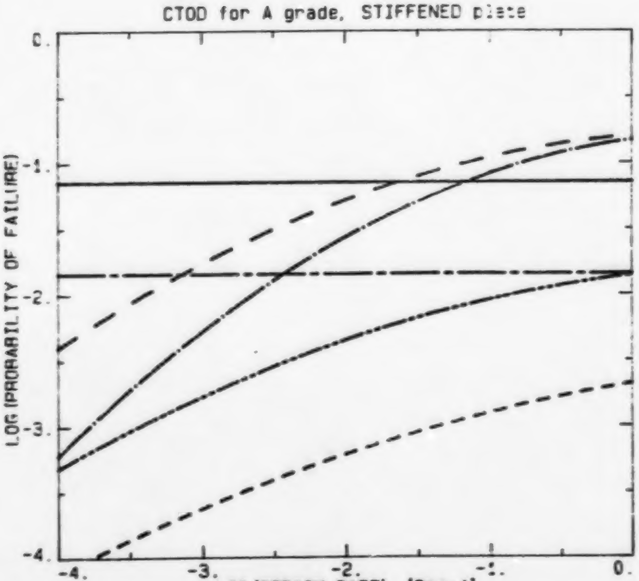

Figure 7.11: Probability of Fracture as a Function of Strain Rate for Stiffened Plate, Grade A Steel

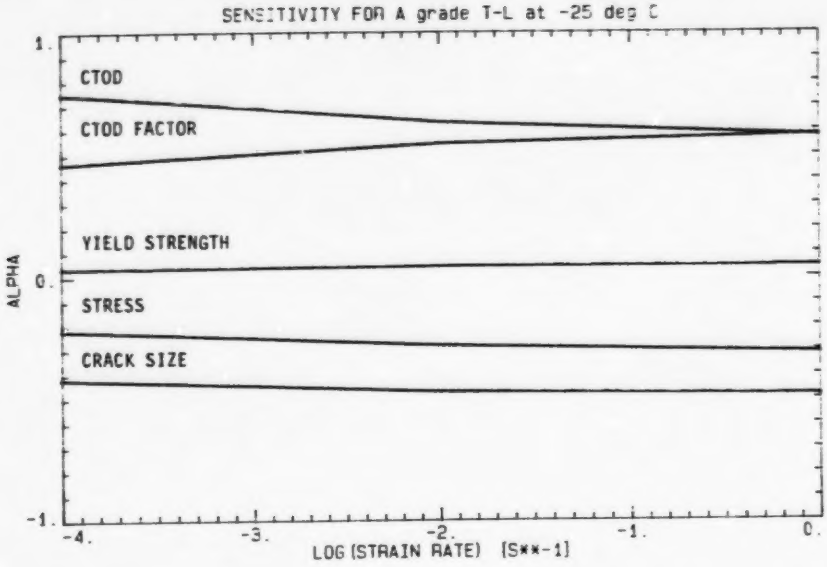

Figure 7.12: Sensitivity Factors vs Strain Rate for A Grade Steel at -25°C (T-L orientation)

Figures 7.13 and 7.14 show that the probability of unstable fracture is very little dependent on strain rate.

From the results presented it can be concluded that lower temperature and higher strength reduce the effect of strain rate on the probability of unstable fracture. This important conclusion should be understood in the context of the limited scope of the present study.

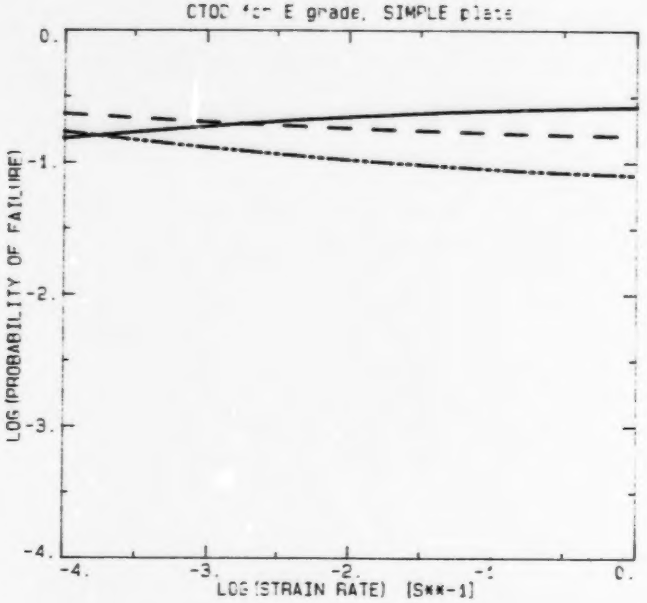

Figure 7.13: Probability of Fracture as a Function of Strain Rate for Simple Plate, Grade E36 Steel

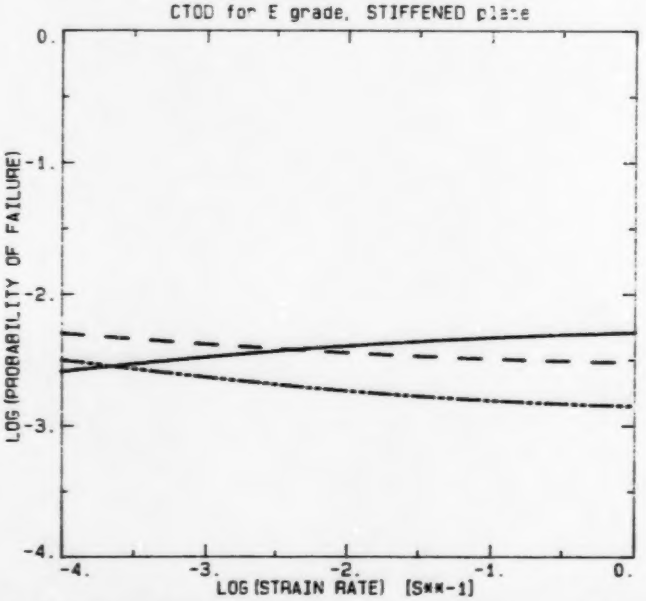

Figure 7.14: Probability of Fracture as a Function of Strain Rate for Stiffened Plate, Grade E36 Steel

Effect of Thickness

The effect of thickness on fracture toughness (transition between plane stress and plane strain states at the crack tip) is a well recognized phenomenon. The data presented in section 6.1.3 was used to simulate unstable fracture in the simple plate and stiffened plate structural elements assuming the crack size distribution found in tankers, under a far field stress of 80 MPa.

Figure 7.15 presents the curves demonstrating the dependance of the probabilities of unstable fracture on plate thickness for A Grade steel. It can be observed that at low temperature (-40°C), the "upper shelf" in the failure probability is reached at approximately 35 mm thickness, while this plateau is reached at about 100 mm at -10/-20°C. At 100 mm thickness there is a negligible difference between the probabilities of failure at -40°C and -10/-20°C.

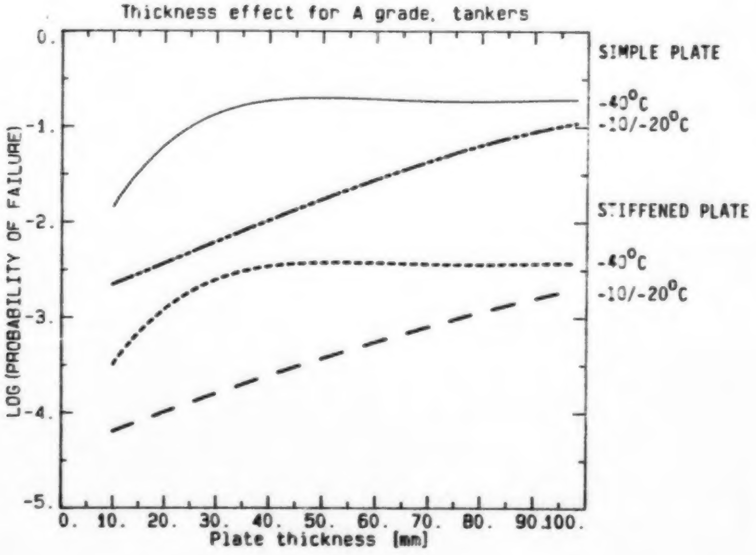

Figure 7.15. Probability of Failure as a Function of Thickness at -40°C and -10/-20°C

These conclusions are further illustrated in Figures 7.16 and 7.17. Figure 7.16 for -10/-20°C shows that the probability of fracture is most sensitive to the CTOD factor and crack size and that the sensitivity to individual variables changes ("redistributes") throughout the entire thickness range. Figure 7.17 shows that at -40°C the sensitivity to all random quantities remains constant at t 30mm.

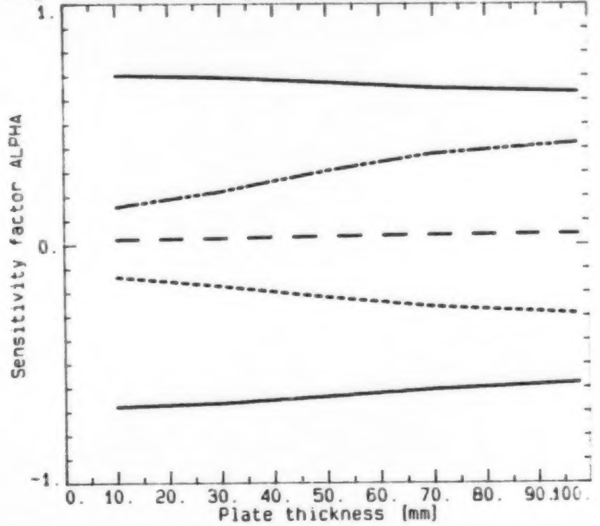

Sensitivity Factors vs Plate Thickness for Simple Plate at -10/-20°C

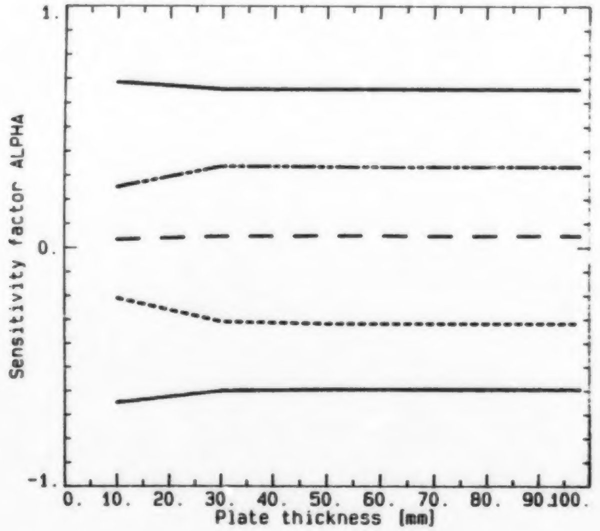

Figure 7.17

Sensitivity Factors vs Plate Thickness for Simple Plate at -40°C

7.1.2 Probability of Plastic Collapse

The failure by plastic collapse was implemented in the probabilistic models developed. Some results for the probability of plastic collapse of structural elements are presented, however, these results should be interpreted with caution. The structural (plate) elements considered here are surrounded by other elements which would support the redistributed load due to plastification and considerably lower the probabilities of plastic collapse of the structural elements.

Figure 7.18 compares the probability of plastic collapse for simple plate and three levels of far-away stress as a function of temperature. The probabilities of failure are very high (approximately 30% at 0°C and 80 MPa stress) and decrease slightly with decreasing temperature due to the increase of the yield strength with decreasing temperature (see Figure 6.24).

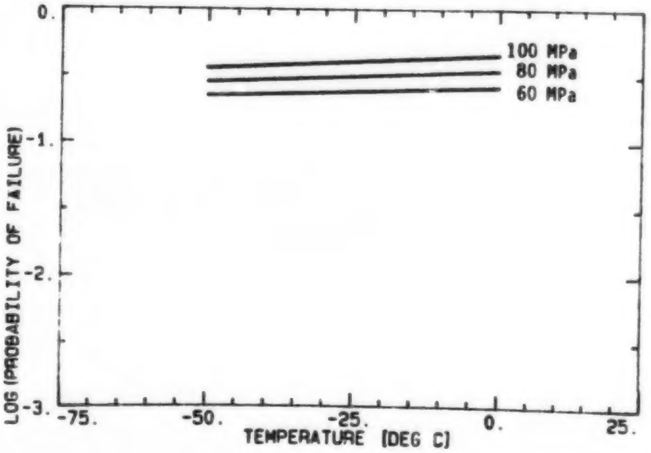

Figure 7.18

Probability of Plastic Collapse as a Function of Temperature

7.1.3 Probability of Failure Considering Unstable Fracture or Plastic Collapse

The probability to obtain failure under either unstable fracture or plastic collapse (called here combined probability of failure, see Eq. 5.32) of failure is calculated as shown in Section 5.4. In PROBAN, this case is treated as a series of two "components", one for unstable fracture and the other one for plastic collapse.

Considering that the probability of plastic collapse for the given examples is much higher than that of unstable fracture, the combined probability of failure would be close to that of plastic collapse.

7.2 Probability of Failure Due to Fatigue Crack Propagation

7.2.1 Simple Plate

Figure 7.19 shows probabilities of failure for unstable fracture and plastic collapse treated as separate events for a far-away stress of 60 MPa as a function of number of years in service. The probability of failure is not sensitive to temperature variation. This is shown by the sensitivity factors in Figure 7.20.

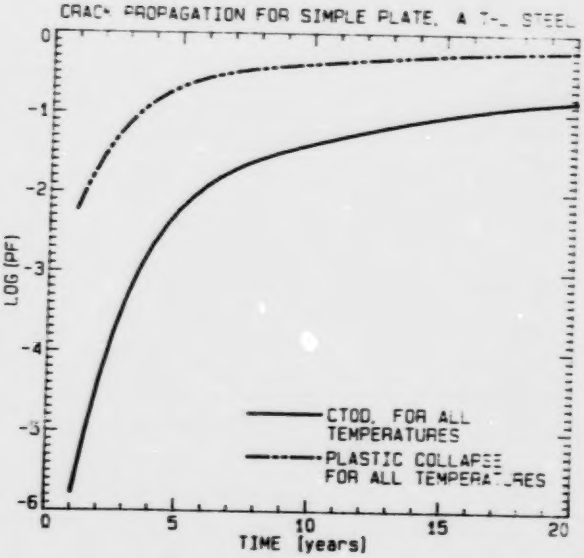

Figure 7.19 Probability of Failure for Unstable Crack Propagation and Plastic Collapse due to Fatigue for A Grade T-L Steel

This Figure shows that the sensitivity of the probability of failure to the two parameters which are influenced by temperature, namely the critical CTOD and the yield strength, is very low. The reason for this low sensitivity can be seen from the formulation of the limit state function and from the values of the random parameters (quantities), associated with the calculation of the probability of failure, at the design point (see Section 3.3). Failure occurs when the actual crack size reaches the critical crack size for unstable fracture.

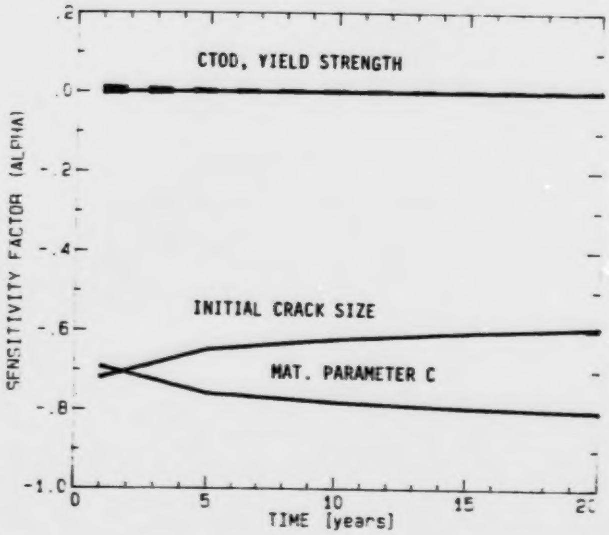

Figure 7.20 Sensitivity Factors as a Function of Time in Service

The actual crack size is obtained by the fatigue propagation of the initial surface crack under cyclic loads of given magnitude and frequency. Since the load effect is described by the number of loading cycles, failure occurs when this number reaches the number of cycles necessary to increase the initial crack size to the critical crack size (see Section 5.3).

The fatigue crack growth occurs in two phases: a) through-thickness fatigue growth of a surface crack; and b) fatigue growth of a through-thickness crack to the critical crack size. During the first phase the surface crack grows through the thickness of the plate to result in a crack of fixed size which depends on the plate thickness and assumed crack geometry (see Section 6.3.3). It was assumed in the calculation that a/2c = 0.4 leading to a through-thickness crack size of 2.5T (T = thickness of the plate). This is the starting dimension of the through-thickness crack size for the second phase. (The critical crack size is always larger than the thickness dimension of the plate and therefore there is no contribution to the probability of failure from this phase, making it temperature independent).

Furthermore, the critical through-thickness crack size at the design point varies relatively little with temperature (e.g. 2443, 2397 and 2029mm at 0, -10 and -30°C respectively). Also, the effect of randomness in the fatigue crack growth parameter C needs to be taken into account. 100% variation of C is commonly accepted (DnV, 1984b). This effect is demonstrated in Figure 7.21. It can be seen that when the critical crack size is such that it falls in the steep (unstable) region of the fatigue crack propagation, the probability of unstable fracture would not be noticeably affected by variation of the critical crack size.

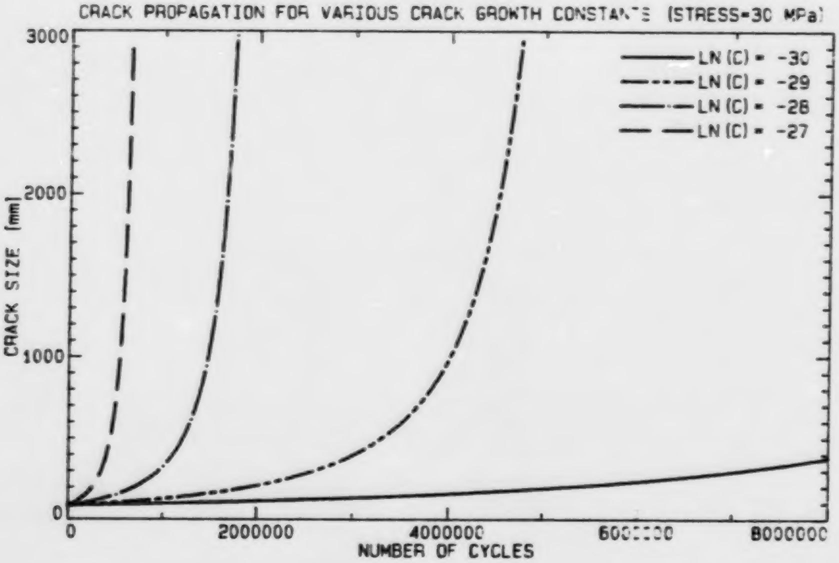

Figure 7.21 Crack Growth as a Function of the Number of Cycles for Various C

This can be further exemplified on a case with an increased far-away stress to 200 MPa, Figure 7.22. Even though there is a slight difference between the curves for various temperatures, the probabilities of failure remain very close to those obtained for far-away stress of 60 MPa, Figure 7.19. This is so despite the fact that the critical crack size decreased approximately ten times.

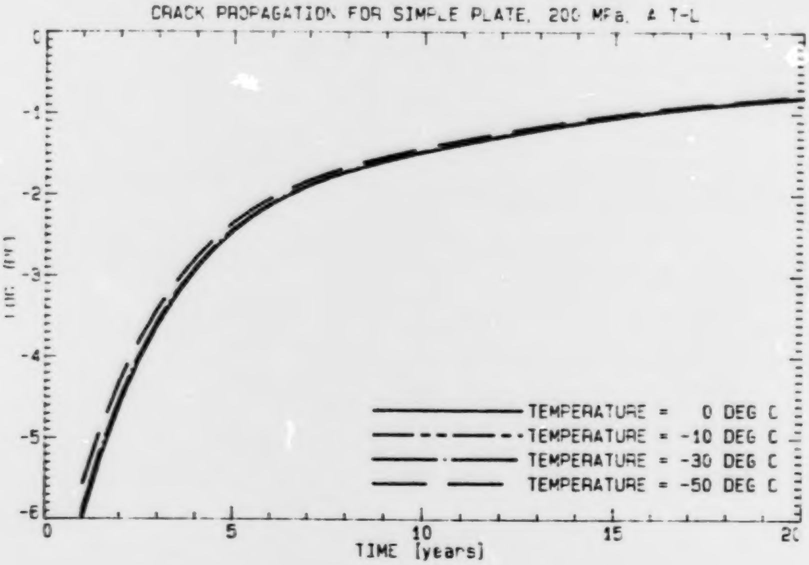

Figure 7.22 Probability of Unstable Fracture for Simple Plate at 200 MPa Far-Away Stress

7.2.2 Welded T-Joint

In the case of the welded T-joint, the stress concentration factor of 1.5 and the residual stress factor of 0.7 increase considerably the probability of unstable fracture, Figure 7.23. Also, for A Grade steel in T-L direction the temperature effect on the probability of failure becomes more pronounced. This is due to a faster growth of the surface crack through the thickness of the plate and to a considerably smaller critical crack size.

Figure 7.24 shows the probability of plastic collapse for the T-joint. As can be seen the probability of plastic collapse is independent of temperature.

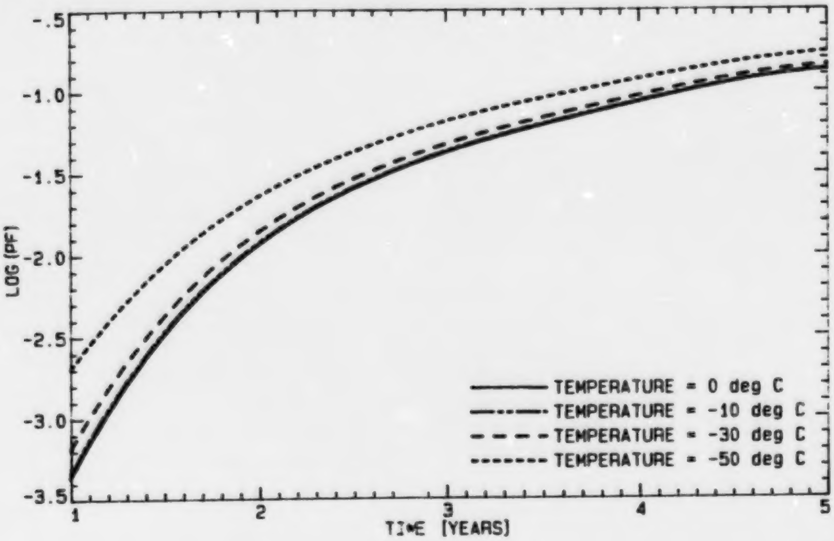

Figure 7.23 Probability of Unstable Fracture for WeldedT-Joint at Far-Away Stress 60 MPa

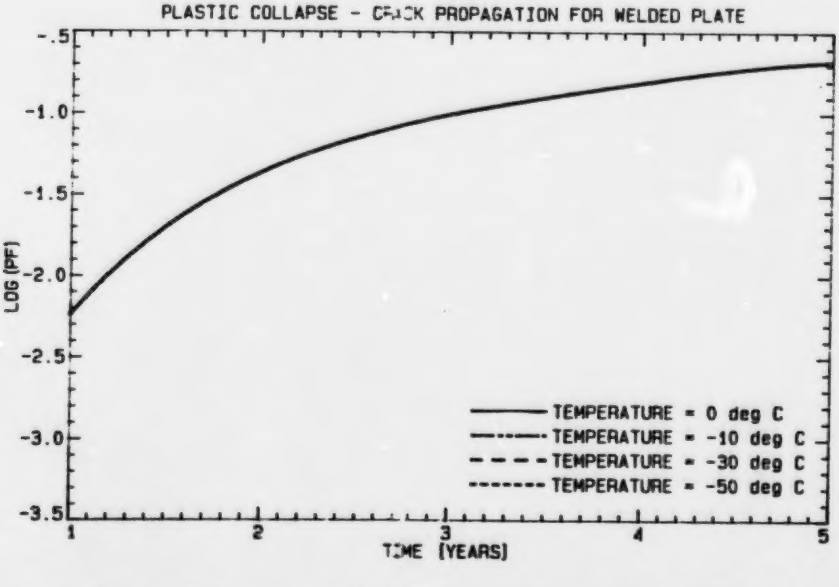

Figure 7.24 Probability of Plastic Collapse for the Welded T-Joint at 60 MPa Far-Away Stress

Still, the probability of unstable fracture is most sensitive to the crack growth parameter C and the initial crack size. Figure 7.25 shows sensitivity factors for individual random quantities at -50°C for A Grade steel in T-L direction.

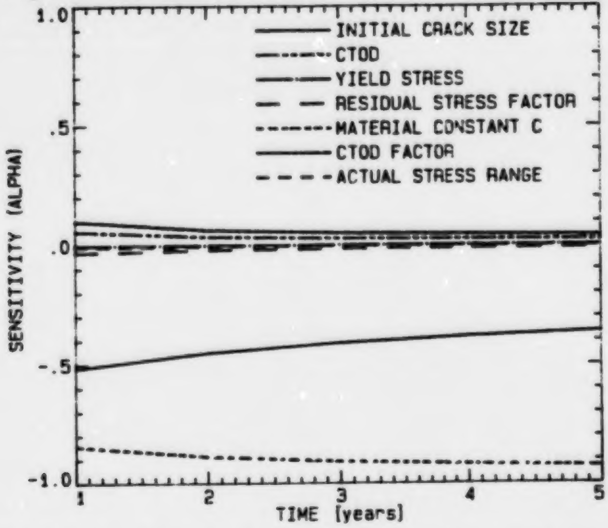

Figure 7.25 Sensitivity Factors as a Function of Time at -50°C for Welded T-Joint and A Grade T-L Steel

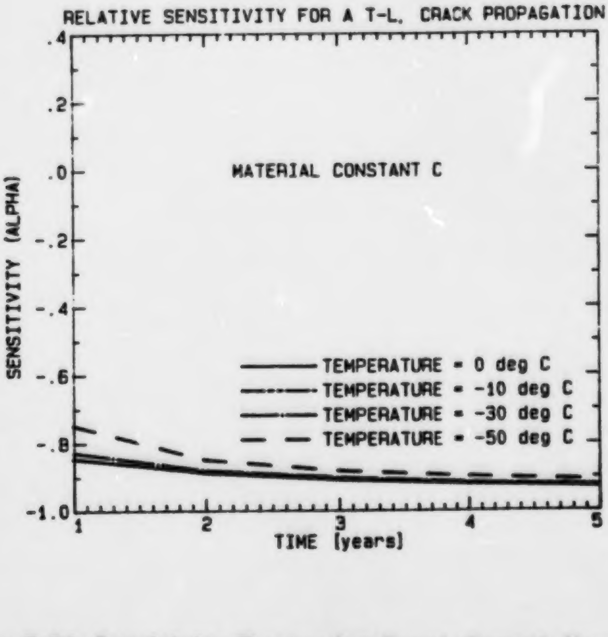

Figure 7.26 Sensitivity Factor for Crack Growth Parameter C

Figures 7.26 to 7.32 show sensitivity factors as a function of time in service for four different temperatures. It can be seen that the effect of the crack growth parameter C is only slightly affected by temperature and increases with increasing service time. The effect of the initial crack size is very pronounced and slightly decreases with time. Also, temperature has only very small effect on the sensitivity to this random quantity.

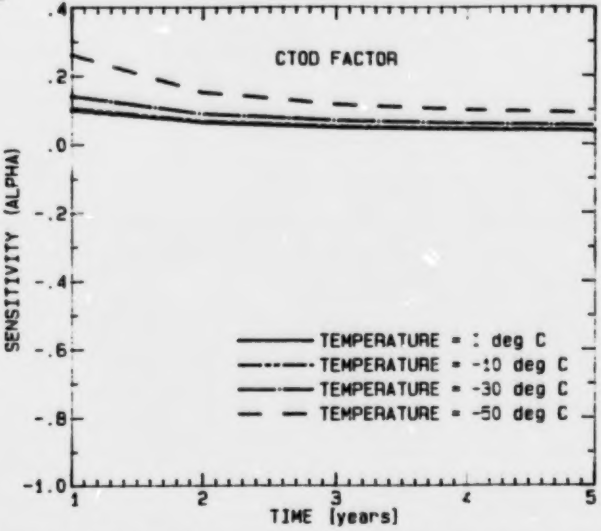

Figure 7.27 Sensitivity to the CTOD Factor

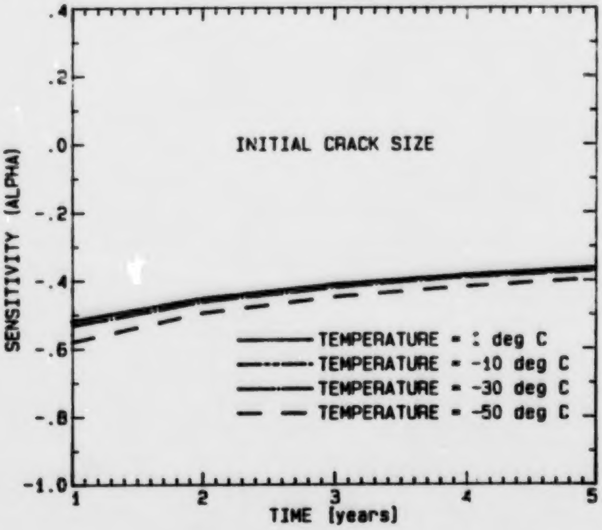

Figure 7.28 Sensitivity to the Initial Crack Size

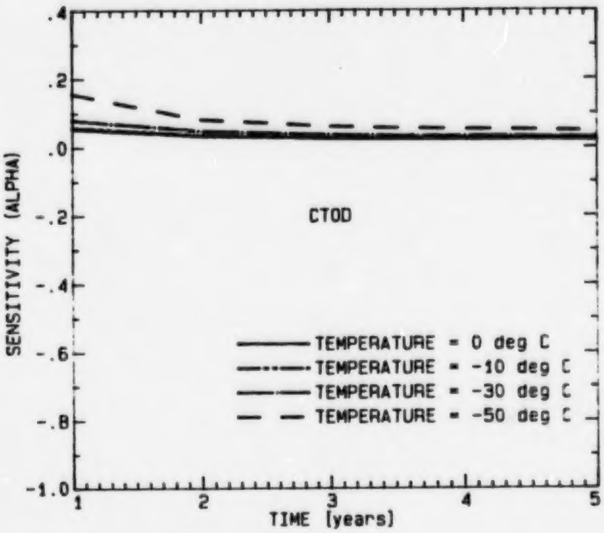

Figure 7.29 Sensitivity to CTOD

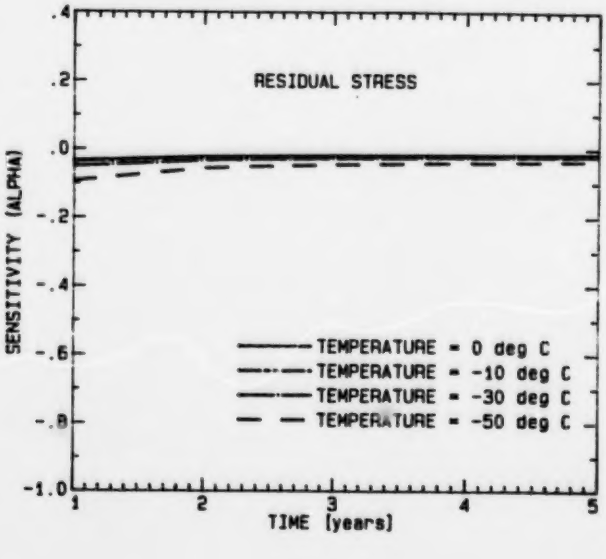

Figure 7.30 Sensitivity to Residual Stresses

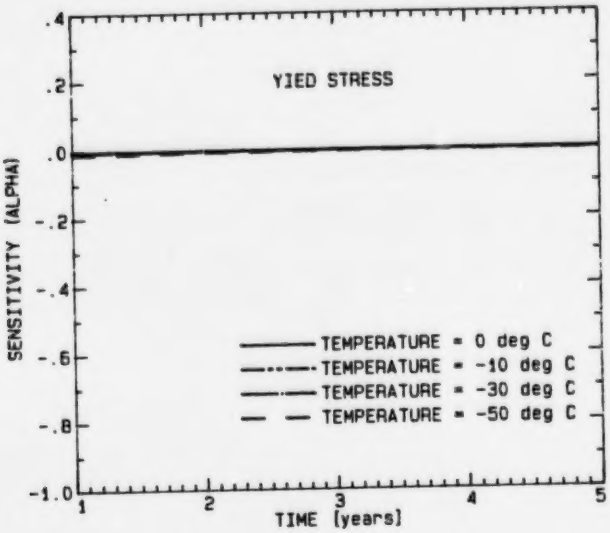

Figure 7.31 Sensitivity to Yield Stress

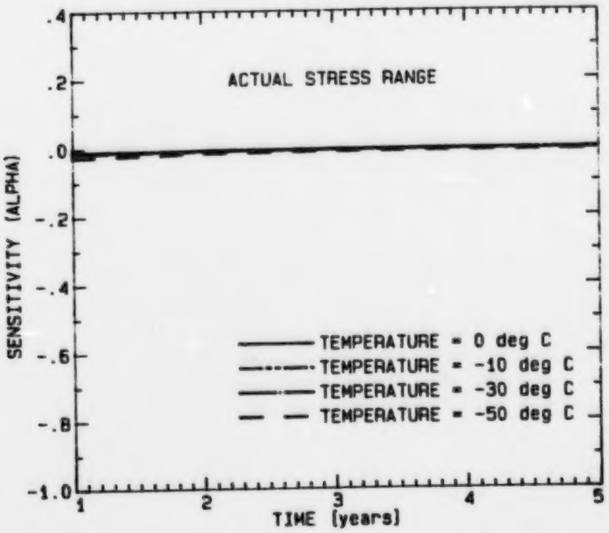

Figure 7.32 Sensitivity to Actual Stress Range

7.3 Probability of Crack Arrest

To study the crack arrest capabilities of EH36 and EH36 Modified steels (see Section 6.1.5), it was assumed that unstable fracture initiates in a lower toughness steel and propagates to reach the width dimension of the strip (frame spacing) before entering the crack arresting steel. Figure 7.33 shows the probability of crack arrest as a function of width (crack size) and temperature for both the standard EH36 as well as the Modified EH36 Grade steel.

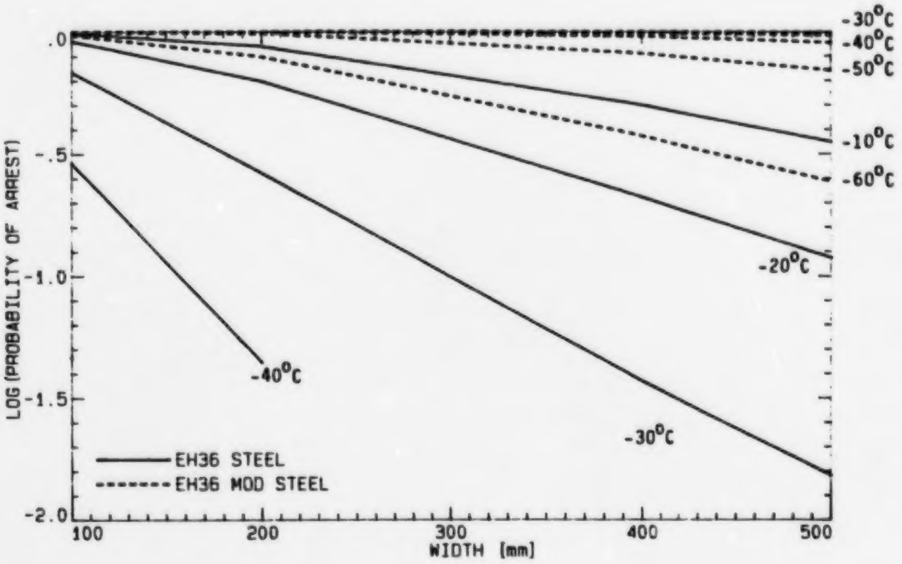

Figure 7.33 Probability of Crack Arrest in EH36 and EH36 Modified Grades

As can be seen from this figure, EH36 has a higher than 50% probability of arresting the crack only down to -10°C with the spacing of the crack arresting strakes w = 300mm. The Modified EH36, however, has a higher than 90% probability level at -50°C for the same configuration.

8. CONCLUDING REMARKS AND RECOMMENDATIONS FOR FUTURE WORK

1. The study showed that probabilistic modelling of such failure modes as plastic collapse or unstable fracture is numerically possible for structural elements, provided that the following is known:

   - elastic characteristics of the element (stress-intensity factor and stress concentration factor);

   - material characteristics of the element (fracture toughness as a function of temperature, strain rate, thickness, etc.);

   - loading characteristics (far-away stress, stress range);

   - fabrication characteristics (initial flaw-size, residual stresses).

2. The limit state function SUBROUTINES DEVELOPED FOR PROBAN handled well numerical iteration processes for complicated stress-intensity factors and stress concentration factors.

3. The investigation of the probability of failure based on measured crack distribution at regular intervals showed that the ship structure is very tolerant to cracks. High probabilities of failure of individual plate elements ($\sim 10^{-1}$) are tolerated without causing catastrophic failure of the whole ship. This reflects the positive effect of structural redundancy in terms of increased target probabilities of failure. The probability of failure here is the two-yearly probability of failure since the crack distribution used was obtained from the two-yearly survey of tankers.

4. The effect of stiffeners on the probability of failure is considerable. The reduced stresses in the plate due to the presence of stiffeners reduce the probability of failure by approximately one order of magnitude.

5. The effect of temperature on the probability of unstable fracture is a reflection of the effect of temperature on fracture toughness. It is interesting to notice that if we accept E36 T-L at 0°C in the static loading regime (probability of failure 0.08) then all steels would perform well down to -43°C, Figure 8.1. This surprising conclusion is a result of very poor toughness properties of the E36 steel in the T-L direction in comparison to other steels investigated.

6. For very low temperatures, when minimum fracture toughness was reached, probability of unstable fracture is insensitive to variation in strain rate. At higher tempeatures, the strain rate variation from low (10^{-4} s^{-1}) to high (100 s^{-1}) causes about one order of magnitude difference in corresponding probabilities of unstable fracture for A Grade steel. The effect is less for E36 Grade steel.

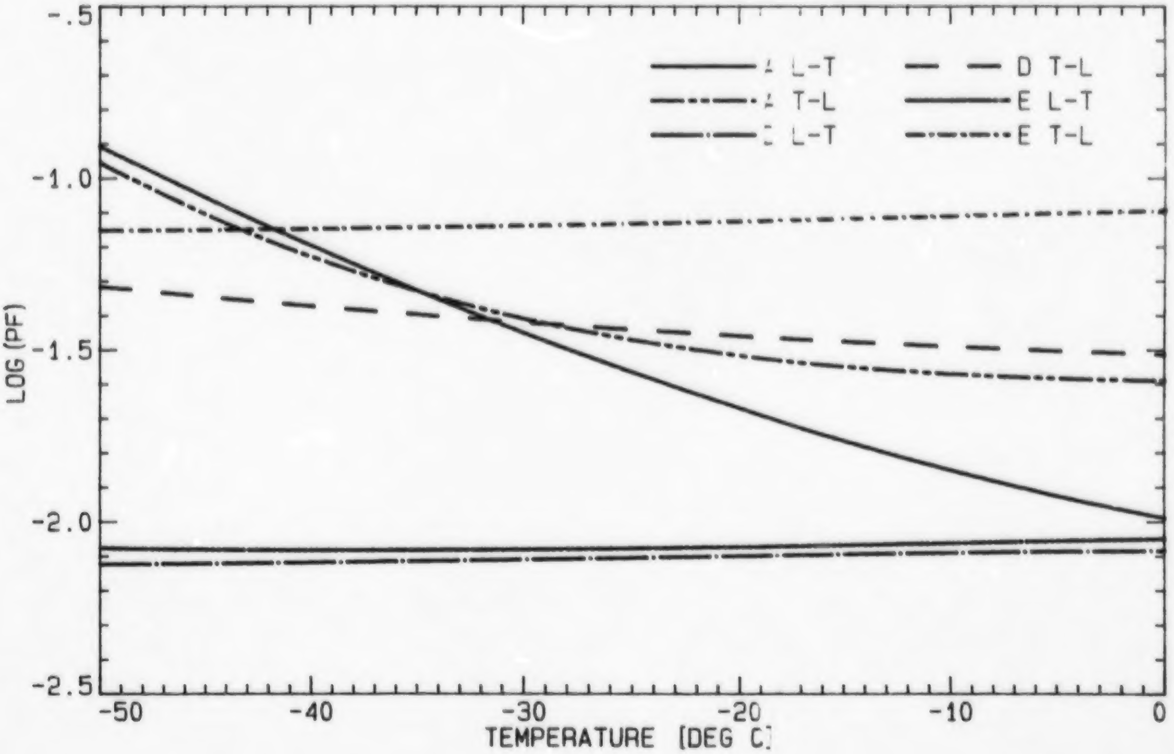

Figure 8.1. Comparison of Probabilities of Unstable Fracture for A, D and E36 Hull Steels as a Function of Temperature

7. Probability of unstable fracture increases by about one order of magnitude in the transition from plane-stress to plane-strain fracture toughness.

8. When fatigue growth of cracks is considered, the temperature effect on the probability of fracture is suppressed by its high sensitivity to the crack growth parameter C and initial flaw size.

9. Material selection criteria should be integrated with the limit state design procedure for structures. It is quite clear that structural redundancy, manufacturing process, load conditions and functional requirements are factors that affect both structures and materials.

10. In view of the interest of designers and fabricators to use extra high strength steels for arctic structures, it is desirable to study the sensitivity of the probability of unstable fracture to various parameters for this family of steels and compare it with traditional normal and high strength steels such as those used in this study.

11. It would be appropriate to class structural elements according to their stress concentration factor and stress intensity factor so that probabilities of failure could be graphically presented for each class of elements.

12. Data base on material and structural performance is needed to validate and improve probabilistic models.

REFERENCES

ABRAHAMSEN, E., NORDENSTROM, N., and ROREN, E.M.Q., (1970), "Design and Reliability of Ship Structures", Spring Meeting, SNAME, Washington, April 1 - 3.

ALMAR-NAESS, A. et al (1985), "Fatigue Handbook - Offshore Steel Structures", Edited by A. Almar-Naess, Tapir Publishing.

ANTONIOU, A.C. (1977), "A Survey on Cracks in Tankers Under Repairs", PRADS -Int. Symp. on Practical Design in Shipbuilding, Tokyo, October.

BISHOP, T.A., MARKWORTH, A.J., and ROSENFIELD, A.R. (1983), "Analyzing Statistical Variability of Fracture Properties", Metallurgical Transactions A, Vol. 14A, April, pp. 687-693.

BISHOP, T.A., RUST, S.W., and TODT, F.R. (1985), "Estimation of Weibull Percentiles Using a Two-Stage Least Squares Procedure", Batelle Columbus Division, Unpublished Report.

BOE, C., JORGENSEN, I., MATHIESEN, T.C., and ROREN, E.M.Q., (1974), "Reliability Design Criteria for Shipping Industry", ASME Winter Annual Meeting, November.

BOKALRUD, T., and Karlsen, A. (1982), "Control of Fatigue Failure in Ship Hulls by Ultrasonic Inspection". Norwegian Maritime Research, NO. 1, pp. 9-15.

BOOTH, E.T., (1981), "SL-7 Extreme Stress Data Collection and Reduction", SSC-304.

BOYD, G.M. (1969), "Fracture Design Practices for Ship Structures", Fracture Vol. V, Chapter 6, Edited by H. Liebowitz, Academic Press.

BS5762 (1979), "Methods for Crack Opening Displacement (COD) Testing", British Standard Institute.

BURDEKIN, F.M., and DAWES, M.G. (1971), "Practical Use of Linear Elastic and Yielding Fracture Mechanics with Particular Reference to Pressure Vessels". Proc. Inst. Mech. Eng. Conf., London, pp. 28-37.

CHANGE, P.Y., and CARROL, T.P., (1981), "Investigation of Steels for Improved Weldability in Ship Construction - Phase II" by P.Y. Change and T.P. Carrol, SSC-305.

CIRIA (1977), "Rationalization of Safety and Serviceability Factors in Structural Codes". Construction Industry Research and Information Association, CIRIA Report No. 63, London.

COMITE EURO-INTERNATIONAL DU BETON, (1976), "First Order Reliability Concepts for Design Codes", Bulletin D'Information No. 112, Munich, July.

COMITE EURO-INTERNATIONAL DU BETON, (1978), "Common Unified Rules for Different Types of Construction and Material", Bulletin D'Information No. 124E, Paris, April.

CROSSLEY, P.B., and RIPLING, E.J., (1980), "Comparison of Crack Arrest Methodologies", Crack Arrest Methodology and Applications, ASTM STP711, Editors G.T. Hahn and M.F. Kanninen, pp. 211-227.

DEPARTMENT OF ENERGY (DOE) (1986), "Offshore Installations: Guidance on Design and Construction".

DET NORSKE VERITAS, (1984a), "Rules for Classification of Steel Ships". Part 3, Ch. 1.

DET NORSKE VERITAS, (1984b), "Fatigue Strength Analysis for Mobile Offshore Units", Classification Note No. 30.2.

DET NORSKE VERITAS, (1977), "Rules for the Design, Construction and Inspection of Offshore Structures".

DET NORSKE VERITAS, (1983), M.V. Arctic Steel Grades.

DIADOLA, J.C., and BASAR, N., (1981), "Probabilistic Structural Analysis of Ship Hull Longitudinal Strength", SSC - 301.

DIAMANTIDIS, D., (1986), "Reliability Aspects for Design and Redesign of Offshore Structures", Proceedings, OMAE, Tokyo, Japan.

FAIN, R.A., and BOOTH, E.T. (1979), "Results of the First Five 'Data Years' of Extreme Stress Scratch Gauge Data Collected Aboard Sea Land's SL-7's", SSC - 286.

FAUCHER, B., and TYSON, W.R. (1988), "A Study of Variability, Size and Temperature Effects on the Fracture Toughness of an Arctic-Grade Steel Plate". Fracture Mechanices, Eighteenth Symposium, ASTM STP 945, Philadelphia.

FAULKNER, D., (1981), "Semi-Probabilistic Approach to the Design of Marine Structures", Extreme Loads Symposium, SNAME, Arlington, October 19 - 20, pp. 213 - 230.

FJELD, S. (1976), "Basis for the Choice of Partial Safety Factors for Offshore Structures", VERITAS Rep. No. 54-90-10.

FJELD, S., ANDERSEN, T., and MYKLATUN, B. (1978), "Risk Analysis of Offshore Production and Drilling Platform". OTC Paper No. 3152, May 8-11, Houston, Texas.

FLINT, A.R., (1979), "The Treatment of Safety for Marine Structures Design Codes", International Symposium on Advances in Marine Technology.

FLINT, A.R., and BAKER, M.J. (1977), "Risk Analysis of Offshore Structures - The Aims and Methods". Proc. on Design and Construction of Offshore Structures". Inst. Civil Eng., London, pp. 87-90.

FURNES, O., and SELE, A., (1981), "Offshore Structures - Implementation of Reliability", Extreme Loads Symposium, SNAME, Arlington, October 19 - 20, pp. 213 - 230.

HARRISON, J.D. (1981), "Material Selection Consideration for Offshore Steel Structures", Paper PS3, Steel in Marine Structures Conference, Commission of the European Communities, Paris, October.

HASOFER, A.M., and LIND, N.C., (1974), "Exact and Invarient Second Moment Code Format", Journal of the Engineering Mechanics Division, ASCE, Vol. 100, No. EMI, February, pp. 111 - 121.

HUTCHINSON, B.L., (1981), "Risk and Operability Analysis in the Marine Environment", SNAME Transactions, Vol. 89, pp. 127 - 154.

INGHAM, T., and HARRISON, R.P. (1981), "A Comparison of Published Methods of Calculation of Defect Significance", Fitness for Purpose Validation of Welded Construction Symp., Paper 46, London, Nov. 17-19.

INTERNATIONAL ASSOCIATION OF CLASSIFICATION SOCIETIES (IACS) (1980), Recommendation No. 7, "Guide for the Use of Hull Structural Steels for Prolonged Exposure to Low Service Temperatures".

INTERNATIONAL ASSOCIATION OF CLASSIFICATION SOCIETIES (IACS) (1979), "Normal and High Strength Structural Steels", W11.

INTERNATIONAL SHIP STRUCTURES CONGRESS, (1987), "Ductile Collapse", ISSC Committee III.1, ISSC '88, Rev. 3, September.

IYER, S.H., TAYLOR, K.V., ASH, P. and GAUTHIER, G., (1980), "A Review of Steel Properties at Low Temperatures", Fenco Report No. 5883 for Transportation Development Centre, December.

JORDAN, C.R., and COCHRAN, C.S., (1978), "In-Service Performance of Structural Details", SSC-272.

JORDAN, C.R., and KNIGHT, L.T., (1979), "Further Survey of In-Service Performance of Structural Details", SSC-294.

KAMATH, M.S. (1981), "The COD Design Curve: An Assessment of Validity Using Wide Plate Tests". Int. J. Press. Vessels and Piping, Vol. 9, No. 2, pp. 79-105.

KARLSEN, A., (1979), "Fracture Toughness of Heavy Welded Joints", DnV Report No. 79-0448.

KARLSEN, A., and FIDJESTOEL, P., (1983), "Evaluation of Steel Grades for M.V. Arctic", DnV Report No. TP4516 for Transportation Development Centre and Canarctic Shipping, March.

LABAS, G., and BERGEZ, D., "A Probabilistic Approach to Crack Initiation", (1986), OMAE, Tokyo, Japan, pp. 56 - 63.

LARSSON, T.-B., LEREIM, J., and SAETHER, S. (1983a), "Influence of Strain Rate on J- and COD-Fracture Toughness of Steel Plates of DnV Qualities NVA, NVD and NVE36", DnV Report No. 83-0194.

LARSSON, T.-B., SLATCHER, S., and LEREIM, J. (1983b), "Influence of PWHT on COD-Fracture Toughness of a C-Mn Structural Steel Weldment", DnV Report No. 83-0060.

LINDEMAN, K., ODLAND, J., and STRENGEHAGEN, J. (1977), "On the Application of Hull Surveillance Systems for Increased Safety and Improved Structural Utilization in Rough Weather". SNAME Publication No. 3.

MADSEN, H.O., KRENK, S., and LIND, N.C. (1986a), "Methods of Structural Safety". Prentice-Hall.

MADSEN, H.O., SKJONG, R., and MOGHTADERI-ZADEH, M., (1986b), "Experience on Probabilistic Fatigue Analysis of Offshore Structures", OMAE, Tokyo, Japan, Vol. pp. 1 - 8.

MADSEN, H.O., SKJONG, R., and KIRKEMO, F. (1985), "Assessment of Pipeline Reliability Under the Existence of Scour Induced Free Spans", Appendix E: Probabilistic Analysis. VERITAS Rep. 85-1039.

MAES, M.A., and JORDAAN, I.J., (1986), "Arctic Environmental Design Using Short Data Extremal Techniques", OMAE, Tokyo, Japan, Vol. IV, pp. 13 - 19.

MANSOUR, A., (1974), "Approximate Probabilistic Method of Calculating Ship Longitudinal Strength," Journal of Ship Research, Vol. 18, No. 3, September, pp. 203 - 213.

MANSOUR, A.E., JAN, H.Y., ZIGELMAN, C.I., CHEN, Y.N., and HARDING, S.J., (1984), "Implementation of Reliability Methods to Marine Structures", SNAME Transactions, Vol. 92, pp. 353 - 382.

MELVE, B., LARSSON, T.-B., and LEREIM, J. (1983), "Fast Fracture-Crack Arrest Testing of a Ship Hull Steel of DnV Quality NVE36 and Pipeline Steel Type 5LX-X65", DnV Report No. 83-0349.

MUNSE, W.H., WILBUR, T.W., TELLALIAN, M.L., NICOLL, K., and WILSON, K. (1982), "Fatigue Characterization of Fabricated Ship Details for Design", SSC - 318.

NAKANO, N., BESSYO, K., TOYOSADA, M., MIYAZAKI, T., and Fujii, E., (1987), "High Strength Steel Plate for Ice-Breaking Vessels Produced by Thermo-Mechanical Control Process", Int. Symp. on Fracture Sponsored by CIM, Winnipeg, Manitoba, August 23 - 26.

OCHI, M.K., (1981), "Principles of Extreme Value Statistics and their Application", Extreme Loads Symposium, SNAME, Arlington, October 19 - 20, pp. 15 - 30.

ODLAND, J., (1975), "Modes of Failure in Ship Structures", Veritas Report No. 75-308. December.

OLDFIELD, W. (1975), "Curve Fitting Impact Test Data: A Statistical Procedure", ASTM Standardization News, November, pp. 24-29.

OLSEN, K., and BRATFOS, H.A., (1982), "Fracture Mechanics Analysis of a Proposed LPG Storage Vessel Design", Veritas Report No. 82-0772, August.

PARIS, P.C., and ERDOGAN, F. (1963), "A Critical Analysis of Crack Propagation Laws". J. Basic Eng, ASME, Vol. 85, pp. 528-534.

PD6493 (1980), "Guidance on Some Methods for the Derivation of Acceptance Levels for Defects in Fusion Welded Joints", Published Document, British Standard Institution.

PENSE, A.W., (1981), "Evaluation of Fracture Criteria for Ship Steels and Weldments", SSC - 307.

PISARSKI, H.G. (1983), "The CTOD Approach to the Specification of Fracture Resistant Welded Steel Structures for Arctic Service", Proc. The Study Session on Fracture Toughness Evaluation of Steels for Arctic Marine Use, Ottawa, Edited by R. Thomsom and C.S. Champion.

RACKWITZ, R. (1976), "Principles and Methods for a Practical Probabilistic Approach to Structural Safety", Sub-Committee for First Order Reliability Concepts for Design Codes of the Joint CEB-CECM-CIB-FIP-IABSE Committee on Structural Safety. CEB Bulletin No. 112.

RACKWITZ, R., and FIESSLER, B. (1978), "Structural Reliability Under Combined Random Load Sequences". Computers & Structures, Vol. 9, pp. 489-494.

ROLF, S.T., and BARSOM, J.M., (1977), "Fracture and Fatigue Control in Structures", Prentice-Hall, Inc.

ROOKE, D.P., and CARTWRIGHT, D.J. (1976), "Compendium of Stress Intensity Factors". Hillingdon Press.

RØREN, E.M.Q., MADSEN, H.O., and LEREIM, J. (1986), "Implementation of Reliability Concepts in Classification Rules". 5th Int. Symp. & Exhibit of Offshore Mechanics and Arctic Eng., OMAE 1986, Tokyo.

SAETHER, S. (1980), "Fracture Toughness of Ship Plates NVA, NVD, NVE36", DnV Report No. 80-1014.

SHIP STRUCTURES COMMITTEE, SNAME, (1978), "The Effect of Strain Rate on the Toughness of Ship Steels", SSC - 275.

SOREIDE, T.H., (1981), "Ultimate Load Analysis of Marine Structures", Tapir, Trondheim.

SOVAK, J.F., CALDWELL, J.W. and SHOEMAKER, A.K., (1981), "Fatigue and Fracture Toughness Characteristics fo SAW and SMA A537 Class I Ship Steel Weldments", SSC-303.

SUKSELAINEN, J., and KUJALA, P., (1983), "Brittle Fracture Risk Assessment of M.V. Arctic", VTT Report No. LAI348G/83 for Canadian Coast Guard, June.

TOMIN, M., and LANTOS, S. (1986), "Evaluation of Fracture Toughness Data with Respect to Reliability of Subarctic and Arctic Structures", DnV Rep. No. CGY/86-049.

TVEDT, L. (1983a), "PROBAN Technical Manual", Veritas Rep. No. 83-0880.

TVEDT, L. (1983b), "PROBAN Users Manual", Veritas Rep. No. 83-0865.

TYSON, W.R., and MARANDET, B., (1988), "Cleavage Toughness Variability and Inclusion Size Distribution of a Weld Metal". Fracture Mechanics, Eighteen Symposium, ASTM STP 945, Philadelphia.

UEG 1985, "Design of Tubular Joints for Offshore Structures", Underwater Engineering Group, London, Volumes 1-3.

WATANABE, M., HOSOKAWA, Y., NAKANO, N., INAMI, A., and OHNISHI, K., (1986), "High Strength Ship Plate (YS36kgf/mm^2, 32kgf/mm^2 Grade) Manufactured by DAC Process", The Sumitomo Search No. 32, May.

WONG, W.K., and ROGERSON, J.H (1983), "A Probabilistic Estimate of the Relative Value of Factors Which Control the Failure by Fracture of Offshore Structures." The Welding Institute Proc. Second Int. Conf. on Offshore Welded Structures, Paper No. 9.

YOSHIKI, M., KANAZAWA, T., and MACHIDA, S., (1968), "Fracture Mechanics Analysis of Stiffener - Type Crack Arrester", JSNA, Japan, Vol. 124, pp. 63-72.

APPENDIX 1

PROBABILITY DISTRIBUTIONS IN PROBAN LIBRARY

The distributions currently included in the library are

BETA	BET
χ^2	CH2
EXPONENTIAL	EXP
GAMMA	GAM
GENERALIZED GAMMA	GGM
GUMBEL	GUM
LOGNORMAL	LNM
LONGUET-HIGGINS	LOH
MAXWELL	MXW
MULTINORMAL	MNR
NORMAL	NRM
ONE SIDED NORMAL	ONE
RAYLEIGH	RAY
STUDENT T	STU
TRUNCATED NORMAL	TRU
UNIFORM	UNI
WEIBULL	WBL

PROBAN can handle any distribution where the inverse transformation

$$\mathbf{X} = T^{-1}(\mathbf{U})$$

is obtained. **U** is a vector of independent standard normal random variables. **X** is the corresponding basic variables, i.e. the variables of the limit state functions.

The BETA distribution

The density function:

$$f(x) = \begin{cases} \dfrac{1}{B(b-a)^{t-1}}(x-a)^{r-1}(b-x)^{t-r-1} & a \leqslant x \leqslant b \\ 0 & \textit{elsewhere} \end{cases}$$

where

$$B = \frac{\Gamma(r)\Gamma(t-r)}{\Gamma(t)} = \beta(r,t-r)$$

with the Γ- and β-functions:

$$\Gamma(r) = \int_0^\infty s^{r-1}e^{-s}\,ds$$

$$\beta(r,t-r) = \int_0^1 s^{r-1}(1-s)^{t-r-1}ds$$

The cumulative distribution:

$$F(x) = \begin{cases} I_y(r,t-r) = \dfrac{\beta_y(r,t-r)}{\beta(r,t-r)} = \dfrac{1}{\beta(a,b)}\displaystyle\int_0^y s^{r-1}(1-s)^{t-r-1}ds & a \leqslant x \leqslant b \\ 0 & \textit{elsewhere} \end{cases}$$

with

$$y = \frac{x-a}{b-a}$$

$I_y(r,t-r)$ is the incomplete beta function.

Restrictions on distribution parameters:

$$r \geqslant 1,\ t \geqslant r,\ b > a$$

Input sequences: There are three possible input sequences for the BETA-distribution:

Sequence 1: This sequence is named "MEAN-VALUE-STANDARD-DEVIATION". Input is "MEAN-VALUE", "STANDARD-DEVIATION, "LOWER-BOUND-FOR-THE-INTERVAL", "UPPER-BOUND-FOR-THE-INTERVAL".

Sequence 2: This sequence is named "MEAN-VALUE-C.O.V.". Input is "MEAN-VALUE", "COEFFICIENT-OF-VARIATION", "LOWER-BOUND-FOR-THE-INTERVAL", "UPPER-BOUND-FOR-THE-INTERVAL".

Sequence 3: This sequence is named "DISTRIBUTION-PARAMETERS". Input is "PARAMETER-R", "PARAMETER-T", "LOWER-BOUND-FOR-THE-INTERVAL", "UPPER-BOUND-FOR-THE-INTERVAL".

Distribution name (input): BETA

Distribution name (output): BETA

The χ^2 distribution

The χ^2 distribution is a special case of the generalized gamma distribution with parameters $a=\frac{\nu}{2}$, $b=1$, $c=2$.

The density function:

$$f(x)=\begin{cases} \frac{1}{2\Gamma(\frac{\nu}{2})}\left(\frac{x-\gamma}{2}\right)^{\frac{\nu}{2}-1}e^{-\frac{x-\gamma}{2}} & x \geqslant \gamma \\ 0 & x < \gamma \end{cases}$$

The cumulative distribution:

$$F(x)=\begin{cases} \frac{\gamma(\frac{\nu}{2},\frac{x-\gamma}{2})}{\Gamma(\frac{\nu}{2})} & x \geqslant \gamma \\ 0 & x < \gamma \end{cases}$$

where the incomplete gamma-function is:

$$\gamma(a,x)=\int_0^x s^{a-1}e^{-s}\,ds$$

Restrictions on distribution parameters:

$$\nu > 0$$

Input options: There are two input options for the χ^2 distribution.

Option 1: This sequence is named "MEAN-VALUE".
The input parameters are "MEAN-VALUE", "SHIFT-PARAMETER".
Option 2: This sequence is named "PARAMETERS."
The input parameters are "PARAMETER-NU", "SHIFT-PARAMETER".

Distribution name (input): CHI-SQUARE

Distribution name (output): CHISQ

The EXPONENTIAL distribution.

The exponential distribution is a special case of the generalized gamma distribution with parameters $a=1, b=1, c=\frac{1}{\lambda}$.

The density function:

$$f(x)=\begin{cases}\lambda e^{-\lambda(x-\gamma)} & x \geq \gamma \\ 0 & x < \gamma\end{cases}$$

The cumulative distribution:

$$F(x)=\begin{cases}1-e^{-\lambda(x-\gamma)} & x \geq \gamma \\ 0 & x < \gamma\end{cases}$$

Restrictions on distribution parameters:

$$\lambda > 0$$

Input options: There are two options for input of distribution parameters:

Option 1: This option is named "MEAN-VALUE-LOWER-LIMIT".
Input is: "MEAN-VALUE", "LOWER-LIMIT"
Option 2: This option is named "DISTRIBUTION-PARAMETERS".
Input is: "PARAMETER-LAMBDA", "LOWER-LIMIT"

Distribution name (input): EXPONENTIAL

Distribution name (output): EXPON

The GENERALIZED GAMMA distribution.

The density function:

$$f(x)=\begin{cases}\dfrac{|b|}{\Gamma(a)c}\left(\dfrac{x-\gamma}{c}\right)^{ab-1}e^{-\left(\frac{x-\gamma}{c}\right)^{b}} & x\geqslant\gamma\\ 0 & x<\gamma\end{cases}$$

The cumulative distribution:

$$F(x)=\begin{cases}1-\dfrac{\Gamma\left(a;\left(\frac{x-\gamma}{c}\right)^{b}\right)}{\Gamma(a)} & b>0, x\geqslant\gamma\\ \dfrac{\Gamma\left(a;\left(\frac{x-\gamma}{c}\right)^{b}\right)}{\Gamma(a)} & b<0, x\geqslant\gamma\\ 0 & x<\gamma\end{cases}$$

Here the Γ-function is

$$\Gamma(a)=\int_0^\infty s^{a-1}e^{-s}\,ds$$

and the complementary incomplete Γ-function is

$$\Gamma(a;x)=\int_x^\infty s^{a-1}e^{-s}\,ds$$

Restrictions on distribution parameters:

$a>0, b\neq 0, c>0$

Input options: There is one option for input of distribution parameters:

Option 1: This option is named "DISTRIBUTION-PARAMETERS". Input is: "PARAMETER-ALPHA", "PARAMETER-BETA", "PARAMETER-C", "SHIFT-PARAMETER-(GAMMA)".

(α,β)
eller
(a,b)

Distribution name: (input): GENERALIZED-GAMMA

Distribution name (output): GNGAM

The GUMBEL distribution.

The distribution is also called the Type I asymptotic extreme value distribution of largest values.

The density function: $\alpha \, \exp(-\alpha(x-\beta) - \exp(-\alpha(x-\beta)))$

$$f(x) = \alpha e^{-\alpha(x-\beta) - e^{-\alpha(x-\beta)}} \qquad -\infty < x < \infty$$

The cumulative distribution:

$$F(x) = e^{-e^{-\alpha(x-\beta)}} \qquad \exp(-\exp(-\alpha(x-\beta)))$$

Restrictions on distribution parameters:

$$\alpha > 0$$

Input options: There are two options for input of distribution parameters:

Option 1: This option is named "MEAN-VALUE-STANDARD-DEVIATION".
Input is "MEAN-VALUE", "STANDARD-DEVIATION.

Option 2: This option is named "MEAN-VALUE-C.O.V.".
Input is "MEAN-VALUE", "COEFFICIENT-OF-VARIATION".

Option 3: This option is named "DISTRIBUTION-PARAMETERS".
Input is "PARAMETER-ALPHA", "PARAMETER-BETA".

Distribution name (input): GUMBEL

Distribution name (output): GUMBE

The LOGNORMAL distribution.

The density function:

$$f(x) = \begin{cases} \dfrac{1}{\sqrt{2\pi}\epsilon(x-\gamma)} e^{-\frac{1}{2}\left(\frac{\ln(x-\gamma)-\xi}{\epsilon}\right)^2} & x > \gamma \\ 0 & x < \gamma \end{cases}$$

The cumulative distribution:

$$F(x) = \begin{cases} \dfrac{1}{2}(1+erf\,(\dfrac{\ln(x-\gamma)-\xi}{\epsilon\sqrt{2}}) & x > \gamma, \ln(x-\gamma)-\xi \geq 0 \\ \dfrac{1}{2} erfc\,(-\dfrac{\ln(x-\gamma)-\xi}{\epsilon\sqrt{2}}) & x > \gamma, \ln(x-\gamma)-\xi < 0 \\ 0 & x < \gamma \end{cases}$$

where

$$erf\,(u) = \frac{2}{\sqrt{\pi}} \int_0^u e^{-s^2} ds$$

$$erfc\,(u) = \frac{2}{\sqrt{\pi}} \int_u^\infty e^{-s^2} ds$$

Restrictions on distribution parameters:

$$\epsilon > 0$$

Input options: There are three options for input of distribution parameters:

Option 1: **This option is named "MEAN-VALUE-STANDARD-DEVIATION". Input is "MEAN-VALUE", "STANDARD-DEVIATION, "SHIFT-PARAMETER-(GAMMA)".**

Option 2: **This option is named "MEAN-VALUE-C.O.V.". Input is "MEAN-VALUE", "COEFFICIENT-OF-VARIATION", "SHIFT-PARAMETER-(GAMMA)".**

Option 3: **This option is named "DISTRIBUTION-PARAMETERS". Input is "PARAMETER-EPSILON", "PARAMETER-KSI", "SHIFT-PARAMETER-(GAMMA)".**

Distribution name (input): LOGNORMAL

Distribution name (output): LOGNR

The LONGUET-HIGGINS distribution.

The density function:

$$f(x) = \frac{2Nx}{r^2}\exp\{-(\frac{x}{r})^2-N\exp[-(\frac{x}{r})^2]\}$$

The cumulative distribution:

$$F(x) = \exp\{-N\exp[-(\frac{x}{r})^2]\}$$

Here N is the number of cycles and r is the r-parameter

Restrictions: $x > 0$, $\exp(-N) \approx 0$

Input options: There is one option for input of parameters of this distribution:

Option 1: The input sequence is named "DISTRIBUTION-PARAMETERS".
Input is "NUMBER-OF-CYCLES:-N", "PARAMETER-R".

Distribution name (input): LONGUET-HIGGINS

Distribution name (output): LONHI

The MAXWELL distribution.

The Maxwell distribution is a special case of the generalized gamma distribution with parameters $a=\frac{3}{2}, b=2, c=\theta$.

The density function:

$$f(x)=\begin{cases}\frac{4}{\sqrt{\pi}}(\frac{x-\gamma}{\theta})^2 e^{-(\frac{x-\gamma}{\theta})^2} & x \geqslant \gamma \\ 0 & x < \gamma\end{cases}$$

The cumulative distribution:

$$F(x)=\begin{cases}\frac{2}{\sqrt{\pi}}\gamma(\frac{3}{2},(\frac{x-\gamma}{\theta})^2) & x \geqslant \gamma \\ 0 & x < \gamma\end{cases}$$

where $\gamma(a,y)$ is the incomplete gamma function.

Restrictions on distribution parameters:

$\theta > 0$

Input options: There is two options for input of distribution parameters:

Option 1: This option is named "MEAN-VALUE-SHIFT-PARAMETER".
Input is "MEAN-VALUE". "SHIFT-PARAMETER-GAMMA".

Option 2: This option is named "DISTRIBUTION-PARAMETERS".
Input is "PARAMETER-THETA". "SHIFT-PARAMETER-GAMMA".

Distribution name (input): MAXWELL

Distribution name (output): MAXWE

The MULTINORMAL distribution.

The density function:

$$\phi(\mathbf{X};\mathbf{C}) = \frac{1}{(2\pi)^{\frac{n}{2}} det\,(\mathbf{C})^{1/2}} \exp(-\frac{1}{2}(\mathbf{X}^T - \mu^T)\mathbf{C}^{-1}(\mathbf{X}-\mu))$$

Here $\mathbf{X}=(X_1,X_2,\cdots,X_n)$ is a random vector, **C** is the correlation matrix, $\mu=(\mu_1,\mu_2,\cdots,\mu_n)$ and det(.) is the determinant.

The cumulative distribution:

$$\Phi(\mathbf{X};\mathbf{C}) = \int_{-\infty}^{X_1}\int_{-\infty}^{X_2}\cdots\int_{-\infty}^{X_n} \phi(\mathbf{s};\mathbf{C})\, ds_1 ds_2 \cdots ds_n$$

Restrictions: The covariance matrix **C** must be positive definite ($\mathbf{x}^T\mathbf{C}\mathbf{x}>0$ for all nonzero choices of **x**.) Thus no linear dependency must exist between variables of the multinormal distribution.

Input to PROBAN: The user is first asked to give the number n of random variables. Having entered $n>0$ the user enters the covariance matrix **C** and thereafter the mean values μ.

Input options: There are two options for input of covariance matrix in PROBAN:

Option 1: The name of this option is "CORRELATION-MATRIX,STANDARD-DEVIATIONS,MEAN-VALUES"
The user enters the strict upper triangle of the correlation matrix rowwise, the standard deviations and the mean values.

Option 2: The name of this option is "COVARIANCE-MATRIX,MEAN-VALUES"
The user enters the upper triangle of the covariance matrix rowwise and the mean values.

Distribution name (input): MULTINORMAL

Distribution name (output): MULNR

The NORMAL distribution.

The density function:

$$f(x) = \frac{1}{\sqrt{2\pi}\sigma} e^{-\frac{1}{2}(\frac{x-\mu}{\sigma})^2} \qquad -\infty < x < \infty$$

The cumulative distribution:

$$F(x) = \begin{cases} \frac{1}{2}(1+erf\,(\frac{x-\mu}{\sigma\sqrt{2}}) & x-\mu \geqslant 0 \\ \frac{1}{2}erfc\,(-\frac{x-\mu}{\sigma\sqrt{2}}) & x-\mu < 0 \end{cases}$$

where

$$erf\,(u) = \frac{2}{\sqrt{\pi}} \int_0^u e^{-t^2} dt$$

$$erfc\,(u) = \frac{2}{\sqrt{\pi}} \int_u^\infty e^{-t^2} dt$$

Restrictions on distribution parameters:

$$\sigma > 0$$

Input options: There are two options for input of distribution parameters:

Option 1: This option is named "MEAN-VALUE-STANDARD-DEVIATION". Input is "MEAN-VALUE", "STANDARD-DEVIATION".

Option 2: This option is named "MEAN-VALUE-C.O.V.". Input is "MEAN-VALUE", "COEFFICIENT-OF-VARIATION".

Distribution name (input): NORMAL

Distribution name (output): NORMA

The ONESIDED NORMAL distribution.

The onesided normal distribution is a special case of the generalized gamma distribution with parameters $a=\frac{1}{2}$, $b=2$, $c=\sigma\sqrt{2}$.

The density function:

$$f(x)=\begin{cases}\dfrac{2}{\sqrt{2\pi}\sigma}e^{-\frac{1}{2}\left(\frac{x-\gamma}{\sigma}\right)^2} & x\geqslant\gamma\\ 0 & x<\gamma\end{cases}$$

The cumulative distribution:

$$F(x)=\begin{cases}erf\left(\dfrac{x-\gamma}{\sigma\sqrt{2}}\right) & x\geqslant\gamma\\ 0 & x<\gamma\end{cases}$$

where

$$erf\ (u)=\frac{2}{\sqrt{\pi}}\int_0^u e^{-s^2}ds$$

Restrictions on distribution parameters:

$\sigma > 0$

Input options: There are two options for input of distribution parameters:

Option 1: This option is named "MEAN-VALUE-SHIFT-PARAMETER".
Input is "MEAN-VALUE", "SHIFT-PARAMETER-(GAMMA)".

Option 2: This option is named "DISTRIBUTION-PARAMETERS".
Input is "PARAMETER-SIGMA", "SHIFT-PARAMETER-(GAMMA)".

Distribution name (input): ONE-SIDED-NORMAL

Distribution name (output): ONSDN

The RAYLEIGH distribution.

The Rayleigh distribution is a special case of the generalized gamma distribution with parameters $a=1, b=2, c=\sqrt{2}\theta$.

The density function:

$$f(x)=\begin{cases}\frac{x-\gamma}{\theta^2}e^{-\frac{(x-\gamma)^2}{2\theta^2}} & x\geqslant\gamma\\ 0 & x<\gamma\end{cases}$$

The cumulative distribution:

$$F(x)=\begin{cases}1-e^{-\frac{(x-\gamma)^2}{2\theta^2}} & x\geqslant\gamma\\ 0 & x<\gamma\end{cases}$$

Restrictions on distribution parameters:

$\theta > 0$

Input options: There are two options for input of distribution parameters:

Option 1: **This option is named "MEAN-VALUE-SHIFT-PARAMETER".**
Input is "MEAN-VALUE", "SHIFT-PARAMETER-(GAMMA)".

Option 2: **This option is named "DISTRIBUTION-PARAMETERS".**
Input is "PARAMETER-THETA", "SHIFT-PARAMETER-(GAMMA)".

Distribution name (input): RAYLEIGH

Distribution name (output): RAYLE

The STUDENT-t distribution.

The density function:

$$f(x) = \frac{1}{\sqrt{n}\,\beta(\frac{1}{2},\frac{n}{2})}(1+\frac{x^2}{n})^{-\frac{1}{2}(n+1)}$$

where β is the beta-function.

The cumulative distribution:

$$F(x) = \begin{cases} \frac{1}{2} I_{\frac{n}{n+x^2}}(\frac{n}{2},\frac{1}{2}) & x \leqslant 0 \\ 1-\frac{1}{2} I_{\frac{n}{n+x^2}}(\frac{n}{2},\frac{1}{2}) & x > 0 \end{cases}$$

where $I_{\frac{n}{n+x^2}}(\frac{n}{2},\frac{1}{2})$ is the incomplete beta function with parameters $r=\frac{n}{2}$, $t=\frac{n+1}{2}$, $a=0$ and $b=1$ at the point $\frac{n}{n+x^2}$.

Restrictions on distribution parameters:

$n \geqslant 2$

Input options: There is one option for input of distribution parameters:

Option 1: This option is named "DISTRIBUTION-PARAMETERS".
Input is "PARAMETER-N".

Distribution name (input): STUDENT-T

Distribution name (output): STUDE

The TRUNCATED NORMAL distribution.

The density function:

$$f(x) = \begin{cases} k f_Y(x) & x_0 \leqslant x \leqslant x_1 \\ 0 & \mathit{else} \end{cases}$$

where $f(x)$ is the normal distribution density function with parameters μ and σ, and the normalizing constant k is :

$$k = \frac{1}{F_Y(x_1) - F_Y(x_0)}$$

where $F_Y(x)$ is the normal cumulative distribution.

The cumulative distribution:

$$F(x) = \begin{cases} k(F_Y(x) - F_Y(x_0)) & x_0 \leqslant x \leqslant x_1 \\ 0 & \mathit{else} \end{cases}$$

Restrictions on distribution parameters:

$$\sigma > 0, x_1 > x_0$$

Input options: There are three options for input of distribution parameters:

Option 1: This option is named "MEAN-VALUE-STANDARD-DEVIATION".
Input is "MEAN-VALUE". "STANDARD-DEVIATION. "LOWER-BOUND-FOR-THE-INTERVAL". "UPPER-BOUND-FOR-THE-INTERVAL".

Option 2: This option is named "MEAN-VALUE-C.O.V.".
Input is "MEAN-VALUE". "COEFFICIENT-OF-VARIATION". "LOWER-BOUND-FOR-THE-INTERVAL". "UPPER-BOUND-FOR-THE-INTERVAL".

Option 3: This option is named "DISTRIBUTION-PARAMETERS".
Input is "PARAMETER-MU". "PARAMETER-SIGMA". "LOWER-BOUND-FOR-THE-INTERVAL". "UPPER-BOUND-FOR-THE-INTERVAL".

Distribution name (input): TRUNCATED-NORMAL

Distribution name (output): TRUNM

The UNIFORM distribution.

The density function:

$$f(x) = \begin{cases} \frac{1}{b-a} & a \leqslant x \leqslant b \\ 0 & else \end{cases}$$

The cumulative distribution:

$$F(x) = \begin{cases} \frac{x-a}{b-a} & a \leqslant x \leqslant b \\ 0 & elsewhere \end{cases}$$

Restrictions on distribution parameters:

$b > a$

Input options: There is one option for input of distribution parameters:

Option 1: This option is named "DISTRIBUTION-PARAMETERS". Input is "LOWER-BOUND-FOR-THE-INTERVAL". "UPPER-BOUND-FOR-THE-INTERVAL".

Distribution name (input): UNIFORM

Distribution name (output): UNIFO

The WEIBULL distribution.

The Weibull distribution is a special case of the generalized gamma distribution with parameters $a = 1, b = \beta > 0, c = \frac{1}{\alpha}$.

The density function:

$$f(x) = \begin{cases} \alpha\beta(x-\gamma)^{\beta-1}e^{-\alpha(x-\gamma)^{\beta}} & x \geqslant \gamma \\ 0 & x < \gamma \end{cases}$$

The cumulative distribution:

$$F(x) = \begin{cases} 1-e^{-\alpha(x-\gamma)^{\beta}} & x \geqslant \gamma \\ 0 & x < \gamma \end{cases}$$

Restrictions on distribution parameters:

$\alpha > 0, \beta > 0$

Input options: There are three options for input of distribution parameters:

Option 1: This option is named "MEAN-VALUE-STANDARD-DEVIATION". Input is "MEAN-VALUE", "STANDARD-DEVIATION, "SHIFT-PARAMETER-(GAMMA)".

Option 2: This option is named "MEAN-VALUE-C.O.V.". Input is "MEAN-VALUE", "COEFFICIENT-OF-VARIATION", "SHIFT-PARAMETER-(GAMMA)".

Option 3: This option is named "DISTRIBUTION-PARAMETERS". Input is "PARAMETER-ALPHA", "PARAMETER-BETA", "SHIFT-PARAMETER-(GAMMA)".

Distribution name (input): WEIBULL

Distribution name (output): WEIBU

APPENDIX 2

DATABASE OF MATERIALS PROPERTIES

TABLE A2.1

Static CTOD Values for Grade A Steel T-L and L-T

TEMP deg C	STEEL GRADE & ORIENT.	Static CTOD Values mm				
75	A, T-L					
50	A, T-L					
22	A, T-L	0.60	0.86	0.79	0.81	0.63
0	A, T-L	0.84				
-25	A, T-L	0.43	0.80	0.67	0.67	0.52
-50	A, T-L	0.08				
-70	A, T-L	0.06	0.05	0.04	0.04	0.04
-100	A, T-L					
-125	A, T-L					
-150	A, T-L					

TEMP deg C	STEEL GRADE & ORIENT.	Static CTOD Values mm		
75	A, L-T			
50	A, L-T			
22	A, L-T	2.20	2.35	2.12
0	A, L-T	1.91		
-25	A, L-T	0.62	0.71	0.80
-50	A, L-T	0.11		
-70	A, L-T	0.08	0.09	0.06
-100	A, L-T			
-125	A, L-T			
-150	A, L-T			

TABLE A2.2

Static CTOD Values for Grade D Steel T-L and L-T

TEMP deg C	STEEL GRADE & ORIENT.	Static CTOD Values mm		
75	D, T-L			
50	D, T-L			
22	D, T-L	0.46	0.51	0.51
0	D, T-L	0.63		
-25	D, T-L	0.62	0.69	0.64
-50	D, T-L	0.65		
-70	D, T-L	0.20	0.21	0.21
-100	D, T-L	0.12		
-125	D, T-L			
-150	D, T-L			

TEMP deg C	STEEL GRADE & ORIENT.	Static CTOD Values mm		
75	D, L-T			
50	D, L-T			
22	D, L-T	1.68	1.80	1.72
0	D, L-T	1.66		
-25	D, L-T	1.97	1.89	1.78
-50	D, L-T	1.97		
-70	D, L-T	1.55	0.87	1.56
-100	D, L-T	0.14		
-125	D, L-T			
-150	D, L-T			

TABLE A2.3

Static CTOD Values for Grade EH 36 Steel T-L and L-T

TEMP deg C	STEEL GRADE & ORIENT.	Static CTOD Values mm					
75	E, T-L						
50	E, T-L						
22	E, T-L	0.22	0.17	0.16	0.31		
0	E, T-L	0.26					
-25	E, T-L	0.20	0.16	0.16	0.16	0.16	
-50	E, T-L	0.15					
-70	E, T-L	0.17	0.17	0.18	0.17	0.17	0.17
-100	E, T-L	0.13					
-125	E, T-L						
-150	E, T-L						

TEMP deg C	STEEL GRADE & ORIENT.	Static CTOD Values mm
75	E, L-T	
50	E, L-T	
22	E, L-T	1.18
0	E, L-T	1.21
-25	E, L-T	1.38
-50	E, L-T	1.11
-70	E, L-T	1.32
-100	E, L-T	0.12
-125	E, L-T	0.13
-150	E, L-T	

TABLE A2.4

Dynamic CTOD Values for Grade A Steel T-L and L-T

TEMP deg C	STEEL GRADE & ORIENT.	Dynamic CTOD Values mm		
75	A, T-L			
50	A, T-L	0.20		
22	A, T-L	0.21	0.20	
0	A, T-L	0.07		
-25	A, T-L	0.07	0.07	0.07
-50	A, T-L	0.04		
-70	A, T-L	0.04		
-100	A, T-L			
-125	A, T-L			
-150	A, T-L			

TEMP deg C	STEEL GRADE & ORIENT.	Dynamic CTOD Values mm		
75	A, L-T			
50	A, L-T	0.23		
22	A, L-T	0.24	0.24	0.25
0	A, L-T	0.22		
-25	A, L-T	0.05		
-50	A, L-T	0.11		
-70	A, L-T	0.09		
-100	A, L-T			
-125	A, L-T			
-150	A, L-T			

TABLE A2.5

Dynamic CTOD Values for Grade D Steel T-L and L-T

TEMP deg C	STEEL GRADE & ORIENT.	Dynamic CTOD Values mm
75	D, T-L	
50	D, T-L	
22	D, T-L	
0	D, T-L	0.28
-25	D, T-L	0.12
-50	D, T-L	0.12
-70	D, T-L	
-100	D, T-L	
-125	D, T-L	
-150	D, T-L	

TEMP deg C	STEEL GRADE & ORIENT.	Dynamic CTOD Values mm
75	D, L-T	
50	D, L-T	
22	D, L-T	0.28
0	D, L-T	0.33
-25	D, L-T	0.21
-50	D, L-T	0.09
-70	D, L-T	
-100	D, L-T	
-125	D, L-T	
-150	D, L-T	

TABLE A2.6

Dynamic CTOD Values for Grade EH 36 Steel T-L and L-T

TEMP deg C	STEEL GRADE & ORIENT.	Dynamic CTOD Values mm		
75	E, T-L			
50	E, T-L			
22	E, T-L	0.35	0.34	0.29
0	E, T-L	0.29		
-25	E, T-L	0.28	0.28	0.43
-50	E, T-L	0.12		
-70	E, T-L	0.13	0.11	
-100	E, T-L			
-125	E, T-L			
-150	E, T-L			

TEMP deg C	STEEL GRADE & ORIENT.	Dynamic CTOD Values mm
75	E, L-T	
50	E, L-T	
22	E, L-T	
0	E, L-T	
-25	E, L-T	
-50	E, L-T	0.19
-70	E, L-T	
-100	E, L-T	
-125	E, L-T	
-150	E, L-T	

TABLE A2.7

Fracture Toughness K_{Ic} for Grade A Steel T-L and L-T

TEMP deg C	STEEL GRADE & ORIENT.	KC Values MPa$\sqrt{m}$				
75	A, T-L					
50	A, T-L					
22	A, T-L	121.0	129.0	174.0	149.0	180.0
0	A, T-L	135.0				
-25	A, T-L	104.0	91.0	73.0	100.0	96.0
-50	A, T-L	40.0				
-70	A, T-L	15.0	53.0	77.0	49.0	24.0
-100	A, T-L					
-125	A, T-L					
-150	A, T-L					

TEMP deg C	STEEL GRADE & ORIENT.	KC Values MPa$\sqrt{m}$		
75	A, L-T			
50	A, L-T			
22	A, L-T	133.0	138.0	
0	A, L-T	166.0		
-25	A, L-T	149.0	147.0	163.0
-50	A, L-T	54.0		
-70	A, L-T	15.0	54.0	
-100	A, L-T			
-125	A, L-T			
-150	A, L-T			

TABLE 2-8

Fracture Toughness K_{Ic} for Grade D Steel T-L and L-T

TEMP deg C	STEEL GRADE & ORIENT.	KC Values MPa√m		
75	D, T-L			
50	D, T-L			
22	D, T-L	141.0	136.0	
0	D, T-L	165.0		
-25	D, T-L	102.0	97.0	91.0
-50	D, T-L	54.0		
-70	D, T-L	53.0	53.0	53.0
-100	D, T-L	76.0		
-125	D, T-L			
-150	D, T-L			

TEMP deg C	STEEL GRADE & ORIENT.	KC Values MPa√m		
75	D, L-T			
50	D, L-T			
22	D, L-T	182.0	167.0	
0	D, L-T	262.0		
-25	D, L-T	250.0	154.0	210.0
-50	D, L-T	182.0		
-70	D, L-T	149.0	149.0	
-100	D, L-T	74.0		
-125	D, L-T			
-150	D, L-T			

TABLE A2.9

Fracture Toughness K_{Ic} for Grade EH 36 Steel T-L and L-T

TEMP deg C	STEEL GRADE & ORIENT.	KC Values MPa$\sqrt{m}$					
75	E, T-L						
50	E, T-L						
22	E, T-L	131.0	133.0	77.0			
0	E, T-L	77.0					
-25	E, T-L	84.0	77.0	81.0	64.0	64.0	
-50	E, T-L	127.0					
-70	E, T-L	102.0	61.0	118.0	107.0	38.0	38.0
-100	E, T-L	61.0					
-125	E, T-L						
-150	E, T-L						

TEMP deg C	STEEL GRADE & ORIENT.	KC Values MPa.$\sqrt{m}$
75	E, L-T	
50	E, L-T	
22	E, L-T	157.0
0	E, L-T	180.0
-25	E, L-T	144.0
-50	E, L-T	182.0
-70	E, L-T	210.0
-100	E, L-T	61.0
-125	E, L-T	74.0
-150	E, L-T	

TABLE A2.10

Dynamic Fracture Toughness K_{Id} for EH 36 Grade Steel

Spec	Temp (^oC)	R (mm)	a_o (mm)	Δa (mm)	y_Q (mm)	y_a (mm)	K_Q/K_{ID}	K_Q (MPa$\sqrt{m}$)	K_{ID} (MPa$\sqrt{m}$)	K_{Ia} (MPa$\sqrt{m}$)	V/C_o
E30	-30	0.5	76.7	42.6	0.66	0.68	0.87	101	88.1	67.9	0.055
E33	-30	0.5	75.7	93.4	0.95	1.01	0.66	146	96.2	57.2	0.128
E37	-30	0.5	75.4	52.3	0.71	0.74	0.81	109	88.2	70.9	0.074
E43	-29	0.5	75.3	35.3	0.59	0.61	0.93	90.5	83.9	65.6	0.030
E22	-33	0.3	75	55.4	0.57	0.60	0.80	87.4	70.0	55.6	0.080
E23	-40	0.3	75	94.0	1.13	1.18	0.66	173	114	66.8	0.128
E34	-37	0.3	75.2	109.5	1.21	1.29	0.62	186	115	-	0.140
E24	-40	0.3	75.4	100.4	1.00	1.08	0.64	153	98.8	51.7	0.132
E28	-36	0.3	75	67	0.86	0.92	0.75	132	99.1	76.7	0.096
E40	-40	0.2	75.1	79.1	0.83	0.86	0.71	127	90.1	62.9	0.111
E21	-36	0.2	74.9	91.7	1.27	1.30	0.67	195	130	79.6	0.124
E42	-40	0.2	74.4	110.3	1.41	1.51	0.61	216	133	-	0.141
E39	-40	0.2	75	100.0	1.43	1.63	0.64	219	141	78.0	0.130

TABLE A2.11

Charpy V-Notch Values for S Grade Steel T-L and L-T

TEMP deg C	STEEL GRADE & ORIENT.	Charpy V-Notch Values J			
75	A, T-L	59.8	66.2		
50	A, T-L	52.8	58.0		
22	A, T-L	33.0	37.9	33.0	32.1
0	A, T-L	12.9	14.8		
-25	A, T-L	5.2	8.0	7.1	
-50	A, T-L	3.2	3.0		
-70	A, T-L	3.0	2.1	2.4	2.5
-100	A, T-L	2.0	2.0		
-125	A, T-L	2.0	2.0		
-150	A, T-L	2.6			

TEMP deg C	STEEL GRADE & ORIENT.	Charpy V-Notch Values J			
75	A, L-T	127.0	127.0		
50	A, L-T	108.0	134.0		
22	A, L-T	21.0	41.0	41.0	39.0
0	A, L-T	15.9	16.0	11.2	
-25	A, L-T	4.1	5.7		
-50	A, L-T	3.0	3.0		
-70	A, L-T	2.7	2.3	2.0	2.1
-100	A, L-T	2.0	2.0		
-125	A, L-T	3.5	2.9		
-150	A, L-T	2.0			

TABLE A2.12

Charpy V-Notch Values for D Grade Steel T-L and L-T

TEMP deg C	STEEL GRADE & ORIENT.	Charpy V-Notch Values J			
75	D, T-L	200.0	196.0	198.0	
50	D, T-L	189.3	192.1	193.2	
22	D, T-L	92.0	84.0		
0	D, T-L	66.0	60.2		
-25	D, T-L	41.0	39.9	49.0	
-50	D, T-L	28.2	26.9	29.0	
-70	D, T-L	20.0	16.0	11.2	9.3
-100	D, T-L	5.2	8.6	5.8	
-125	D, T-L	3.7	2.4		
-150	D, T-L	2.3			

TEMP deg C	STEEL GRADE & ORIENT.	Charpy V-Notch Values J			
75	D, L-T				
50	D, L-T				
22	D, L-T	210.0	205.0		
0	D, L-T	206.2	202.1		
-25	D, L-T	163.1	206.0		
-50	D, L-T	11.6	18.1	155.0	140.0
-70	D, L-T	11.8	10.0	6.9	32.1
-100	D, L-T	7.0	3.0	9.5	
-125	D, L-T	5.8	4.0		
-150	D, L-T	2.7			

TABLE A2.13

Charpy V-Notch Values for EH 36 Grade Steel T-L and L-T

TEMP deg C	STEEL GRADE & ORIENT.	Charpy V-Notch Values J		
75	E, T-L			
50	E, T-L			
22	E, T-L	50.0		
0	E, T-L	50.5	50.0	
-25	E, T-L	32.0	30.9	
-50	E, T-L	23.2	22.5	
-70	E, T-L	14.2	13.3	15.0
-100	E, T-L	9.7	10.5	14.0
-125	E, T-L	6.0	6.0	
-150	E, T-L	4.1		

TEMP deg C	STEEL GRADE & ORIENT.	Charpy V-Notch Values J		
75	E, L-T			
50	E, L-T			
22	E, L-T	117.0		
0	E, L-T	124.6	121.0	
-25	E, L-T	130.1	99.0	
-50	E, L-T	60.0	87.0	74.0
-70	E, L-T	36.0	35.2	29.1
-100	E, L-T	14.1	8.1	12.2
-125	E, L-T	7.3	8.2	
-150	E, L-T	2.0		

TABLE A2-14

CTOD and J_{Ic} for Grade A Steel T-L for Different Strain Rates

Temp. (^oC)	Specimen	COD_c (mm)	J_{IC} (N/mm)	CODd (mm)	Jd (N/mm)	$\dot{\varepsilon}$ (s^{-1})
22	17	0.60	64.0			$5 \cdot 10^{-5}$
"	16	0.86	72.0			"
"	15	0.79	131.0			"
"	14	0.81	96.0			"
"	1	0.63	140.0			"
"	20			0.21	120.0	2.7
"	25			0.20	112.0	2.7
20	29			0.04 , 0.08	43.1	0.44
"	36			0.48 , 0.41	239.8	0.03
0	2	0.84	79.4			$5 \cdot 10^{-5}$
"	21			0.07	32.0	2.7
- 25	11	0.43	47.4			$5 \cdot 10^{-5}$
"	12	0.80	35.8			"
"	10	0.67	23.0			"
"	13	0.67	43.5			"
"	3	0.52	39.7			"
"	32			0.07	17.6	2.7
"	26			0.07	22.1	2.7
"	31			0.07	32.0	2.7
- 25	23			0.07 , 0.10	47.8	$1.0 \cdot 10^{-3}$
"	35			0.06 , 0.08	52.9	$8.8 \cdot 10^{-3}$
"	28			0.02 , 0.04	19.8	0.15
"	34			0.02 , 0.04	20.2	0.26
- 50	4	0.08	7.0			$5 \cdot 10^{-5}$
"	24			0.04	8.0	2.7
- 70	7	0.06	1.0			$5 \cdot 10^{-5}$
"	6	0.05	12.0			"
"	8	0.04	5.1			"
"	9	0.04	10.0			"
"	5	0.04	2.6			"
"	22			0.04	9.6	2.7

TABLE A2.15

CTOD and J_{Ic} for Grade A Steel L-T for Different Strain Rates

Temp (^oC)	Spec	COD_c (mm)	J_{IC} (N/mm)	CODd (mm)	Jd (N/mm)	$\dot{\varepsilon}$ (s^{-1})
22	11	2.20	76.8			$5 \cdot 10^{-5}$
"	10	2.35	-			"
"	1	2.12	83.2			"
"	12			0.24	112.0	2.7
"	14			0.24	112.0	2.7
"	16			0.25	96.0	2.7
0	2	1.91	119			
"	13			0.22	96.0	2.7
- 25	8	0.62	96.0			$5 \cdot 10^{-5}$
"	9	0.71	93.4			$5 \cdot 10^{-5}$
"	3	0.80	115.2			$5 \cdot 10^{-5}$
"	15			0.05	9.3	2.7
- 25	20			0.02 ,0.06	22.3	0.20
- 50	4	0.11	12.8			$5 \cdot 10^{-5}$
"	17			0.11	26.9	2.7
- 70	6	0.08	1.0			$5 \cdot 10^{-5}$
"	7	0.09	12.8			$5 \cdot 10^{-5}$
"	5	0.06	-			$5 \cdot 10^{-5}$
"	19			0.09	16.0	2.7

TABLE A2-16

CTOD and J_{Ic} for Grade D Steel T-L for Different Strain Rates

Temp (^{o}C)	Spec	COD$_c$ (mm)	J_{IC} (N/mm)	CODd (mm)	Jd (N/mm)	$\dot{\varepsilon}$ (s^{-1})
22	5	0.46	85.8			$5 \cdot 10^{-5}$
"	11	0.51	-			$5 \cdot 10^{-5}$
"	10	0.51	80.6			$5 \cdot 10^{-5}$
0	2	0.63	117.8			$5 \cdot 10^{-5}$
"	14			0.28	228.2	2.7
- 25	12	0.62	44.8			$5 \cdot 10^{-5}$
"	13	0.69	41.0			$5 \cdot 10^{-5}$
"	4	0.64	35.8			$5 \cdot 10^{-5}$
"	15			0.12	72.0	2.7
- 50	1	0.65	12.8			$5 \cdot 10^{-5}$
"	17			0.12	24.0	2.7
- 70	3	0.20	12.0			$5 \cdot 10^{-5}$
"	7	0.21	12.0			$5 \cdot 10^{-5}$
"	6	0.21	12.0			$5 \cdot 10^{-5}$

TABLE A2.17

CTOD and J_{Ic} for Grade D Steel L-T for Different Strain Rates

Temp (^{o}C)	Spec	COD_c (mm)	J_{IC} (N/mm)	CODd (mm)	Jd (N/mm)	$\dot{\varepsilon}$ (s^{-1})
22	10	1.68	143.4			$5 \cdot 10^{-5}$
"	9	1.80	-			$5 \cdot 10^{-5}$
"	11	1.72	121.6			$5 \cdot 10^{-5}$
"	14			0.28	192.0	2.7
0	1	1.66	297.0			$5 . 10^{-5}$
"	17			0.33	224.0	2.7
- 25	3	1.97	271.4			$5 \cdot 10^{-5}$
"	4	1.89	102.4			$5 \cdot 10^{-5}$
"	2	1.78	192.0			$5 \cdot 10^{-5}$
"	15			0.21	108.2	2.7
- 50	5	1.97	143.4			$5 \cdot 10^{-5}$
"	28			0.09	46.1	2.7
- 70	7	1.55	96.0			$5 \cdot 10^{-5}$
"	8	0.87	96.0			$5 \cdot 10^{-5}$
"	6	1.56	-			$5 \cdot 10^{-5}$

TABLE A2.18

CTOD and J_{Ic} for Grade EH 36 Steel T-L for Different Strain Rates

Temp (°C)	Spec	COD_c (mm)-	J_{IC} (N/mm)	CODd (mm)	Jd (N/mm)	$\dot{\varepsilon}$ (s^{-1})
22	15	0.22	74.2			$5 \cdot 10^{-5}$
"	16	0.17	76.8			$5 \cdot 10^{-5}$
"	14	0.16	25.6			$5 \cdot 10^{-5}$
"	1	0.31	-			$5 \cdot 10^{-5}$
"	31			0.35	180.2	2.7
"	32			0.34	222.1	2.7
"	26			0.29	214.4	2.7
0	2	0.26	25.6			$5 \cdot 10^{-5}$
"	20			0.29	192.0	2.7
- 25	3	0.20	30.7			$5 \cdot 10^{-5}$
"	6	0.16	25.6			$5 \cdot 10^{-5}$
"	7	0.16	28.2			$5 \cdot 10^{-5}$
"	4	0.16	17.9			$5 \cdot 10^{-5}$
"	5	0.16	17.9			$5 \cdot 10^{-5}$
"	34			0.28	168.0	2.7
"	28			0.28	192.0	2.7
"	25			0.43	288.0	2.7
- 25	24			0.11 ,0.17	126.9	0.082
"	30			0.12 ,0.18	146.3	0.43
"	23			0.13 ,0.19	147.5	0.77
- 50	8	0.15	70.4			$5 \cdot 10^{-5}$
"	27			0.12	32.0	2.7
- 70	10	0.17	44.8			$5 \cdot 10^{-5}$
"	12	0.17	16.6			$5 \cdot 10^{-5}$
"	11	0.18	60.0			$5 \cdot 10^{-5}$
"	17	0.17	50.0			$5 \cdot 10^{-5}$
"	18	0.17	6.4			$5 \cdot 10^{-5}$
"	13	0.17	6.4			$5 \cdot 10^{-5}$
"	21			0.13	48.0	2.7
"	19			0.11	30.1	2.7

TABLE A2.19

CTOD and J_{Ic} for Grade EH 36 L-T for Different Strain Rates

Temp (^{o}C)	Spec.	COD_c (mm)	J_{IC} (N/mm)	CODd (mm)	Jd (N/mm)	$\dot{\varepsilon}$ (s^{-1})
22	5	1.18	107.5			$5 \cdot 10^{-5}$
0	1	1.21	140.8			$5 \cdot 10^{-5}$
- 25	2	1.38	89.6			$5 \cdot 10^{-5}$
- 50	3	1.11	143.4			$5 \cdot 10^{-5}$
"	-			0.19	101.8	2.7
- 70	4	1.32	192.0			$5 \cdot 10^{-5}$

TABLE A2.20

Yield Strength for Grade A Steel T-L and L-T

TEMP deg C	STEEL GRADE & ORIENT.	LOWER YIELD MPa AVG.	LOWER YIELD MPa STD.	UPPER YIELD MPa AVG.	UPPER YIELD MPa STD.
50	A, T-L	219.7	8.8	268.9	10.8
0	A, T-L	245.1	9.8	278.8	11.2
-75	A, T-L	329.0	13.2	370.8	14.8

Note: Variation of the yield strength is assumed to be 4%

TEMP deg C	STEEL GRADE & ORIENT.	LOWER YIELD MPa AVG.	LOWER YIELD MPa STD.	UPPER YIELD MPa AVG.	UPPER YIELD MPa STD.
50	A, L-T	207.6	8.3	244.2	9.8
23	A, L-T	228.8	9.2	232.5	9.3
0	A, L-T	241.6	9.7	270.3	10.8
-25	A, L-T	262.6	10.5	311.5	12.5
-75	A, L-T	336.9	13.5	392.4	15.7

Note: Variation of the yield strength is assumed to be 4%

TABLE A2.21

Yield Strength for Grade D Steel T-L and L-T

TEMP deg C	STEEL GRADE & ORIENT.	LOWER YIELD MPa AVG.	LOWER YIELD MPa STD.	UPPER YIELD MPa AVG.	UPPER YIELD MPa STD.
23	D, T-L	288.1	11.5	293.3	11.7
-25	D, T-L	295.9	11.8	339.5	13.6
-50	D, T-L	322.2	12.9	399.2	16.0
-75	D, T-L	336.9	13.5	415.0	16.6
-100	D, T-L	417.4	16.7	469.7	18.8

Note: Variation of the yield strength is assumed to be 4%

TEMP deg C	STEEL GRADE & ORIENT.	LOWER YIELD MPa AVG.	LOWER YIELD MPa STD.	UPPER YIELD MPa AVG.	UPPER YIELD MPa STD.
23	D, L-T	266.6	10.7	277.1	11.1
-25	D, L-T	293.1	11.7	340.7	13.6
-50	D, L-T	319.7	12.8	357.2	14.3
-75	D, L-T	347.8	13.9	373.1	14.9
-100	D, L-T	395.3	15.8	413.6	16.5

Note: Variation of the yield strength is assumed to be 4%

TABLE A2.22

Yield Strength for Grade EH 36 Steel T-L and L-T

TEMP deg C	STEEL GRADE & ORIENT.	LOWER YIELD MPa AVG.	LOWER YIELD MPa STD.	UPPER YIELD MPa AVG.	UPPER YIELD MPa STD.
0	E, T-L	377.0	15.1	423.1	16.9
-50	E, T-L	438.0	17.5	496.3	19.9
-100	E, T-L	516.0	20.6	567.2	22.7

Note: Variation of the yield strength is assumed to be 4%

TEMP deg C	STEEL GRADE & ORIENT.	LOWER YIELD MPa AVG.	LOWER YIELD MPa STD.	UPPER YIELD MPa AVG.	UPPER YIELD MPa STD.
-50	E, L-T	441.9	17.7	509.2	20.4
-75	E, L-T	453.5	18.1	508.0	20.3
-125	E, L-T	540.2	21.6	644.1	25.8

Note: Variation of the yield strength is assumed to be 4%